Ecosystem Feedback from Animal-Vegetation Interactions: A Modeling Approach

Zur Erlangung des akademischen Grades eines

DOKTORS DER NATURWISSENSCHAFTEN

(Dr. rer. nat.)

von der KIT Fakultät für

Bauingenieur-, Geo- und Umweltwissenschaften

des Karlsruher Instituts für Technologie (KIT)

genehmigte

DISSERTATION

von

M.Sc. Meteorologie: Jens Krause

aus Garmisch-Partenkirchen

Tag der mündlichen Prüfung: 28.04.2025

Sprache der mündlichen Prüfung: Englisch

Referentin: Prof. Dr. Almut Arneth

Koreferent: Prof. Dr. Thomas Hickler

Karlsruhe 2025

Abstract

Animal biodiversity faces significant threats from anthropogenic activities. It is well understood in principle that animals play an important role in ecosystem dynamics, but how exactly the presence or absence of full trophic chains affect, e.g., vegetation growth, composition and biogeochemical cycling is still unknown. To address these challenges, it is crucial to improve our understanding of the dynamic interactions between animals and vegetation. Process-based modelling has proven to be a powerful tool for assessing ecological functioning. This thesis presents a novel coupling of two process-based models: the Dynamic Global Vegetation Model (DGVM) LPJ-GUESS and the Madingley model, a framework for simulating multi-trophic animal functional diversity. Through three experiments, I evaluate and compare different versions of the coupled model system.

First, I compare outputs from the "offline" coupled version of the model system to Madingley's "default" version for four ecosystem types around the globe. Using LPJ-GUESS as an input to Madingley's herbivory results in significant shifts in simulated animal populations, with trends toward smaller body sizes and increased abundance. The shifts in body mass and animal distributions can be traced back to ecological processes, allowing in-depth analysis of heterotrophic responses to changes in leaf biomass. Power-law relationships for herbivore consumption to NPP and herbivore biomass to NPP derived from both model versions demonstrate substantial improvement in response to the LPJ-GUESS "offline" coupling compared to the "default" state. The results of this experiment encourage further development of the coupled process-based model systems as a viable way to assess multi-trophic interconnections between animal populations and the ecosystem's vegetation.

Second, I present the fully coupled "online" version of the model system that allows for bidirectional interactions between the availability of green vegetation biomass, herbivory, and the whole trophic chain and vice versa. In this "online" version, an overall reduction of -5% in ecosystem net primary productivity (NPP), -9% in leaf area index (LAI) and -10% in vegetation carbon mass is evident, compared to LPJ-GUESS without herbivory. Boreal ecosystems exhibit the most pronounced impacts, with vegetation carbon mass reductions reaching -42% in some regions. I evaluate LPJ-GUESS output against remote sensing datasets and flux measurements and find that the "online" coupled model system preserves LPJ-GUESS's ability to simulate realistic biome distributions and carbon pools. I again compare power-law relationships of herbivore population dynamics for all three different versions of the Madingley model and conclude that the "online" version surpasses both other versions in terms of representing the power-law relationships derived from empirical data.

Finally, I employ the fully coupled version of the model system to investigate the effects of large animal removal on the simulated vegetation. In two separate cases, I either remove large

herbivores or large carnivores from the simulation after the system reaches an equilibrium state. In the case of large herbivore removal, leaf carbon mass increases in boreal biomes (+10%), tropical rainforests (+5%) and moist savannas (+6%). Conversely, removing large carnivores reduces leaf carbon mass in boreal biomes (-11%), tropical rainforests (-19%) and moist savannas (-19%). When comparing the effects of large animal removal under climate change, vegetation shifts caused by climate change outweigh the effects of large animal removal in the boreal biomes. In Africa, the effect of large carnivore removal is of a similar magnitude as the effects of CO_2 fertilisation (but reducing overall productivity). Simulations of animal population recovery reveal that ecosystems require centuries to recover from the complete removal of large animals, whereas recovery occurs more rapidly when such populations are preserved in areas that are unaffected by the removal. These results emphasise the critical role of conserving animal biodiversity in the face of climate change.

In conclusion, the results of this thesis highlight the important contribution of process-based modelling towards a better understanding of the complex interconnections between animals and vegetation. It demonstrates how coupling dynamic vegetation and animal population models enhances our understanding of multi-trophic ecosystem dynamics and broadly underpins the important role of animals in ecosystem functioning.

Zusammenfassung (German)

Die biologische Artenvielfalt, welche für das Funktionieren und die Stabilität von Ökosystemen von entscheidender Bedeutung ist, wird durch den Menschen erheblich bedroht. Die prinzipiell wichtige Rolle, welche Tiere für die dynamischen Prozesse von Ökosystemen spielen, ist unbestritten. Wie genau jedoch die An- oder Abwesenheit vollständiger trophischer Ketten beispielsweise das Wachstum, die Zusammensetzung und den biogeochemischen Kreislauf der Vegetation beeinflusst, ist nicht quantifiziert. Ein verbessertes Verständnis von Ökosystemfunktion und deren Artenzusammensetzung benötigt u. a. auch ein besseres Verständnis der dynamischen Interaktionen zwischen Tieren und Pflanzen. Zu diesen Interaktionen gehört der Blattfraß durch Herbivoren, mit tiefgreifenden und vielfältigen Auswirkungen auf die Vegetation. Bislang fehlen umfassende, groß angelegte, quantitative Abschätzungen dieser Effekte. Prozessbasierte Modelle haben sich als mächtiges Werkzeug zur Bewertung ökologischer Prozesse erwiesen. Diese Dissertation stellt eine neuartige Kopplung zweier prozessbasierter Modelle vor: das Dynamische Globale Vegetations Modell (DGVM) LPJ-GUESS und das Madingley-Modell, ein Modell zur Simulation multi-trophischer funktioneller Diversität von Tieren. In drei Experimenten werden verschiedene Versionen des gekoppelten Modellsystems präsentiert, bewertet und verglichen.

Zunächst vergleiche ich Ergebnisse der „offline“ gekoppelten Version des Modellsystems mit der „default“ Version von Madingley für vier ausgewählte Biome. Es zeigen sich signifikante Verschiebungen in den simulierten Tierpopulationen, mit Trends zu geringerer Körpermasse und höherer Abundanz. Die Verschiebungen in Körpermasse und dem resultierendem Größenspektrum lassen sich auf ökologische Prozesse zurückführen und ermöglichen eine detaillierte Analyse der vielschichtigen Reaktionen der Tierpopulation auf die Veränderungen der Blattbiomasse. Aus den Ergebnissen beider Modellversionen wurden Potenzgesetze zwischen Herbivorenmasse und Nettoprimärproduktion (NPP) sowie zwischen der von Herbivoren konsumierten Biomasse und NPP abgeleitet. Diese Potenzgesetze zeigen, dass nur das „offline“ gekoppelte Modellsystem Tierpopulationen simuliert, die ähnlich zu Potenzgesetzen in empirischen Datensätzen sind. Die Ergebnisse dieses Experiments bekräftigen den Nutzen weiterer Entwicklung prozessbasierter Modellsysteme als gangbare Methode zur Bewertung multi-trophischer Wechselwirkungen zwischen Tierpopulationen und der Vegetation von Ökosystemen.

Im zweiten Experiment stelle ich die „online“ Version des Modellsystems vor, die bidirektionale Rückkopplungen zwischen grüner Pflanzenbiomasse, ihrem Konsum durch Herbivoren und der gesamten trophischen Pyramide ermöglicht. Verglichen mit der “offline” Version, ist in der „online“ Version eine Reduktion der NPP um -5%, des LAI um -9% und der Vegetationskohlenstoffmasse um -10% zu beobachten. Boreale Ökosysteme zeigen die stärksten Auswirkungen, mit Reduktionen der Kohlenstoffmasse um bis zu -42 % in manchen Regionen. Die Ergebnisse der LPJ-GUESS Simulationen werden mit Fernerkundungsdaten und Flux-Tower-Messungen

verglichen. Es zeigt sich, dass das “online” gekoppelte Modellsystem die Fähigkeit von LPJ-GUESS bewahrt und realistische Biomenverteilungen und Kohlenstoffpools simuliert. Außerdem vergleiche ich Potenzgesetze für alle drei Versionen des Madingley-Modells und komme zu dem Schluss, dass die „online“ Version beide anderen Versionen übertrifft, wenn es darum geht, Tierpopulationen zu simulieren, deren Populationsdynamik ähnlich zu Potenzgesetzen empirischer Daten ist.

Im dritten Experiment modifiziere ich die „online“ Version des Modellsystems um die Auswirkungen der Entnahme großer Tiere auf die simulierte Vegetation zu untersuchen. In zwei separaten Szenarien entfernte ich entweder große Herbivoren oder große Karnivoren aus der Simulation. Diese Entnahme findet statt, nachdem das Modellsystem einen Gleichgewichtszustand erreicht hat. Bei der Entnahme großer Herbivoren steigt die Blattkohlenstoffmasse in borealen Biomen (+10%), tropischen Regenwäldern (+5%) und feuchten Savannen (+6%). Im Gegensatz dazu führt die Entnahme großer Karnivoren zu einer Verringerung der Blattkohlenstoffmasse in borealen Biomen (-11%), tropischen Regenwäldern (-19%) und feuchten Savannen (-19%). Die Auswirkungen der Entnahme großer Tiere wird in borealen Ökosystemen von allgemeinen Ökosystemverschiebungen durch den Klimawandel überschattet. In Afrika ist die Auswirkung der Entfernung großer Karnivoren ähnlich groß, wie die Effekte der CO_2 -Düngung. Allerdings werden weitere, verheerende Effekte des Klimawandels nicht im Modell berücksichtig, weshalb die Entnahme von großen Karnivoren nicht als Kompensation für die Auswirkungen des Klimawandels verstanden werden kann. Simulationen zur Erholung der Tierpopulationen zeigen, dass Ökosysteme Jahrhunderte benötigen, um sich von der vollständigen Entnahme großer Tiere zu erholen, während diese Erholung deutlich schneller erfolgt, wenn ähnliche Tierspezies in nicht betroffenen Gebieten erhalten bleiben. Diese Ergebnisse unterstreichen die entscheidende Rolle des Schutzes der Artenvielfalt im Kontext des Klimawandels.

Abschließend zeigen die Ergebnisse dieser Dissertation die wichtige Rolle, die prozessbasierte Modelle zum besseren Verständnis der komplexen Wechselwirkungen zwischen Tieren und Vegetation beitragen können. Sie demonstrieren, wie die Kopplung dynamischer Vegetations- und Tierpopulationsmodelle unser Verständnis von komplexen Dynamiken in Ökosystemen verbessern kann und betont die Bedeutung des Schutzes der Biodiversität für die Resilienz von Ökosystemen.

Eidesstattliche Versicherung gemäß § 13 Absatz 2 Satz 1 Ziffer 4 der Promotionsordnung des Karlsruher Instituts für Technologie (KIT) für die KIT-Fakultät für Bauingenieur-, Geo- und Umweltwissenschaften.

1. Bei der eingereichten Dissertation zu dem Thema "Ecosystem Feedback from Animal-Vegetation Interactions: A Modeling Approach" handelt es sich um meine eigenständig erbrachte Leistung.
2. Ich habe nur die angegebenen Quellen und Hilfsmittel benutzt und mich keiner unzulässigen Hilfe Dritter bedient. Insbesondere habe ich wörtlich oder sinngemäß aus anderen Werken übernommene Inhalte als solche kenntlich gemacht.
3. Die Arbeit oder Teile davon habe ich bislang nicht an einer Hochschule des In- oder Auslands als Bestandteil einer Prüfungs- oder Qualifikationsleistung vorgelegt.
4. Die Richtigkeit der vorstehenden Erklärungen bestätige ich.
5. Die Bedeutung der eidesstattlichen Versicherung und die strafrechtlichen Folgen einer unrichtigen oder unvollständigen eidesstattlichen Versicherung sind mir bekannt.

Ich versichere an Eides statt, dass ich nach bestem Wissen die reine Wahrheit erklärt und nichts verschwiegen habe.

Ort und Datum Unterschrift

This thesis is submitted as a monography and consists of three main Chapters (Chapters 3 - 5). Chapter 3 has also been published in a peer-reviewed journal. Chapter 3 has been submitted and is currently under revision. Chapter 3 has also been prepared with the intention of being submitted. The Chapters are as follows:

3. How more sophisticated leaf biomass simulations can increase the realism of modelled animal populations.
This Chapter is based on the paper, Krause, Harfoot, Hoeks, Anthoni, Brown, Rounsevell, Arneth (2022). How more sophisticated leaf biomass simulations can increase the realism of modelled animal populations, Ecological Modelling, 471, https://doi.org/10.1016/j.ecolmodel.2022.11006. We published a Corrigendum to the last figure of the paper under
https://doi.org/10.1016/j.ecolmodel.2024.110706

4. Modelling Herbivory Impacts on Vegetation Structure and Productivity
This Chapter is based on the draft, Krause, Anthoni, Harfoot, Kupisch, Arneth (2024). Modelling Herbivory Impacts on Vegetation Structure and Productivity, submitted for open review in Geoscientific Model Development. The open review discussion is available under
https://egusphere.copernicus.org/preprints/2024/egusphere-2024-1646/#discussion

5. The Effect of Large Animal Removal and Conservation under the Future of Climate Change

Due to the papers being published (or in preparation for publication), and therefore involving the work of co-authors, I detail my contribution to the Chapters 3-5 as follows:

3. I led the experiment design, implemented the "offline" coupling interface for the Madingley model, performed the simulation, analysis and evaluation, and led the writing of the paper.

4. I led the experiment design, implemented the "online" coupling interface for both LPJ-GUESS and the Madingley model, performed the simulation, analysis and evaluation, and led the writing of the paper.

5. I led the experiment design, implemented the animal removal functionality in the Madingley model, performed the simulation and analysis, and wrote the Chapter.

Detailed information about every author's contributions can be found in the Credits and Authorship Statement at the end of the thesis.

Contents

List of Tables

List of Figures

List of Abbreviations

Abbreviation	Meaning
AFT	Animal Functional Type
AVHRR	Advanced Very-High-Resolution Radiometer
DIC	Carbon in dissolved form
CO_2	Carbon Dioxide
CRUJRA	Climatic Research Unit and Japanese Reanalysis Data
C3	3-Carbon Compound
C4	4-Carbon Compound
DGVM	Dynamic Global Vegetation Model
ESA	European Space Agency
FLUXNET	No specific acronym; name of a flux-tower measurement network
GPP	Gross Primary Production
GLEAM	Global Land Evaporation Amsterdam Model
iLAMB	International Land Model Benchmarking
[kg C]	Kilogram Carbon
LandSyMM	Land System Modular Model
LAI	Leaf Area Index
LPJ-GUESS	Lund-Potsdam-Jena General Ecosystem Simulator
MODIS	Moderate Resolution Imaging Spectroradiometer
NPP	Net Primary Production
PFT	Plant Functional Type
[Pg]	Petagram (1 Pg = 10^{15} g)
RCP	Representative Concentration Pathway
SIMFIRE-BLAZE	No specific acronym; name of the fire model used in our simulations
UNFCCC	United Nations Framework Convention for Climate Change

1 Introduction

Animals can play a key role in controlling the state and function of all terrestrial ecosystems (Schmitz et al. 2014). By consuming autotrophic biomass, herbivores enhance light transfer into plant canopies and affect net carbon assimilation. Cascading trophic effects triggered by top predators or the largest herbivores propagate through food webs, regulating levels of herbivory and affecting soil carbon and nitrogen cycling through excreta and dead bodies. Nevertheless, the impact of animals so far has been often disregarded, especially in ecosystem modelling. In this thesis, I investigate the role of animals in the carbon cycle and explore potential feedback between animal population dynamics and the underlying vegetation by coupling two different model approaches to present a model system that incorporates the advantages of both a dynamic global vegetation model and an animal population model of functional diversity.

The introduction of this thesis begins by providing an overview of the expanding research field exploring interactions between animals and their underlying vegetation. I will then highlight the emergence of model-based studies investigating these complex interconnections. Subsequently, I will review the development and recent advancements in Dynamic Global Vegetation Models (DGVMs) and the Madingley model, both of which are elemental to the work presented in this thesis. Finally, I will outline the structure of this thesis and the key research questions it aims to address.

1.1 The Developing Interest in Animal Impact on Ecosystem Functioning

Animal biodiversity has key roles for ecosystem state and functioning (Cardinale et al. 2011; Edenius et al. 2002; Ripple et al. 2015; Schmitz et al. 2014; Sobral et al. 2017; Wilmers and Schmitz 2016) but the degree to which animal-vegetation interactions affect carbon-, nutrient-, and water cycles globally, and how these interactions may change over time, remains unclear. The scientific community still debates whether an increase in the abundance of herbivores enhances ecosystem productivity by accelerating nutrient cycles (Enquist et al. 2020), reduces overall autotroph biomass through damaging plant individuals (Jia et al. 2018) or shifts the distribution of plant species (Schmitz et al. 2014). These diverse responses to a similar modification highlight the overall complexity of animal impacts on plants, making it urgently necessary to improve understanding of the interconnections between animals and the vegetation within ecosystems.

Adding to the urgency is the reported decline in global biodiversity in response to anthropogenic activities such as habitat modification, harvesting and, increasingly, anthropogenic climate change (Arneth et al. 2020; Cardinale et al. 2012; Pacifici et al. 2015). A better understanding of how changes and losses of plant and animal functional diversity will affect ecosystem functioning is also needed from the perspective of an ecosystem's role in both climate change mitigation and

climate change adaptation. However, the diverse mixture of species and the interconnectivity in food webs makes quantifying the links between ecosystem biogeochemical cycling and an ecosystem functional diversity a challenge (Schmitz et al. 2018).

Although animals constitute a much smaller proportion of global biomass compared to plants (Bar-On et al. 2018), the implicit assumption that they play a minor role in terrestrial carbon cycling is increasingly being challenged by a growing body of literature. Already some decades ago, studies such as Edenius et al. (2002) have explored the interactions between moose populations and natural boreal forests, revealing that moose browsing is focused on Scots pine and creates spatial heterogeneity by forming and exploiting gaps in vegetation. Similarly, Bonan (1992), Kielland and Bryant (1998), and Schmitz et al. (2003) have reported that moose can reduce the primary productivity of boreal forests, underscoring their influence on ecosystem structure and carbon cycling. Holdo et al. (2009) extrapolated impacts of strongly reduced wildebeest populations due to rinderpest, hypothesising that similar future die-offs could lead to significant increases in grass biomass, albeit altering fire regimes, and potentially shift the ecosystem toward becoming net carbon sources. Hooper et al. (2012) suggested that the presence or absence of herbivores and carnivores within ecosystems can drive changes on a scale comparable to major abiotic environmental pressures such as global warming, increased CO_2 levels, or nitrogen pollution. Schmitz et al. (2014) advocated for the inclusion of animal-mediated carbon dynamics in carbon cycling assessments. Their work outlined how animals influence terrestrial and marine ecosystems, a concept visually summarised in Figure **1.1** (adapted from Schmitz et al. (2014)).

The role of large animals is of particular concern. Ripple et al. (2015) reported that around 60% of large herbivore species face extinction; their loss would profoundly impact ecosystem functioning, with implications for carbon storage and nutrient cycles. Wilmers and Schmitz (2016) emphasised the top-down control of large predators in regulating carbon dynamics. Based on measurements, they estimated that wolf predation on moose in boreal forests of North America might enhance NPP and NEP by up to 30%, as reduced herbivory pressure allows deciduous tree growth. In contrast, wolves in Rocky Mountain grasslands reduce the positive effects of grazers on nutrient cycling, thereby lowering ecosystem NPP. Sobral et al. (2017) demonstrated that in the Amazon, large-bodied animals affect the carbon cycle both directly through metabolism and indirectly by altering vegetation composition via seed dispersal. A recent meta-analysis by Trepel et al. (2024) reviewed 5.990 observations from 297 studies to quantify the impacts of large wild herbivores. Their analysis revealed that herbivores generally reduce average plant biomass, primary productivity, and plant cover but increase spatial heterogeneity in plant biomass and cover.

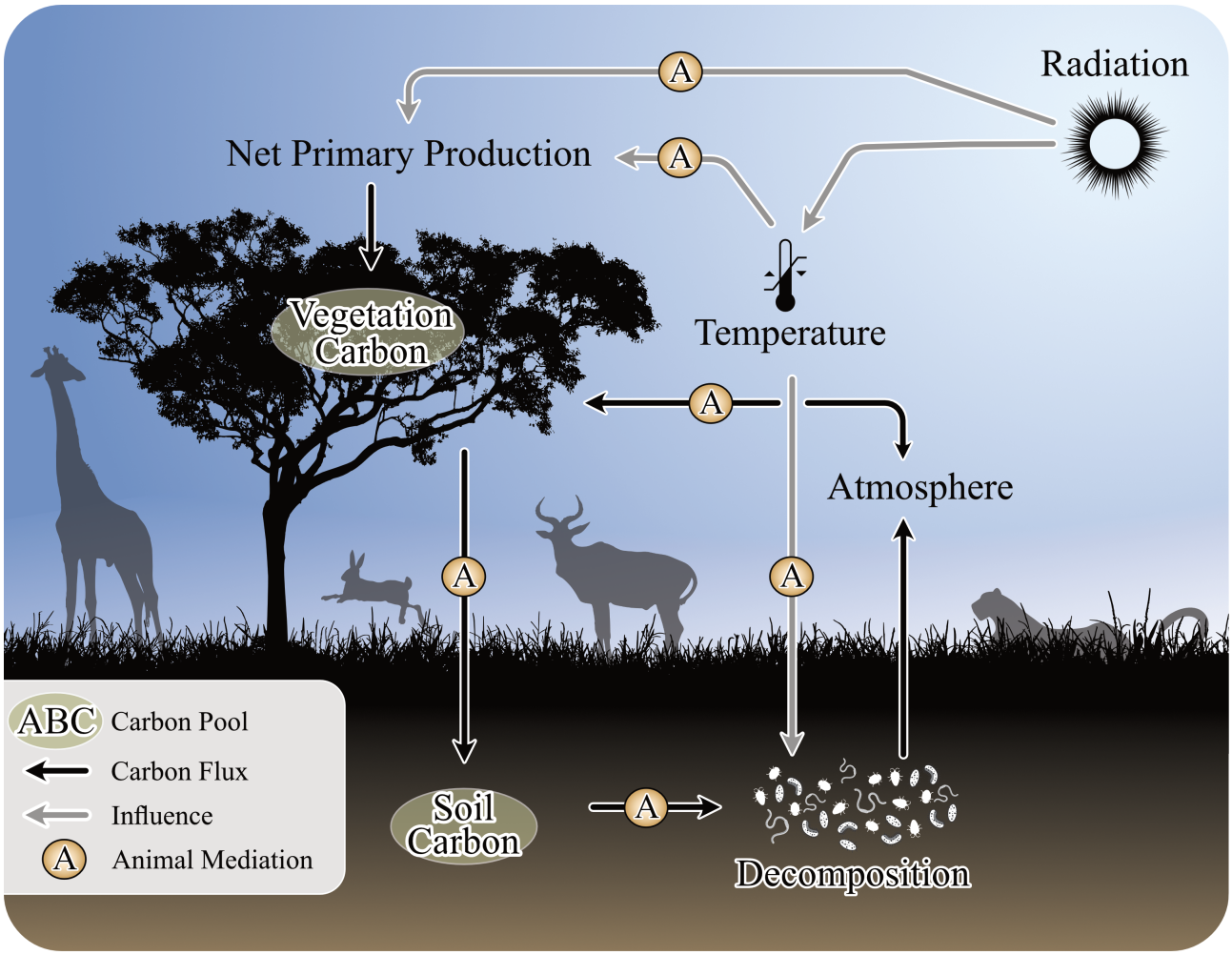

Figure 1.1 A schematic of how animals can influence carbon exchange and storage. The panel depicts exchanges between terrestrial and atmospheric reservoirs. Animals can mediate the uptake and release of CO_2 (and hence NPP) by influencing the amount of plant biomass present in an ecosystem. Animals can influence biophysical conditions such as albedo (with impacts also on local temperatures) through the destruction of vegetation. Animals also affect decomposition and wildfires, which impacts the release of CO_2. This also affects the amount (and elemental quality, not the subject of this thesis) of C entering the soil.
Caption and Figure adapted from Schmitz et al. (2014), usage licensed under license number 5951360240934 by Springer Nature.

1.2 Using Process-Based Modelling

Field experiments are providing valuable insights into how animals control ecosystems, revealing their significant influence on biogeochemical cycles, vegetation dynamics, and carbon storage. However, observation-based studies often struggle to capture long-term and large-scale effects. This, together with the complexity of trophic interactions, emphasises the need for a holistic approach. To bridge these limitations, modelling studies have proven to be powerful tools to

explore the broader effects of animals on ecosystem state and functioning, offering a means to integrate field-based findings into dynamic, system-wide frameworks.

Pachzelt et al. (2015) integrated a physiological grazer population model with a dynamic vegetation model known as the Lund-Potsdam-Jena General Ecosystem Simulator (LPJ-GUESS). They identified net primary productivity (NPP) and the duration of the dry season as critical factors influencing grazer population size in African savannahs. They found that the presence or absence of grazers substantially impacted the standing grass and tree vegetation biomass, as well as the area vulnerable to burning. Similarly, Riggs et al. (2015) coupled a landscape fire succession model with a multi-species herbivory module to examine ungulate herbivory's role in shaping fire regimes. Even though herbivory was found to play a role within single stands, across larger scales, herbivory did not significantly impact respiration, primary production, carbon mass or the area burned. Dangal et al. (2017) employed a grazer population dynamics model linked to a dynamic land ecosystem model, successfully simulating observed populations of livestock species. They demonstrated that herbivore presence reduced NPP across nine modelled regions while revealing a vulnerability of herbivores to climate extremes. Berzaghi et al. (2019) incorporated the impacts of forest elephant disturbances into an ecosystem demography model. They reported that the resulting reduction in tree stem density altered competition for light and water and enhanced above-ground biomass. Malhi et al. (2022) and Schmitz et al. (2018) underscored the potential of animals to mitigate climate change effects. Their reviews showed that animals can influence fire regimes, terrestrial albedo, and vegetation and soil carbon stocks, presenting a compelling case for integrating fauna into climate resilience strategies. Vegetation-animal interactions also challenge long-standing assumptions about historical landscapes. Pearce et al. (2023) recently challenged the assumption of pre-human Europe being dominated by dense, closed-canopy forests, proposing instead that light woodlands and open vegetation might have dominated more than 50% of the land surface.

These studies collectively emphasise the important and diverse roles of animals in controlling ecosystems and highlight the value of incorporating animal-ecosystem interactions into process-based models to better understand and predict ecological outcomes under changing environmental conditions. However, many of the previous studies focus on distinct animal species or species classes and neglect complexities such as the top-down control predators impose on herbivores and omnivores and, thus, food webs in ecosystems. However, Malhi et al. (2022) highlighted the importance of advancing global dynamic model approaches that incorporate the impacts of animals on ecosystems more broadly, including under, e.g. climate change. As an example, they pointed to the Madingley model presented by Harfoot et al. (2014), advocating for its further development. Their statement reads as follows:

Quote from Malhi et al. (2022)

"In addition to empirical studies focused on building the evidence base, a logical step forward would be the development of models incorporating both biodiversity and climate change measures, as well as realistic representations of large animal impacts. The first generation of Earth system models that incorporate animals have begun to appear, e.g. Harfoot et al. (2014), but these models do not yet effectively simulate the key processes and dynamic feedback effects we outline in this paper. These are needed to reliably explore the climate change mitigation and adaptation outcomes of restoration scenarios with and without large wild animals on the timescales of decades to centuries."

In this thesis, I contribute towards this goal by coupling the Madingley model with LPJ-GUESS.

1.3 Simulating the Land Biosphere with Dynamic Global Vegetation Models

Early DVGMs were formed by the idea of combining the most pronounced and impactful processes from plant geography, plant physiology, biogeochemistry, vegetation dynamics, and biophysics, which were until then pursued by disconnected research groups (Prentice et al. 2004). After having recognised the importance of terrestrial biospheric sinks for anthropogenic carbon emissions in the Kyoto Protocol to the United Nations Framework Convention for Climate Change (UNFCCC, 1997), DGVM development shifted towards incorporating anthropogenic influences in the form of agriculture, urbanisation and forest management (Prentice et al. 2004).

Incorporating agricultural influences of humans in DGVMs was initialised by the parameterisation of distinct crop functional types (Bondeau et al. 2007; Levis et al. 2012; Lindeskog et al. 2013), expanded with dedicated bioenergy crops (Beringer et al. 2011; Mayer 2017). Management methods, including tillage, irrigation, grassland management and flexible growing seasons (Bondeau et al. 2007; Jägermeyr et al. 2015; Levis et al. 2014; Lindeskog et al. 2013; Pugh et al. 2015; Rolinski et al. 2017; Stocker et al. 2014) quickly expanded the potency of DGVM simulations. Together with the incorporation of nitrogen (and in some cases, phosphorous) cycling, which enabled crop fertilisation and the capacity to represent land-cover transitions and forest management (Arneth et al. 2017; Bayer et al. 2017; Olin et al. 2015b; Olin et al. 2015a; Shevliakova et al. 2009; Stocker et al. 2014; Wilkenskjeld et al. 2014), DGVMs are well-equipped to answer complex and timely research questions, although important improvements are still lacking (e.g. Allen et al. (2015).

With the increasing complexity of land-use and land-cover change simulations in DGVMs, it becomes relevant to explore additional research fields that could significantly influence simulated vegetation dynamics. One such field is the study of animal impacts on ecosystem states and

functions, particularly since Schmitz et al. (2014) called to fully "animate" the carbon cycle. Given the common modular design approach of DGVMs (Prentice et al. 2004), coupling such a model with an equally sophisticated animal simulation model is a logical step forward. Such integration would provide a more holistic understanding of ecosystem dynamics, capturing the intricate feedback between vegetation and herbivory. As mentioned above, the Madingley model makes a fitting candidate for such a process-based multi-trophic herbivory module.

The Madingley model predicts fluxes of biomasses between above-ground autotrophs and heterotrophs by modelling the fundamental processes affecting the ecology of these organisms. Trophic structures in the modelled ecosystems emerge from the representation of individual and community-level biological processes, and interactions between organisms and their environment. Madingley has proven to reproduce patterns and functional processes in animal populations and has been used to model terrestrial and marine ecosystems (Enquist et al. 2020; Harfoot et al. 2014), to analyse complex food chains (Hoeks et al. 2020) and was employed as foundation for a high-resolution migration model (Hoeks et al. 2021). The original version of Madingley models vegetation, which drives herbivory, by employing an empirical carbon cycling model (M. J. Smith et al. 2013), in which primary production is determined by the Miami Model (Lieth 1975). However, the Miami Model does not capture important dynamics such as interannual variability and trends in vegetation composition and productivity introduced by weather, climate change, carbon-nitrogen interactions and changes in atmospheric CO_2, which modern dynamic vegetation models do. This limits Madingley's applicability to explore future global environmental change impacts on ecosystem functional diversity. This makes it a perfect match for a DGVM that would also benefit from a sophisticated herbivory approach, like LPJ-GUESS.

1.4 Thesis Structure and Objectives

The work presented here is the first step towards creating a fully coupled multi-trophic model of functional diversity, which combines the advantages of complex process-based vegetation and animal modelling, allowing comprehensive assessment of animal-vegetation feedback in ecosystems.

The main research questions of this thesis are:

- Do process-based simulations of natural vegetation improve the realism of animal populations modelled by the Madingley Model?
- How do multi-trophic food chains impact ecosystem productivity, and which feedback can be found between herbivores and the underlying vegetation layer?
- How does the absence of large mammalian herbivores or carnivores alter the vegetation cover, and how do different future climate scenarios affect these impacts?

To answer these questions, this thesis is divided into three main Chapters (Chapters 3-5). The methodology used in each Chapter is described in Chapter 2.

Chapter 3 is based on the paper "How more sophisticated leaf biomass simulations can increase the realism of modelled animal populations" by Krause et al. (2022) and Krause et al. (2024), published in Ecological Modelling. Chapter 4 builds upon a manuscript in review in Geoscientific Model Development, with the title "Modelling Herbivory Impacts on Vegetation Structure and Productivity". Chapter 5 will be submitted later this year.

Chapter 3 describes the implementation of leaf biomass data extracted from an independent LPJ-GUESS simulation. The research questions addressed are:

- Does forcing the Madingley model with prescribed leaf biomass from LPJ-GUESS have significant consequences for the modelled animal population composition and dynamics?
- How do overall animal biomass levels respond to more sophisticated leaf biomass levels?
- How do these effects differ between different biomes?
- Are the resulting changes reflecting an improvement in model realism?

Chapter 4 expands on the model development of Chapter 3 and describes how implementing bidirectional feedback impacts the formerly unaffected vegetation modelled in LPJ-GUESS. The key research questions addressed in the Chapter are:

- What are key implications for simulated vegetation in LPJ-GUESS under herbivory pressure from animals in Madingley?
- What are potential spatial response patterns, and how do they correspond with ecosystem productivity and dominant tree species?
- How do the results from the coupled version compare to those of an uncoupled version in the light of external datasets, and do they portray an improvement in terms of realism?

Chapter 5 is based on the same model version as Chapter 4, with minor additions. I added the option to remove animals from the coupled model system to investigate the following research questions:

- How does the removal of large (>21kg) herbivores or carnivores generally affect the animal population and vegetation composition in different biomes?
- Does the magnitude of climate change outweigh the responses to large mammal removal, and how do both effects combine?
- To what extent can the removal of large animals be reversed if all large animals from a functional group are completely wiped out?

A general conclusion and outlook with respect to the overall research questions is presented in Chapter 6, providing a broader perspective on the findings of this thesis.

As much of the work presented in the following includes some input from the co-authors of the published/prepared versions of the Chapters, I will generally use “we” instead of “I” throughout Chapters 2-5.

2 Methods

This Chapter introduces the two models central to this thesis and outlines the experiment in which they were utilised. We begin with a detailed description of the LPJ-GUESS model, focusing on its representation of vegetation dynamics and carbon allocation processes. This is followed by an in-depth explanation of the Madingley model, highlighting its ecological processes and the mechanisms it captures. Subsequently, the methods applied in each of the three experiments are described individually.

2.1 The LPJ-GUESS Dynamic Global Vegetation Model

LPJ-GUESS is a process-based DGVM that can be applied regionally and globally, typically at a half-degree resolution. It is forced with multiple years of climate data to ensure sufficient variability for computing the model stochastics, interannual disturbances and the model spin-up (B. Smith et al. 2014). This climate data includes daily or monthly-averaged time series for precipitation sum, minimum, maximum and mean air temperature at two meters height and shortwave radiation. In addition, its fire module BLAZE also requires relative humidity, wind speed and surface air pressure. Additional forcing is annual atmospheric CO_2 and nitrogen deposition.

LPJ-GUESS combines the advantages of a global macroscopic nutrient cycle and carbon assimilation model with the advantages of an individual-based growth model (B. Smith et al. 2014; Wårlind et al. 2014). To reduce computational demand, plant individuals are represented by age-cohorts, which share key ecological and physiological properties (Table **2.1**).

Table 2.1 The basic traits alongside a set of selected parameterisations of all simulated Plant Functional Types.

Trait	**Code**	**BNE**	**BINE**	**BNS**	**IBS**	**TeNE**	**TeBS**	**TeBE**	**TrBE**	**TrIBE**	**TrBR**	**C3G**	**C4G**	**LSE**	**LSS**
Climate Type	**B**oreal, **Te**mperate, **Tr**opical	B	B	B	B	Te	Te	Te	Tr	Tr	Tr				
Life Form	**T**ree, **L**ow-Shrub, **G**rass	T	T	T	T	T	T	T	T	T	T	G	G	L	L
Leaf Physiognomy	**Ne**edleleaved, **Br**oadleaved	Ne	Ne	Ne	Br	Ne	Br	Br	Br	Br	Br			Ne	Br
Phenology	**E**vergreen, **S**ummergree **R**aingreen	E	E	S	S	E	S	E	E	E	R				
Photosynthesis Pathway		C3	C3	C3	C3	C3	C3	C3	C3	C3	C3	C3	C4	C3	C3
Light Behavious	**S**hade-**I**ntolerant **S**hade-**T**olerant	ST	SI	ST	ST	ST	ST	ST	ST	SI	ST			SI	SI
Photosynthetic	Min to Max Temp. [°C]	-4 to 38				-2 to 38			2 to 55			-5 to 45	6 to 55	-4 to 38	
Activity Range	Optimum Temp. Low - High	10 to 25				15 to 25			25 to 30			10 to 30	20 to 45	10 to 25	
Survival Temp. [°C]		-31	-31	no lim	-30	-2	-14	-1	15.5			no lim	15.5	-32.5	-40
Leaf Turnover Rate [frac/yr]		0.33	0.33	1	1	0.33	1	0.33	0.5	0.5	1	1		0.33	1
Drought Resistance Coefficient (1 = maximum sensitivity)		0.0001												0.1	
Fire Resistance		0.3			0.1	0.3	0.1	0.3	0.1	0.1	0.3	0.5		0.12	
Respiration Coefficient		1				1			0.15			1	0.15	1	1
Minimum Forest Floor PAR for Grass Growth or Tree Establishment [10^6 J m^{-2} day^{-1}]		0.35	2.5	0.35	2.5	0.35			0.35	2.5	0.35	1		1	
Madingley Stock	**E**vergreen, **D**eciduous	E	E	D	D	E	D	E	E	E	D	D	D	E	D

Distinct properties like their life form (tree or herbaceous plant), bioclimatic preferences, photosynthesis pathway (C3 or C4), phenology (raingreen, summergreen or evergreen) or growth strategies (shade-tolerant or intolerant) separate the plants into plant functional types (PFTs). Plants compete for nitrogen, light, water and space. Annual processes, like biomass allocation, leaf, root and sapwood turnover, disturbances or mortality, are simulated at the beginning of the year. Short-term processes like soil hydrology, stomata regulation, photosynthesis, plant respiration, decomposition and phenology are simulated on a daily basis (B. Smith et al. 2014). The overall accuracy of these modelled processes and interactions has been evaluated extensively (e.g., Hickler et al. 2006; Lindeskog et al. 2013; B. Smith et al. 2014; Wramneby et al. 2008), and LPJ-GUESS has shown skills in capturing large-scale vegetation patterns and vegetation dynamics. We use LPJ-GUESS to simulate natural vegetation without utilising its capabilities to simulate crop growth, forest management or land-use change.

2.1.1 Vegetation Structure and Dynamics

PFT age-cohorts are each represented by one average individual plant. These individuals are described by their foliage, fine root, sapwood and heartwood biomass calculated in $\mathrm{kg\,C\,m^{-2}}$. In the following, individuals in LPJ-GUESS refer to the average individual of an age-cohort, assuming that all plant individuals within a cohort retain the same size, age and form as they grow (B. Smith et al. 2014).

PFTs are growing on patches of land, each representing the maximum area of influence of a large individual tree (typically 1000 $\mathrm{m^{-2}}$). The model simulates multiple independent patches simultaneously within each grid cell, with the typical number of patches ranging from 10 to 50 (Figure **2.1**). Model outputs are derived by averaging across all simulated patches. These patches are subject to stochastic effects, like patch-destroying events with an expected return interval of 100 years. Vegetation dynamics are based on approaches used in forest gap models (Bugmann 2001). Fire dynamics are also calculated on a patch level, with fires destroying only a fraction of a patch. For our simulations, the SIMFIRE-BLAZE fire model, which is integrated into LPJ-GUESS, was used (Rabin et al. 2017).

Under initial conditions - such as those following a patch-destroying disturbance event - vegetation succession commences with the establishment of different PFTs governed by their bioclimatic limits and light (nutrient and water) conditions at the forest floor (B. Smith et al. 2014).

Succession in LPJ-GUESS typically begins with herbaceous PFTs, followed by shade-intolerant trees characterised by relatively short average lifespans, poor tolerance to resource stress and rapid height growth. In contrast, shade-tolerant trees show slower height growth rates but a longer average life span and a higher tolerance to resource stress. Consequently, shade-tolerant

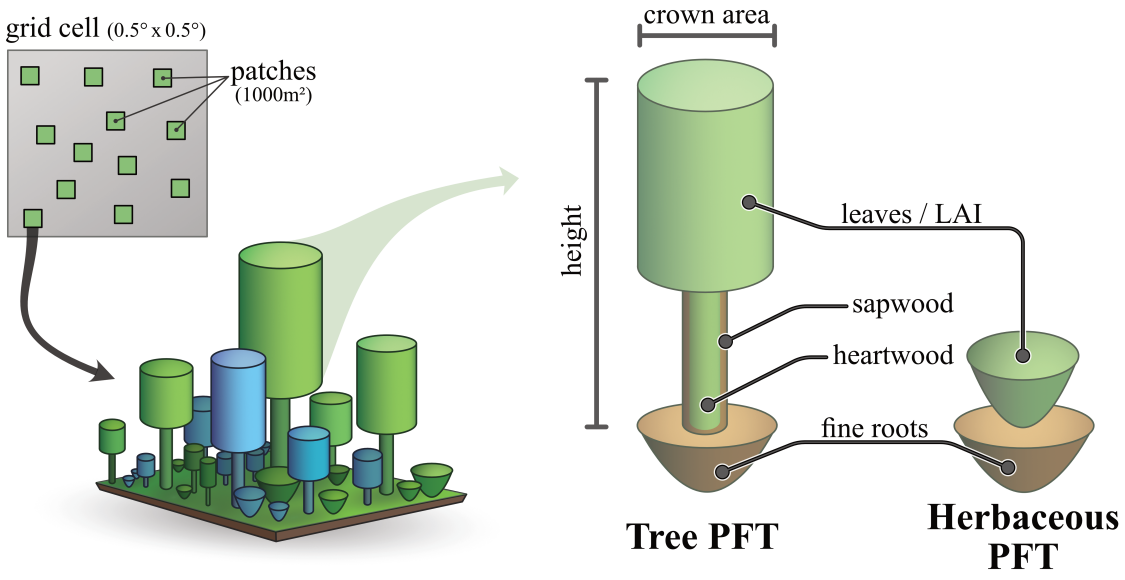

Figure 2.1 A visual representation of the simulated vegetation in LPJ-GUESS. The top left shows a grid cell that is represented by several independent patches. Each patch provides space and resources for plant individuals from all woody and herbaceous PFTs to grow, including some stochastic processes. Grid cell ecosystem properties and fluxes are derived as the average of the individual patches. The right side shows the basic structure of these woody and herbaceous plant functional types. Based on Figure B1 from B. Smith et al. (2014), licensed under CC BY 3.0. The original figure is available at https://doi.org/10.5194/bg-11-2027-2014. License details: http://creativecommons.org/licenses/by/3.0/.

trees typically succeed shade-intolerant trees during the progression of succession (B. Smith et al. 2014).

2.1.2 Growth and Carbon Allocation

The exchange of CO_2 between the vegetation and the atmosphere is modelled daily following a photosynthesis and stomatal conductance sub-model (Collatz et al. 1991). Plant growth is calculated on an individual level as the surplus of the photosynthesis rate after subtracting maintenance and growth respiration costs, yielding a daily increment of NPP. This daily increment is aggregated over the simulation year and allocated to various plant compartments at the end of the year after accounting for turnover rates of leaves and fine roots, as well as sapwood-to-heartwood transfers. Of the annual NPP, 10% is reserved for reproductive costs, while the remainder is distributed towards leaves, fine roots and, for woody PFTs, sapwood (Figure **2.1**) (B. Smith et al. 2014).

Sapwood plays a critical role in water transport to supply leaves. According to the pipe model theory, a cross-sectional sapwood area is assumed to be maintained proportionally to the total leaf area (McDowell et al. 2002; B. Smith et al. 2014). As trees grow, their stem diameter increases in relation to their height (Huang et al. 1992).

After accounting for the sapwood growth, the remaining NPP is divided between leaves and fine roots. The fractional allocation is determined by water (and nitrogen) stress experienced in the preceding growing season. Water stress, manifested as reduced photosynthesis due to stomatal closure under limited soil water availability, leads to an increased allocation to fine roots as an adaptive strategy. The greater the stress, the more biomass is directed towards fine roots to mitigate water deficits. At the beginning of each year, plants regrow leaf carbon mass based on their turnover rate, which is prescribed by their functional group as leaf longevity (Table **2.1**).

2.2 The Madingley Model

The Madingley Model is a mechanistic and process-based model designed to simulate the dynamics of animal communities globally. By representing the critical biological processes of metabolism, reproduction, herbivory, predation, mortality and migration, the model seeks to capture emergent patterns of biomass and abundance distributions across multiple trophic levels and functional groups (Figure **2.2**). The Madingley Model groups animals based on functional traits into Animal Functional Types (AFTs). This enables the simulation of complex ecological interactions within and between these groups. We modified the latest model version (as published e.g. in Hoeks et al. (2020)) to run on a half-degree grid and a monthly timestep

for any number of years. This thesis focuses on coupling Madingley with a terrestrial vegetation model, so marine realm formulations (Harfoot et al. 2014) are excluded from further discussion. The following descriptions are based on formulations presented in Harfoot et al. (2014), who provide the most comprehensive description of the model's methodology.

2.2.1 Autotrophs as Basis of the Trophic Pyramid

The Madingley model requires deciduous and evergreen leaf biomass stock to feed herbivores. These stocks, which represent a bottom-up control of the simulated trophic pyramid, are modelled in the original Madingley version (Harfoot et al. 2014) with the carbon cycle model of M. J. Smith et al. (2013), based on the Miami model by Lieth (1975). The Miami model predicts the total annual net primary production (NPP) on a grid cell level based on the yearly mean temperature T and total precipitation sum p. The annual NPP is converted to wet matter via an estimate of 9.813 wet matter g/gC (Kattge et al. 2011). The resulting annual NPP is then split into monthly fractions. Leaf mortality and carbon partitioning to leaves are parametrised through near-surface temperature. The resulting monthly wet matter leaf biomass increment is divided into an evergreen and a deciduous stock, with the evergreen-to-deciduous ratio being based on the fraction of the year prone to frost. This simplified approach to determining the basis of the modelled trophic pyramid is replaced by the coupling we created in our work. Chapters 2.3 and 2.4 describe how we implemented this coupling.

2.2.2 Cohort Dynamics and Ecological Processes

Figure **2.2** shows a schematic of the model processes based on Harfoot et al. (2014). In the following, we will provide an overview of each individual process that is resolved by the Madingley Model.

Categorical Cohort Traits

The Madingley model represents various animal species by grouping similar individuals into cohorts. Within each cohort, all individuals are assumed to possess identical properties and are represented by a single representative individual alongside a specified abundance. Key ecological traits defining these functional groups include (i) feeding strategy, categorising cohorts as herbivores, carnivores, or omnivores; (ii) reproductive strategy, classified as iteroparous or semelparous; and (iii) thermoregulation strategy, identified as either endothermic or ectothermic. The combination of these traits yields nine distinct functional groups, with the exception of endothermic semelparous cohorts, which do not exist. Additionally, the functional group of a cohort determines its assimilation efficiency, minimum juvenile body size, and maximum adult body size. A summary of functional group traits is provided in Table **2.2**.

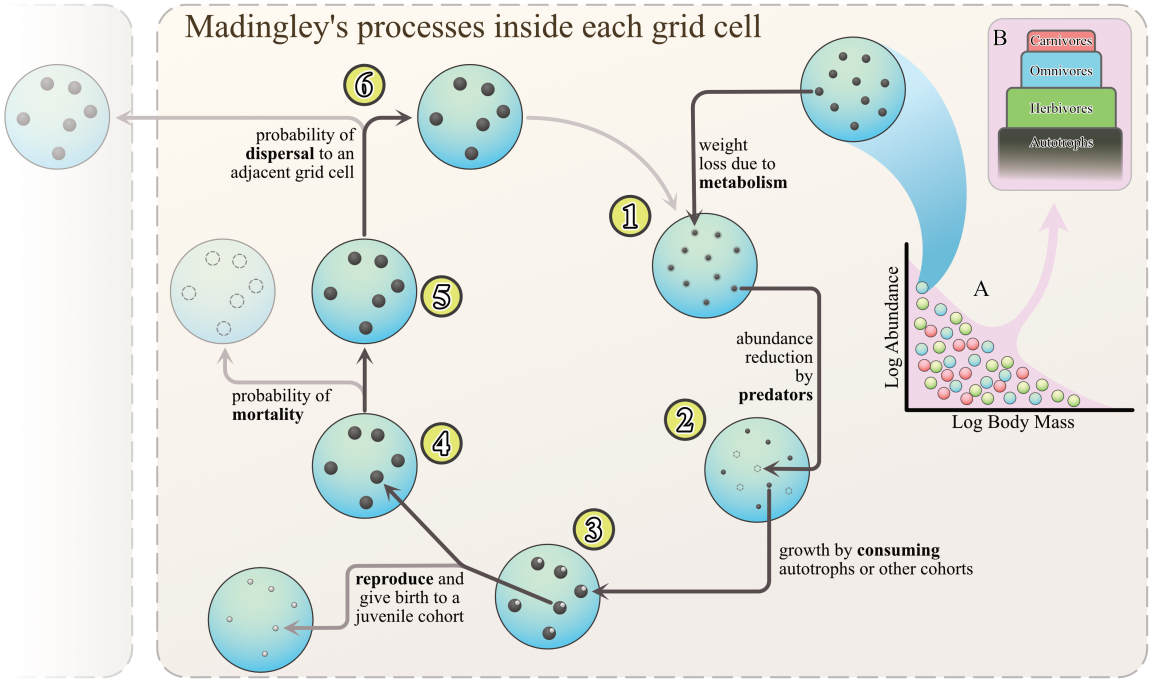

Figure 2.2 An illustrative example of the Madingley Model. The structure and functioning of the modelled ecosystem emerges from the processes that are represented in the model: Metabolism (1), Predation (2), Feeding (3), Reproduction (4), Mortality (5) and Dispersal (6). Each ecological process is applied to cohorts (represented as blue circles) rather than individuals and affects their ecological properties (principally body mass and abundance, represented as the diameter and number of black dots in each circle, respectively). The resulting diverse animal population (A) aggregates to overall ecosystem-wide biomass levels (B). Based on Figure 1 from Harfoot et al. (2014), licensed under CC BY 4.0. The original figure is available at https://doi.org/10.1371/journal.pbio.1001841.
License details: http://creativecommons.org/licenses/by/4.0/.

Table 2.2 A detailed overview of all terrestrial Animal Functional Types in Madingley and their corresponding key ecological traits. Based on Table 2 from Harfoot et al. (2014), licensed under CC BY 4.0. The original figure is available at https://doi.org/10.1371/journal.pbio.1001841.
License details: http://creativecommons.org/licenses/by/4.0/.

Feeding Mode	Reproductive Strategy	Thermoregulation Strategy	Min. Body Mass	Max. Body Mass	Herbivory Assimilation Efficiency	Carnivory Assimilation Efficiency
Herbivore	Iteroparity	Endotherm	1.5 g	5.000 kg	0.8	0
Omnivore	Iteroparity	Endotherm	3 g	200 kg	0.65	0.65
Carnivore	Iteroparity	Endotherm	3 g	400 kg	0	0.8
Herbivore	Iteroparity	Ectotherm	0.0004 g	10 g	0.8	0
Omnivore	Iteroparity	Ectotherm	0.0004 g	20 g	0.65	0.65
Carnivore	Iteroparity	Ectotherm	0.0008 g	20 g	0	0.8
Herbivore	Semelparity	Ectotherm	0.0004 g	1 kg	0.8	0
Omnivore	Semelparity	Ectotherm	0.0004 g	2 kg	0.65	0.65
Carnivore	Semelparity	Ectotherm	0.0008 g	2 kg	0	0.8

Continuous Cohort Traits

Within each model grid cell, multiple competing cohorts of the same functional group may coexist. To distinguish cohorts within the same functional groups, all cohorts also inherit two constant traits and several dynamic traits. The constant traits remain unchanged throughout the simulation and define the cohort's body mass at birth (referred to as juvenile body mass) and its body mass at reproductive maturity (referred to as adult body mass). The dynamic traits contain the abundance of individuals, their age, the current wet matter body mass of each individual in the cohort (referred to as individual body mass), and a stored reproductive mass for each individual (referred to as reproductive body mass). Together, these traits define the life trajectory of each individual living in that cohort: After being born with its juvenile body mass, an individual's body mass increases until it reaches its adult body mass. Beyond this point, further growth contributes towards the reproductive body mass pool instead of increasing the individual body mass. Eventually, the cohort gives birth to a new cohort, which inherits its parent's functional group and an adult body mass trait drawn randomly around its parent's adult body mass (Harfoot et al. 2014).

Cohort growth is realised by updating the individual's body mass each timestep according to the effects of ecological processes and interactions with stocks and other cohorts within the same grid cell. The growth is accounted for as follows:

$$M_{i,t+\Delta t} = M_{i,t} + \Delta M_i^{ass} - \Delta M_i^{met} - \Delta M_i^{repr}, \tag{2.1}$$

with ΔM_i^{ass} as the total biomass sum assimilated through herbivory and carnivory, ΔM_i^{met} as the total biomass lost through metabolism and ΔM_i^{repr} as biomass lost by allocation to reproduction.

Herbivorous Assimilation

Herbivorous cohorts feed upon leaf biomass and assimilate biomass through Madingley's herbivory process. Every cohort has a daily time fraction where it is considered active, whereas it is considered dormant for the rest of the day. A cohort's active time is based on its thermoregulation strategy and the climatic conditions of its surroundings. The active time and the cohort's current body mass determine the autotroph biomass that a herbivorous cohort experiences during each time step. While searching for food, these herbivores experience 10% of the leaf biomass of every autotroph stock within the grid cell. This fixed fraction accounts for (i) cohorts not being able to search the whole grid cell within one month, (ii) cohorts not being able to access all parts of a plant due to vertical structure and plant defence mechanisms, and (iii) cohorts not targeting every part of a plant, since most animals are preferential feeders.

The formulation for herbivory relies on several assumptions: (i) autotroph biomass and herbivore cohorts are well mixed throughout each grid cell; (ii) each herbivore cohort encounters

a 10% fraction of the total grid cell's autotroph biomass; and (iii) all herbivores experience the vegetation independently without any priorities or advantages (Harfoot et al. 2014).

Carnivorous Assimilation

Carnivorous cohorts prey upon other cohorts within the same grid cell through Madingley's predation process. Similar to herbivores, carnivorous cohorts are considered active during a fraction of the day. The probability of them capturing prey is modelled based on the framework described by, where the likelihood of a predation event is governed by a normal distribution centred around an optimal proportion of the prey's body mass relative to the predator's body mass. Consequently, the probability of successful predation is determined by the cumulative density of organisms whose body mass falls within the predator-specific prey bin.

The formulation for carnivory relies on several assumptions: (i) predator and prey cohorts are well mixed throughout each grid cell; (ii) predator cohorts can experience all other cohorts sharing the same grid cell; and (iii) while searching for one prey, predators can simultaneously encounter another prey - given they are not limited by search time (Harfoot et al. 2014).

Omnivorous Assimilation

Omnivorous cohorts assimilate biomass through both Madingley's herbivory and carnivory processes. Like all other cohorts, omnivorous cohorts are considered active during a fraction of the day. During this active period, they are assumed to divide their time between searching for leaf biomass to consume and hunting other animals. Consequently, omnivores spend less time hunting prey than carnivores and less time-consuming leaf biomass than herbivores. As an additional disadvantage, omnivores have a lower efficiency at converting and assimilating biomass to body mass through herbivory or carnivory.

The formulations for omnivory rely on the combined assumptions for its herbivory and carnivory processes (Harfoot et al. 2014).

Metabolic Cost

All cohorts simulated by the model must fulfil their metabolic cost to survive and increase in body mass. The metabolic cost for each timestep takes into account the proportion of the current timestep for which environmental conditions are suitable for the cohort. Each cohort has a metabolic cost associated with its field metabolic rate (during its active time) and its basal metabolic rate (while it is dormant). The total metabolic cost for a given timestep is calculated as the sum of these two components. This approach accounts for animals reducing their metabolic rate when facing harsh environmental conditions.

The formulations for metabolism are based on the assumption that endothermic organisms maintain a body temperature of 310 K at all times (Harfoot et al. 2014).

Reproduction

If a cohort's body mass surpasses its adult body mass, further growth ceases, and assimilated

biomass is contributed to the reproductive biomass pool. The increment of this pool per timestep is calculated as a surplus of assimilated biomass after accounting for metabolic costs. This ensures that the individual body mass no longer increases once the cohort reaches maturity. It also provides a buffer to sustain the cohort during timesteps where its metabolic cost cannot be fully met.

When a cohort's ratio of the total body mass (including its reproductive biomass) to adult body mass exceeds a critical threshold, a reproduction event occurs. During this event, the cohort uses its entire reproductive biomass pool to produce offspring. For semelparous cohorts, which reproduce only once during their lifespan, a portion of the parent's own body mass is additionally sacrificed to increase the reproductive biomass pool (Harfoot et al. 2014). The newly born juvenile cohort inherits its parent's functional group, as well as an adult body mass stochastically drawn around the parent's adult body mass.

Non-Predation Mortality

Madingley models three types of non-predation mortality: (i) background mortality, (ii) starvation mortality and (iii) senescence mortality. Background mortality accounts for cohorts' deaths resulting from accidents and disease. Starvation mortality occurs when an organism's metabolic demand exceeds its ability to sustain itself. It is dependent on the cohort's current body mass in relationship to its maximum body mass ever reached. Senescence mortality reflects age-related increases in mortality risk by assuming an exponentially increasing risk after reaching maturity.

While cohorts are subjected to the risk of background and starvation mortality during their entire lifespan, the senescence mortality risk is only applied to adult cohorts (Harfoot et al. 2014).

Dispersal

In terrestrial model domains, Madingley incorporates two types of types of dispersal mechanisms to facilitate cohort migration between adjacent grid cells. The first dispersal type is diffusive natal dispersal. It represents a random movement of juvenile cohorts. Each cohort inherits a characteristic dispersal distance, which scales with body mass (Harfoot et al. 2014). During each time step, the dispersal distance is accumulated to determine the total distance moved since the last dispersal event. Once this cumulative distance exceeds the size of the grid cell, the cohort is moved in a random direction to an adjacent grid cell. The movement direction is modified by overlaying a background probability to capture large-scale movement patterns while maintaining the cohort's freedom of movement. This type of dispersal is applied to immature organisms under the implicit assumption that they are searching for new territory.

The second dispersal type is behaviour-mediated dispersal of adult cohorts as a response to two environmental challenges: (i) mate-driven dispersal when reproduction is limited by low encounter rates and (ii) resource-driven dispersal when faced with unsuitable feeding conditions.

The first condition is triggered when a cohort's individual density falls below a body mass-related threshold, while the second condition is triggered when the amount of body mass lost during a time step exceeds the starvation threshold.

To manage total cohort numbers within a grid cell, it is assumed that all individuals in a cohort disperse collectively. When the number of cohorts within one grid cell exceeds a specific limit, the model searches for similar cohorts of the same functional group and merges them (Harfoot et al. 2014).

2.2.3 The Natural Advantage of Large Animals

Larger animals tend to have a natural advantage over smaller animals in Madingley for various reasons. The missing vertical vegetation structure in the Madingley model is the most relevant factor causing the issue. In reality, smaller animals climb trees and branches to reach for leaves further away from the stem. The reach of an animal is primarily determined by its weight - the lighter an animal is, the further it can traverse a branch without breaking it. Large mammals are typically ground dwellers - with some famous evolutionary exceptions, like giraffes and sauropods. However, every animal cohort in Madingley has access to 10% of the grid cell's leaf biomass. This fixed factor (see Chapter **2.2.2**, "Herbivorous Assimilation") incidentally introduces a uniform vertical reach for all animals. If this assumption were valid, it would imply that large animals could also access higher levels of the vegetation canopy, which, in fact, are primarily accessible to smaller animals. Losing this exclusive access for smaller animals introduces a disadvantage.

2.3 Development of the LPJ-GUESS/Madingley Model System

This section describes how the coupling between LPJ-GUESS and Madingley was implemented. Throughout this thesis, we refer to three distinct stages of the coupled model system: the "default," "offline," and "online" coupled versions. Figure **2.3** provides a comprehensive overview of the model versions associated with this terminology.

2.3.1 Offline Coupling: Aggregating Leaf Biomass Information in LPJ-GUESS to be passed on to Madingley

At present, LPJ-GUESS cannot model daily or monthly leaf growth and regrowth, which is needed by Madingley. Growth seasonality dynamics are incorporated through a phenology factor f_{ph}. This factor equals 1 for evergreens but varies between 0 and 1 for deciduous plants, reflecting environmental and climatic conditions throughout the year. Following the approach of Kautz

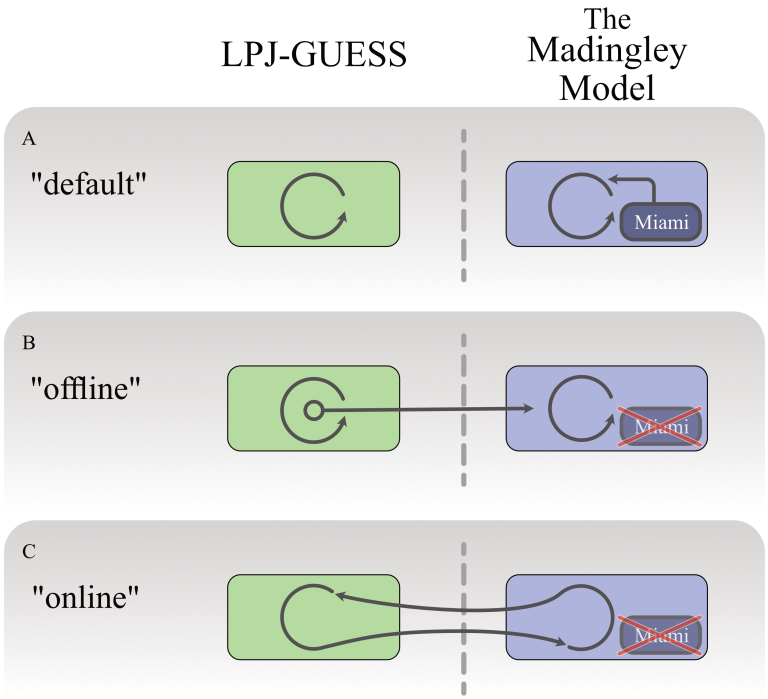

Figure 2.3 Illustration of the nomenclature used to describe the different model versions. (A) The "default" versions of LPJ-GUESS and Madingley operate independently without influencing each other. (B) The "offline" coupled version of Madingley, where leaf biomass input data is derived from the "default" LPJ-GUESS model. Note that there is no "offline" version of LPJ-GUESS. (C) The "online" coupled versions of both models, where simulations are interdependent, with significant mutual influence on their outcomes.

et al. (2018), an individual's daily leaf biomass $m_{C,leaf}(day)$ is estimated by multiplying its annual potential leaf biomass with the phenology factor:

$$m_{C,leaf}(day) = m_{C,annual} \cdot f_{ph}(day) \tag{2.2}$$

We estimate monthly leaf carbon values by averaging daily leaf carbon masses. These estimates are either accounted towards an evergreen or a deciduous leaf carbon mass pool per grid cell. Table **2.1** provides detailed information on which PFTs are accounted towards which stock. The aggregate of the individual leaf carbon masses in LPJ-GUESS into an evergreen leaf carbon mass per grid cell (respectively for deciduous and grasses) is therefore calculated as the following:

$$m_e = \sum m_i \mid \forall i \text{ in evergreen individuals} \tag{2.3}$$

$$m_d = \sum m_i \cdot f_{ph} \mid \forall i \text{ in deciduous individuals} \tag{2.4}$$

The aggregated sum is then passed to Madingley using a file-transfer method, replacing Madingley's original parameterised autotroph stocks (see Chapter **2.2.1**, Miami model). Using file

transfer ensures that updates of both models can easily be integrated and gives flexibility such that LPJ-GUESS can be coupled to different versions of Madingley, while Madingley, in turn, could be coupled to a number of different vegetation models. Coupling via file exchange also allows for the tracking of the exchanged data without the need for any further processing memory. Figure **2.4** shows a simplified technical blueprint to illustrate how we realised the "offline" coupling of the two models.

Madingley model development for Chapter **3** is based on the C++ Madingley model version presented by Hoeks et al. (2020), which originally cycles a single year of environmental input data throughout the simulation. Climate affects not only vegetation but also animals' metabolism due to its ecto- and endothermic thermoregulation method. To ensure that the animals in Madingley are exposed to the same climate used for the vegetation prediction in LPJ-GUESS, we expanded the length of Madingley's environmental forcing from the single-year cycle to a 30-year time series.

For the experiments presented in Chapter **4** and **5**, the Madingley model was driven using a monthly average of long-term climate data. To accommodate this data within the model, we divided the climate files into chunks that the Madingley model recombines during the simulation. This workaround is necessary since the Madingley model inherits a technical limitation, restricting it from processing climate data longer than a maximum of 60 years.

2.3.2 Online Coupling: Feedback Link Between Madingley and LPJ-GUESS

In the second step, we implemented bidirectional coupling between LPJ-GUESS and Madingley. Typically, LPJ-GUESS processes the entire time series for a single grid cell before proceeding to the next. This approach is computationally efficient, as it minimises memory usage by focusing on one grid cell at a time. However, this structure poses a challenge for extracting information across the entire model domain on a monthly basis. While this limitation was not an issue when Madingley was forced with prescribed vegetation biomass, addressing it became essential for the "online" coupled version of the model system. To overcome this limitation, we switched the spatial and temporal simulation loops for the "online" coupled version based on the LPJ-GUESS version r10042. This modification allowed the system to handle the entire LPJ-GUESS model domain for a given timestep before progressing to the next timestep. This adjustment was critical for enabling interaction and synchronisation between LPJ-GUESS and Madingley for a coupled configuration.

We expanded the file-exchange approach described in Chapter **2.3.1**. An illustration of the coupled model system's timestep loop, as well as the different spin-up phases, can be found in Figure **2.5**.

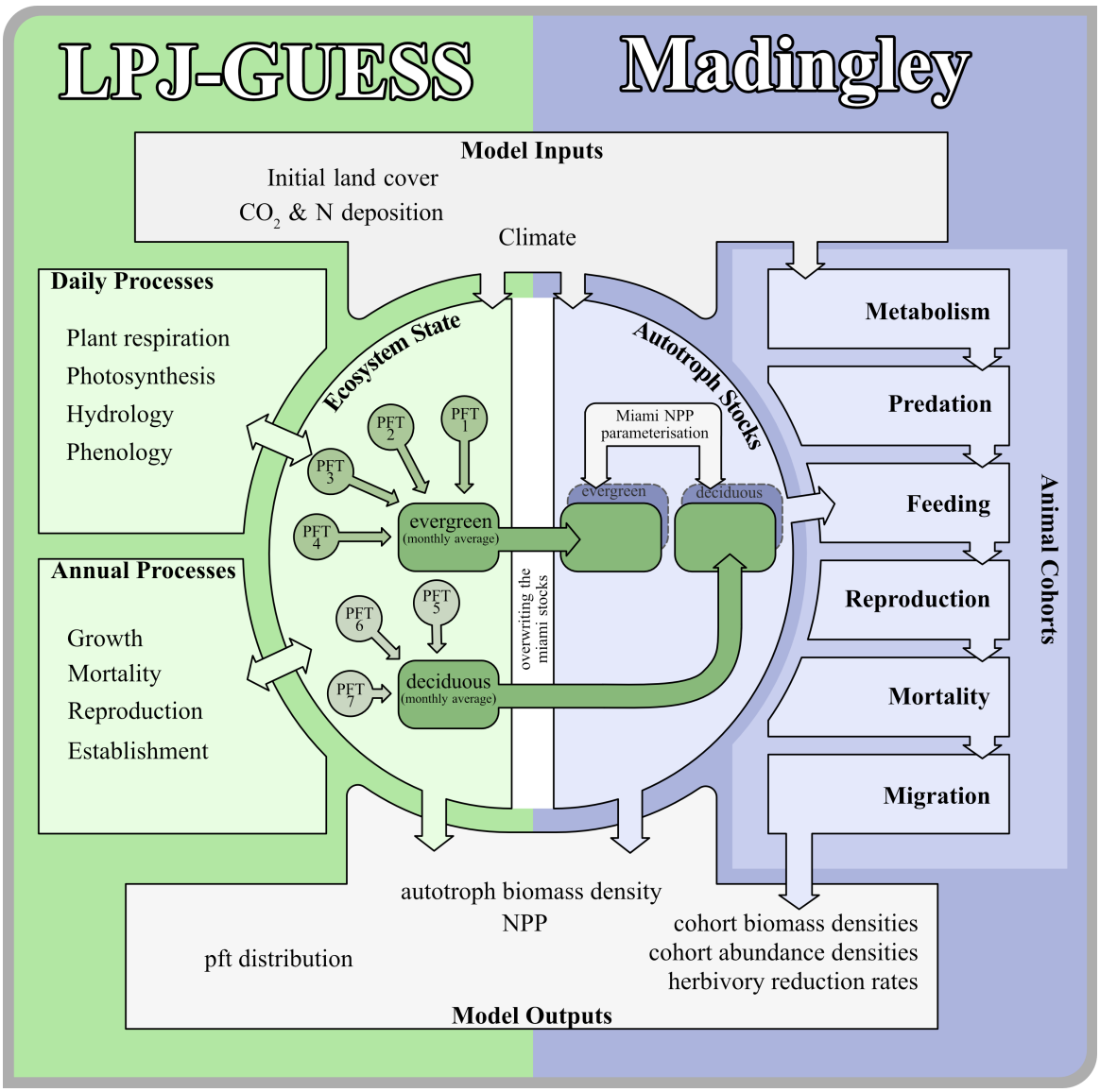

Figure 2.4 Technical illustration of the offline coupling. The left side shows a simplification of the LPJ-GUESS processes and the aggregation of PFTs into evergreen and deciduous grid cell sums. The right side shows a simplification of the Madingley process routine and the overwriting of the Miami NPP vegetation model.

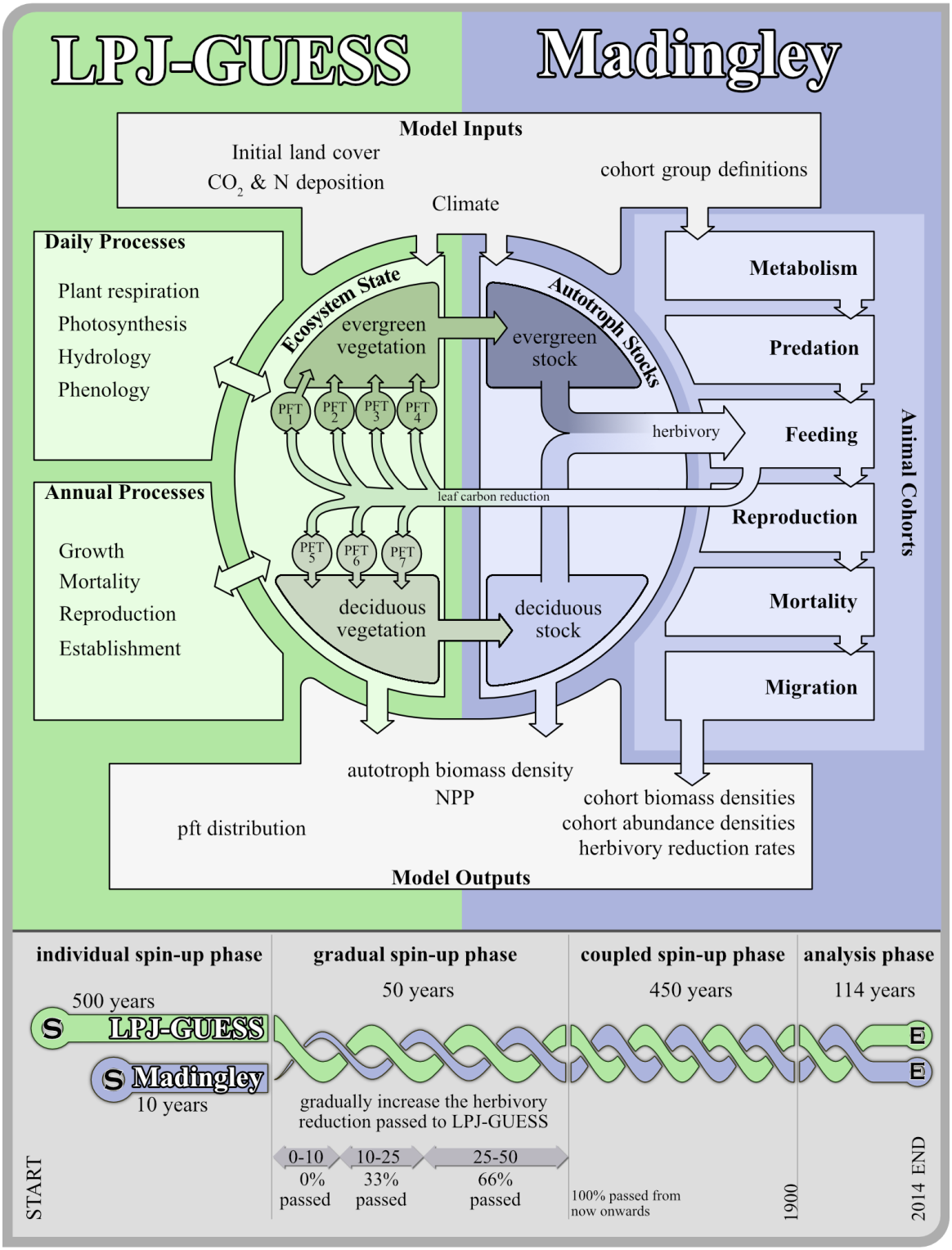

Figure 2.5 Technical illustration of the fully coupled model system. The upper panel shows how both models exchange data and how the time loop is synchronised. The lower panel shows how the coupling is initialised and run.

Spin-Up

Both models need to run through an offline and a coupled spin-up phase. Madingley starts with autotrophs, herbivores, omnivores, and carnivores, which have the exact same biomass density. During the first years of spin-up, the interactions between the groups and the simulated physiological processes in Madingley rapidly shift the cohort and autotroph biomass density towards more realistic magnitudes. Typically, this phase is completed after five simulation years, using a monthly timestep. LPJ-GUESS establishes its vegetation starting from bare soil, including an upscaled 10.000-year loop, which accounts for the fact that soil carbon in some regions needs much longer to reach an equilibrium. After the simplified soil spin-up, vegetation establishment and growth result in increasing litter input, which gradually decomposes and builds up carbon and nitrogen pools in the soil (B. Smith et al. 2014). Thus, a longer offline spin-up phase is needed. Five hundred years has proven to be a sufficient timespan for LPJ-GUESS.

The Coupling Loop

After both models complete the offline spin-up phase, the data exchange between the models is enabled, and a coupled online spin-up phase of 500 years is initiated to equilibrate LPJ-GUESS vegetation with Madingley herbivory and Madingley's trophic pyramid with LPJ-GUESS vegetation biomass. During the first 50 years of this joint spin-up phase, the percentage of leaf biomass reduction in LPJ-GUESS in response to Madingley herbivory is gradually increased so as to not kill off plant age-cohorts with initially unrealistically high herbivory rates. After 50 years, 100% of the herbivory reduction is passed to LPJ-GUESS, and the models are considered fully coupled at this timestep.

We assume that the animals will digest all the biomass they have eaten within one timestep. Since Madingley does not yet have a coupled carbon-nitrogen cycle, we here simplify the impacts of herbivory on the nitrogen cycle by adding all eaten leaf nitrogen mass directly towards the litter pool in LPJ-GUESS at the time of the defoliation event, given that animal faeces and carcasses are enriched in nitrogen. Analogously, all leaf carbon mass removed gets accounted towards the carbon litter pool. This latter assumption results in an overestimation of carbon remaining in the system since animals respire carbon during growth. We, therefore, concentrate our initial analysis, presented in Chapter **4** and **5**, on the impacts of herbivory on photosynthesis and growth and will quantify the impacts of plant-animal interactions on total ecosystem carbon and nitrogen cycling in a future analysis with an updated version of Madingley which incorporates the animal stoichiometry and explicit C and N cycling (in prep.).

As described in Chapter **2.3.1** , we aggregate a grid cell's leaf carbon mass of the PFT age-cohorts on a monthly basis. Based on their corresponding PFT, the leaf carbon mass of an age-cohort is either accounted towards an evergreen leaf carbon stock or a deciduous leaf carbon stock. Herbaceous PFTs are again accounted towards the deciduous leaf carbon stock. The monthly leaf carbon sums are then passed to Madingley through the file exchange interface.

In the case of evergreen carbon mass, only one-third of the carbon mass is passed on. This is due to different assumptions in the two models regarding vegetation regrowth: The original Madingley model is calibrated with a monthly regrowing vegetation stock for both deciduous and evergreen plants. In contrast, LPJ-GUESS regrows leaves of its age-cohorts at the start of each year. Giving herbivores access to the complete evergreen vegetation stock would cause unrealistically high damage to the evergreen PFTs at the start of each year – also due to the seasonality of deciduous trees, which leads to only evergreens being available as a nutrition source. Furthermore, evergreen PFTs in LPJ-GUESS have a 3-year leaf lifespan. This results in damage to evergreen leaves persisting three times longer than damage to deciduous PFTs. Our feedback allocation method partially compensates for the higher risk of growing long-lived leaves and the lack of defence mechanisms, which long-lived tree species typically invest more into (Coley and Aide 1991). The formulations for aggregating the individual leaf carbon masses in "online" LPJ-GUESS into an evergreen leaf carbon mass per grid cell m_e (respectively m_d for deciduous and grasses) can be summarised as the following:

$$m_e = \sum m_i \cdot \frac{1}{3} \mid \forall i \text{ in evergreen individuals} \tag{2.5}$$

$$m_d = \sum m_i \cdot f_{ph} \mid \forall i \text{ in deciduous individuals} \tag{2.6}$$

After receiving the vegetation data from LPJ-GUESS, Madingley runs its ecological processes, which result in a reduction of the leaf biomass by the herbivores and omnivores. This reduction of the stock biomass r_e and r_d is recorded and returned to LPJ-GUESS. Subsequently, LPJ-GUESS determines the corresponding amount of biomass to be removed based on the input from Madingley. The defoliation method used to calculate this biomass removal follows a similar approach to the methods described by Kautz et al. (2018). The reduction is calculated as separate evergreen and deciduous herbivory reduction fractions f_e and f_d :

$$f_e = \frac{r_e}{3 \cdot m_e}, f_d = \frac{r_d}{m_d} \tag{2.7}$$

which is then weighted with f_{ph} and applied to every age-cohort's maximum annual leaf carbon mass. This assures that a PFT age-cohort that did not contribute to the original leaf stock that was supplied to herbivores and omnivores is not damaged by herbivory. This would be an issue, e.g. early in the season when f_{ph} is still zero for some age-cohorts. The new individual's leaf carbon mass is then calculated for evergreen or deciduous PFTs like the following:

$$m_{i,new} = m_i - m_i \cdot f_e \mid \forall i \text{ in evergreen individuals} \tag{2.8}$$

$$m_{i,new} = m_i - m_i \cdot f_d \cdot f_{ph} \mid \forall i \text{ in deciduous individuals} \tag{2.9}$$

2.3.3 Animal Removal Methodology

We modified the "online" version of the model system to determine how large animal removal affects the state of animal populations and vegetation dynamics alike - both with and without the influence of climate change. To conduct these experiments, we implemented an animal removal method.

In the Madingley model, each individual has an adult body mass, which serves as a threshold that distinguishes juveniles from adult cohorts. Once a cohort is classified as an adult, it begins acquiring biomass for reproduction. Upon the birth of a juvenile cohort, that new cohort's adult body mass trait is determined based on their parent's adult body mass trait. When removing cohorts from the simulation, we use the adult body mass trait as the selection criterion. This ensures that no juveniles are kept in the simulation that would eventually grow to an adult body mass that surpass the defined removal threshold. In Madingley, cohorts' adult body mass can also naturally evolve toward heavier weights through iterative increases across generations. To prevent the reappearance of large animals throughout the simulation, it is essential to remove cohorts consecutively. Therefore, we removed herbivores or carnivores annually. Specifically, if a cohort's adult body mass is found to exceed a set removal threshold at the end of a year, its abundance is set to 0, effectively removing it from the simulation. The biomass of such removed cohorts is discarded and has no influence on the ongoing simulation. Instabilities in the bidirectional coupled model system are avoided by implementing the removal gradually, starting with adults heavier than 41 kg. Every following year, the removal threshold is lowered by 1 kg until the lower limit of 21 kg is reached. This lower limit is based on Hoeks et al. (2020) who defined this threshold based on Malhi et al. (2016).

2.3.4 Updated Carnviory Process

Hoeks et al. (2020), on which we base the experiment presented in Chapter **5**, changed the preferred predator-prey body mass ratio from 0.1 to 1.0 for predators with an adult body mass heavier than 21 kg, based on the allometric relationships described in Carbone et al. (1999). However, this results in a step change such that carnivores weighing 20.9 kg prey on animals weighing 2.09 kg, while carnivores weighing 21 kg prefer prey that also weighs 21 kg. This creates a predation gap between 2.09 and 21kg, which is especially evident in the reproduction success rates of cohorts within this size category (Figure **2.6**). The juveniles of large carnivores play a unique role here; they have exclusive access to prey within the size range of the predation gap. However, their number is small compared to the overall carnivore population, so they cannot effectively fill the gap. To address this issue, we implemented a linear increase of carnivores' optimal prey body mass ratio from 0.1 at 2.9 kg to 1.0 at 21 kg (Figure **2.6**). This was especially

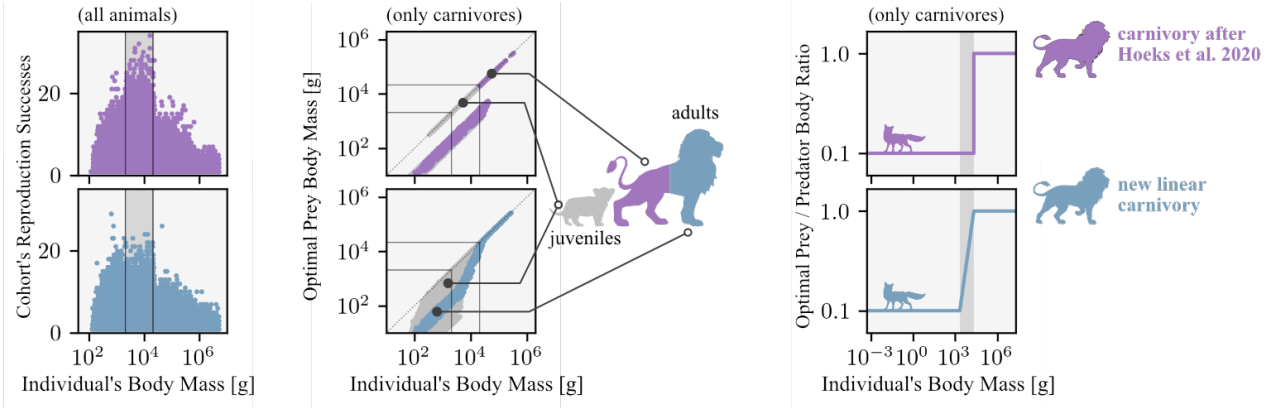

Figure 2.6 The implementation of a linear increase in optimal predator-prey body mass ratio. Throughout the figure, violet indicates data from a simulation with carnivory following (Hoeks et al. 2020), while blue indicates data from a simulation with the updated carnivory process. The greyed-out areas in the left and right panels indicate the size range of the identified predation gap. The left panel shows the number of reproductive successes of all endothermic cohorts alive at the end of the simulation. The middle panel shows carnivores' optimal prey body mass plotted against their body mass (juveniles are plotted in grey). The right panel shows the sharp transition of the carnivore's optimal predator-prey ratio from 0.1 to 1.0 after (Hoeks et al. 2020) (top) and the new linear transition (bottom).

needed since removing large carnivores (>21 kg), as done in Chapter **5**, otherwise lifts the carnivory pressure of all cohorts larger than 2kg.

2.4 Experiment Setups for Chapter 3: How more sophisticated leaf biomass simulations can increase the realism of modelled animal populations

In Chapter **3**, we compare Madingley's "default" version to the "offline" coupled version to determine the impact of the LPJ-GUESS vegetation on simulated animal populations.

LPJ-GUESS requires multiple years of climate data to ensure sufficient variability for computing the model's stochastics, interannual disturbances and the model spin-up. For the simulations for Chapter 3, we chose to recycle the CRUJRA v2.1 climatology (Harris 2020) based on the years 1950 to 1979. This approach allowed us to compare vegetation simulated with LPJ-GUESS and Miami, since Miami was parameterised based on empirical data available during the 1960s. We recycled atmospheric CO_2 concentrations ranging from 311 to 335 ppm during the LPJ-GUESS simulations. Since the CRUJRA dataset has a 6-hour resolution, we used a daily postprocessing method. LPJ-GUESS uses 30 patches per grid cell to ensure stochastic stability. Since we focus

on carbon cycling, we kept the nitrogen deposition constant at 2 $\mathrm{kg\,N\,ha^{-1}\,yr^{-1}}$ (B. Smith et al. 2014).

For the Madingley model, we used the same CRUJRA v2.1 climate data, but due to Madingley's monthly timestep, the data required additional processing into monthly intervals. All Madingley simulations include the same definitions of animal functional groups described in Chapter **2.2.1** (see Table **2.2**). Each grid cell was initialised with 100 cohorts of each functional group with initial body masses that were drawn randomly from the cohort's juvenile and adult body mass. During a simulation, the total number of cohorts that are allowed to coexist in one grid cell is limited to 1000.

Both model setups represent a solid and stable version of the model. The additional time needed to precompile the LPJ-GUESS is small in comparison to the average Madingley runtime, which is quite time-consuming and memory-consuming. This makes global simulations, especially when producing highly detailed cohort output, highly challenging. Thus, we decided to carry out smaller-scale simulations at different locations instead of a continental or global run. Other recent studies with Madingley followed a similar approach (Newbold et al. 2020) or used a coarser grid for their simulations (Hoeks et al. 2020). We performed simulations for four locations representing three different types of forest ecosystems and one savanna ecosystem (Table **2.3** and Figure **2.7**). Each location was resolved by a grid of three-by-three cells, spanning a 1.5° latitude by 1.5° longitude model domain with a resolution of 0.5° in each direction. Both Madingley and LPJ-GUESS run on a half-degree resolution, so we did not need to up- or downscale any of the exchanged data.

We compared Madingley output simulated with its standard Miami-based vegetation with simulations in which, at the beginning of each timestep, the leaf biomass was replaced by the modelled leaf biomass from LPJ-GUESS, summed up for deciduous and evergreen PFTs. In Chapter 3.1, we present four experiments to test how LPJ-GUESS vs. Miami vegetation affects model stability, community structures and individual traits. For all four experiments, we compare the "default" and "offline" versions of Madingley and highlight the effects which the LPJ-GUESS vegetation implies on the Madingley model.

In the first experiment, we ran an ensemble of ten long-term simulations to investigate the development of leaf biomass and heterotrophic functional-group dynamics. Each simulation covered 1000 years of simulation time. The objective here was to test whether Madingley's model dynamics reach equilibrium conditions with LPJ-GUESS, as well as with Miamis vegetation input. We assume the model system has reached its dynamic equilibrium stage when aggregated biomass densities of both autotroph stocks and heterotroph cohorts stop trending up- or downwards over a period of 50 years.

For the second experiment, we compared the evergreen-to-deciduous ratio of the simulated vegetation from both LPJ-GUESS and the Miami Model. The objective here was to visualise

Table 2.3 A detailed list of all simulation domains for Chapters 3, 4 and 5, as well as the cropped analysis locations for Chapter 4. All model domains have a resolution of 0.5°. The total model domain for Chapter 4 was created by merging the European and African model domains at 30° N, where both domains were overlapping for 0.5°.

Domain Tag	Longitudes	Latitudes	Biome Type	Additional Information
		Chapter 3		
FIN	24°E - 25°E	61°N - 62°N	Boreal Coniferous Forest	
GER	11°E - 12°E	50°N - 51°N	Temperate Mixed Forest	
UGA	31°E - 32°E	0°N - 1°N	Tropical Rainforest	
SAF	28°E - 29°E	26°S - 25°S	Subtropical Savanna	
		Chapter 4		
Europe	20°W - 50°E	30°N - 70°N		Northern part of the model domain
Africa	20°W - 50°E	30°S - 30.5°N		Southern part of the model domain
E1	11°E - 13°E	51°N - 53°N	Temperate Mixed Forest	Cropped from "Europe" domain
E2	37°E - 39°E	56°N - 58°N	Boreal Coniferous Forest	-""-
E3	22°E - 24°E	60°N - 62°N	Boreal Mixed Forest	-""-
E4	24°E - 26°E	67°N - 69°N	Boreal Grassland	-""-
E5	6°W - 4°W	38°N - 40°N	Mediterranean Forest	-""-
A1	14°E - 16°E	2°S - 0°N	Tropical Rainforest	Cropped from "Africa" domain
A2	22°E - 24°E	12°S - 10°S	Subtropical Forest	-""-
A3	34°E - 36°E	1°N - 3°N	Moist Savanna	-""-
A4	7°W - 5°W	14°N - 16°N	Subtropical Savanna	-""-
A5	25°E - 27°E	28°S - 26°S	Subtropical Grassland	-""-
		Chapter 5		
EU1	6°E - 37°E	48°N - 53°N	Temperate Mixed Forest	
EU2	34°E - 40°E	52°N - 64°N	Boreal Coniferous Forest	
AF1	15°E - 28°E	5°S - 5°N	Tropical Rainforest	
AF2	28°E - 40°E	5°S - 5°N	Moist Savanna	

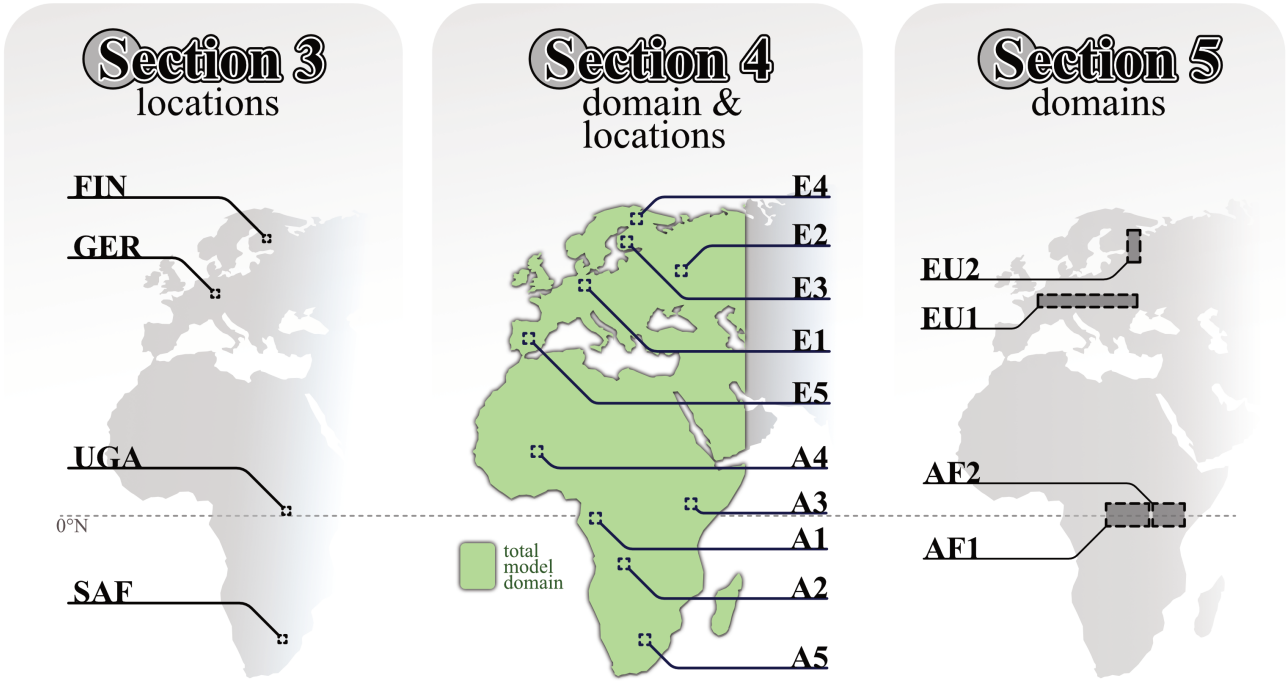

Figure 2.7 Model domains for Chapters 3, 4 and 5. The analysis locations of Chapter 4 are cropped from the total model domain coloured in green. Detailed domain information can also be found in Table **2.3**.

the differences between the two vegetation models. Since these differences are the key drivers for all coupling-related changes, understanding them is essential for the interpretation of all other experiments.

In our third experiment, we focussed on how the coupling alters the basic shape of the trophic pyramid and how it affects the animal population on a community level as a whole. To do so, we investigated the biomass pools of the trophic pyramid and the fluxes between those pools. We used an ensemble of ten simulations to capture stochastic variation within the pools. Shifts in leaf biomass density are likely to affect the size distribution of animals as a result of the bottom-up regulation of autotrophs in the trophic pyramid, so we also compared the emergent size distribution of cohorts driven by the two vegetation models.

After investigating the effects of our coupling on the community level, our fourth experiment focussed on the effects on an individual level by taking a closer look at power-law relationships between individual body mass and growth rate per timestep, days needed to reach maturity, lifespan and lifetime reproduction successes.

The simulations for the third and fourth experiments differ in terms of simulation length due to the determined time needed for the model to reach its dynamic equilibrium (as found in experiment 1, see results in Chapter 3.1.1). The tropical rainforest simulations covered 600 years

of simulation time, while all other setups covered 250 years of simulation time. We extracted detailed information on cohort characteristics during the last year of every simulation.

To set the effects of our coupling into context, we compared NPP simulated with LPJ-GUESS and the Miami model at the four experiment locations. Since the NPP parameterised by the Miami Model forms the foundation of the "default" simulations, we wanted to test if the NPP simulated by LPJ- GUESS is more realistic. For the comparison, we used NPP data derived from the MODIS 17ASHGFv061 dataset (Running and Zhao 2021) as the average NPP of the area corresponding to the model domains. The MODIS data layers are derived from the radiation use efficiency concept (Hatfield and Dold 2019) and, therefore, are also a model product.

Cebrian (2004) derived power-law relationships between NPP, herbivore biomass and consumption by primary consumers, which have been derived from a large body of literature. It is worth noting thatCebrian (2004) combined herbivore consumption and detritus consumption in one pool as primary consumption, while Madingley only includes herbivores. We derived power-laws for the same functional relationships from the last ten years of each simulation.

2.5 Experiment Setups for Chapter 4: Modelling Herbivory Impacts on Vegetation Structure and Productivity

In Chapter 4, we compare the "default" versions of LPJ-GUESS and Madingley to the fully coupled "online" version of the model system.

We simulate the impacts of animal herbivory for the European-African continents, i.e., a model domain that captures a large variety of biomes and climates (20°W – 50°E, 35°S – 75°N). We use historical climate data input from the CRUJRA v2.1 dataset (Harris 2020), and historic CO_2 concentrations from 1901 onwards (Meinshausen et al. 2017). During the spin-up phases, both models repeatedly cycle the climate data from 1901 to 1930, applying a standard CO_2 concentration of 296 ppm. LPJ-GUESS uses 30 patches per grid cell to ensure stochastic stability. Throughout the whole simulation, the nitrogen deposition was kept constant at 2 $\mathrm{kg\,N\,ha^{-1}\,yr^{-1}}$ (B. Smith et al. 2014).

The Madingley model was forced with a monthly average of the climate forcing used by LPJ-GUESS. Its model domain was seeded with 50 cohorts of each functional group, while the maximum number of cohorts allowed per grid cell was set to 500. This reduction compared to the maximum number of cohorts in Chapter **3** accounts for the increase in computational demand given the larger model domain. All simulations include the same definitions of animal functional groups described in Chapter **2.2.2** (see Table **2.2**).

The simulation was run over the period from 1901 to 2014. Changes in continental-scale NPP, vegetation composition, carbon, and autotrophic respiration are presented as percentage increases

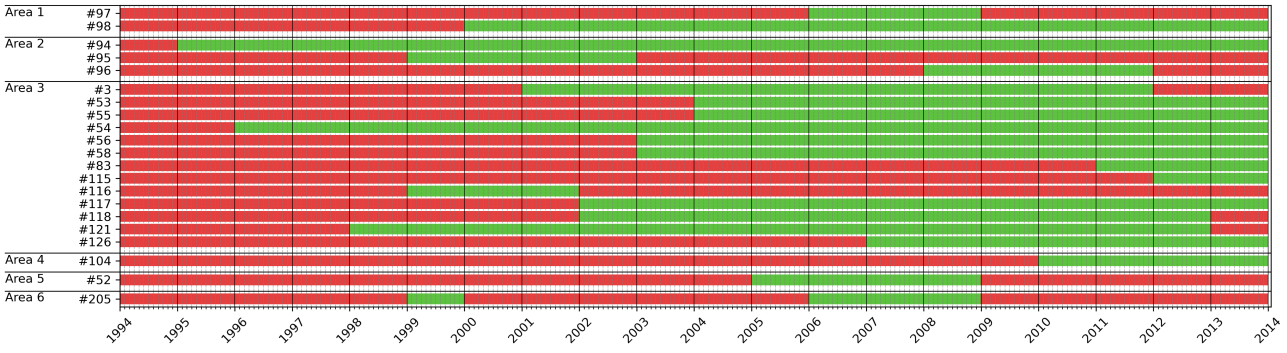

Figure 2.8 Timeline of data availability from FLUXNET stations, which were selected for 4.5. Green indicates available data while red indicates no available data.

or decreases in the "online" coupled simulation when compared to the "default" LPJ-GUESS simulation. Second, we analyse the distributions of the dominant PFTs, as determined by the maximal leaf area index (LAI), throughout the model domain. We chose LAI as metric for PFT dominance since the PFT with the highest LAI is also the PFT with the largest surface available for photosynthesis within a grid cell. To examine the impacts of vegetation-animal interactions in more detail, we further identified ten locations, shown in Table **2.3** and Figure **2.7**. We arranged them from highest productivity (A1 & E1) to lowest productivity (A5 & E5).

We compared the model output of the stand-alone LPJ-GUESS model and the coupled model system against monthly gross primary production (GPP) flux estimates from the FLUXNET network and against satellite data, which are available via the International Land Modelling Benchmark Project (Collier et al. 2018) and are designed to be used for benchmarking ecosystem models. Since the FLUXNET measurement sites encompass the local site climate, but the simulation uses gridded 0.5° climate input, we preferentially aimed for regions within the simulation grid, which include multiple FLUXNET stations and averaged the measured fluxes within the area. This was only possible in Europe because there are only five FLUXNET stations in Africa. Thus, we compared FLUXNET station GPP data to the GPP of the corresponding simulated grid cell for three African stations. The FLUXNET dataset covers a time span from 1994 to 2014, but the individual stations only provide data for a fraction of the time span (see Figure **2.8**). We averaged the available monthly GPP fluxes of the FLUXNET stations and compared them to the simulated annual GPP flux between 1994 and 2014.

We compared the simulation output also to GPP data from the FLUXCOM dataset (Tramontana et al. 2016), LAI from an AVHRR dataset (Fang et al. 2019), evapotranspiration from the GLEAM v3.3a dataset (Miralles et al. 2011) and woody vegetation carbon from a combination of multiple datasets (Pugh et al. 2023; Saatchi et al. 2011; Thurner et al. 2014). The underlying data is of a much higher resolution than the 0.5° resolution of LPJ-GUESS, but the International Land Model Benchmarking project (iLAMB) maintains a collection of downscaled 0.5° datasets. Notably, the AVHRR data is also a model product and includes human land use. To estimate

the magnitude of human influence, the iLAMB-datasets contain additional uncertainty estimates based on human impact factors like forest management and land use.

Forest vegetation (above- and belowground) carbon estimates in Thurner et al. (2014) cover northern boreal and temperate forests, including the European region of our model domain, for which Thurner et al. (2014) indicate low-medium uncertainty in their estimates. The data was compared to the simulated vegetation carbon from 1980 to 2000. For tropical forest and savanna total biomass estimates, we used the African fraction of the Saatchi et al. (2011) dataset (35°N - 35°S, 20°W - 50°E), which covers the time period 1995-2005. They estimate a relatively high (30-45%) uncertainty, especially in the tropical rainforest. The impact of human timber extraction is included in the estimates derived from remote-sensing information, while we simulate potential natural vegetation, including simplified estimates of natural disturbances and wildfires. Pugh et al. (2023) provided data that combined remotely sensed disturbance intervals with LPJ-GUESS-derived vegetation carbon for the years 2001-2014. To minimise human influence in our comparison, we chose the low disturbance natural vegetation scenario from Pugh et al. (2023), in which they focussed on protected areas to keep human influence in their estimates to a minimum.

We compared our simulations against a dataset that intends to quantify aboveground biomass on non-cropland and non-pasture vegetation (thus also excluding grassland), i.e., present land use distributions. It is based on the ESA 100m aboveground biomass dataset (Santoro and Cartus 2021) and the ESA 300m land cover dataset (ESA Land Cover Climate Change Initiative: Global Land Cover Maps, Version 2.0.7, 2024). For the comparison to our simulations, we assumed that aboveground biomass represents 70% of the total vegetation biomass since LPJ-GUESS does not explicitly model aboveground biomass.

Finally, we compared power-law relationships between NPP, herbivore biomass and consumption by primary consumers from each model version against similar relationships derived by Cebrian (2004).

In the "online" version of the LPJ-GUESS-Madingley model system, no other effects like the acceleration of the nutrient cycles (Enquist et al. 2020) or shifts in plant species distribution through selective feeding (Schmitz et al. 2014; Staver and Bond 2014) are parameterised. Thus, the general trends we see in vegetation and process responses are caused by the monthly removal of green biomass.

2.6 Experiment Setups for Chapter 5: The Effect of Large Animal Removal and Conservation under the Future of Climate Change

In Chapter **5**, we use the "online" coupled model system and apply animal removal and climate change scenarios to the simulated ecosystems.

We used simulated atmospheric climate data from ISIMIP3b MPI-ESM1-2-HR (Gutjahr et al. 2019; Lange and Büchner 2021). In Chapter **5**, this data is used in two ways. For the recycled climate approach, we repeatedly use detrended historical data from 1850 to 1880 with a constant CO_2 concentration of 283 ppm for the entire simulation. In the climate scenario approach, the same detrended data and CO_2 concentration are used only during the 500-year coupled spin-up phase. Afterwards, historical climate and CO_2 data are applied from 1850 to 2014, followed by RCP 2.6 or RCP 7.0 climate projection data until 2100. To integrate these RCP climate projections within the coupled LPJ-GUESS version, we had to modify the standard netCDF input module. LPJ-GUESS uses 30 patches per grid cell to ensure stochastic stability. Throughout the whole simulation, the nitrogen deposition was kept constant at 2 $\mathrm{kg\,N\,ha^{-1}\,yr^{-1}}$ (B. Smith et al. 2014).

The Madingley model was forced with a monthly average of the climate forcing used by LPJ-GUESS. Its model domain was seeded with 50 cohorts of each functional group, while the maximum number of cohorts allowed per grid cell was set to 500.

We carried out three experiments to determine the effect of large animal removal under different boundary conditions. We conducted simulations for all three experiments across four model domains: two in Europe and two in Africa, allowing us to compare different biomes. For Europe, we chose one region where temperate mixed forest is prominent and a second region representative of boreal ecosystems covered by evergreen forests. For Africa, we chose two model domains that are adjacent to one another. The first represents the tropical rainforest biome in the center-equatorial region, and the second represents the moist savanna biome at the east of the equatorial region of Africa (see Table **2.3** and Figure **2.7**).

For the first experiment, we used the recycled climate approach. This experiment investigates the isolated effect of animal removal without climate- or CO_2-change-driven responses. After the coupled spin-up phase, either large carnivores or large herbivores are removed for the remainder of the simulations. In the following 200 years, the model system reactions to the removal are analysed. Addition simulations, where no animals are removed, serve as control runs. We highlight shifts in AFT biomass densities (timeline and size spectrum) and PFT carbon mass distributions (timeline) compared to these control runs to visualise the effect of the animal removal.

For the second experiment, we forced the model system with RCP 2.6 and 7.0 climate projections. Carnivores or herbivores are removed consecutively from 1950 onwards. We compare

the PFT leaf carbon mass distribution response to the animal removal under both RCP scenarios to investigate how animal removal enhances or diminishes the effects of climate change. Also, we highlight responses within the animal populations under the pressure of climate change and animal removal.

For our third experiment, we investigate the ecosystem's potential to recover naturally from the removal of large mammals. In this experiment, we again follow the recycled climate approach. While Madingley simulates large herbivores and carnivores in both the tropical rainforest (AF1) and savannas (AF2), savannas are known to inhabit substantially larger herbivores and carnivores than rainforests in reality. Therefore, we chose the AF2 model domains for this experiment. In contrast to experiment one, the continuous animal removal is ended after being applied for 100 years. In the following 200 years, the model can recover from the former animal removal. We present the recovery as herbivore and carnivore biomass density timelines, as well as population dynamics and PFT distribution timelines. Finally, we compared the recovery potential between a simulation where large herbivores were removed from the entire model domain and a simulation where they were preserved in parts of the domain.

Within these three experiments, different simulation modifiers were presented: (i) biome type, (ii) the climate forcing type, and (iii) the applied animal removal method. The modifiers resulted in 36 simulations for experiments one and two, plus three simulations to model the recovery potentials for experiment three.

3 How more sophisticated leaf biomass simulations can increase the realism of modelled animal populations

3.1 Results

In this Chapter, we present the results of our first experiment, focusing on the comparison between the "offline" coupling to Madingley and the "default" version of the model. Long-term simulations are analysed to determine the time required for the model system to reach an equilibrium state. This is followed by an examination of shorter simulations to highlight changes in canopy composition and their impacts on animal communities and individuals. Finally, we evaluate both versions of Madingley against power-law relationships derived from empirical data.

Compared to the submitted paper Krause et al. (2022) we changed the descriptions of the model versions (originally labeled "M-M" and "M-LPJG") to be consistent with the nomenclature defined in Figure **2.3**.

3.1.1 Long-term Analysis

The left side of Figure **3.1** shows biomasses simulated by Madingley's "default" version, while the right side shows those simulated by the "offline" version. The "default" simulations reach a state of dynamic equilibrium after about 100 years. The time needed for a simulation to reach equilibrium in the "offline" coupled version ranges from about 100 years (locations FIN, GER, SAF, see Table **2.3** and Figure **2.7**) to about 500 years (UGA).

Simulated leaf biomass density in the two vegetation models differs markedly. As modelled by LPJ-GUESS, the amount of evergreen leaf biomass in the "offline" simulations barely changes over the course of a year, in contrast to the seasonal oscillation seen in deciduous leaf biomass. This is clearly visible, for example, in the boreal and temperate climate regions with a high seasonality – represented by FIN and GER. In contrast, Madingley's "default" version simulates strongly fluctuating evergreens and deciduous stocks while also having a higher amplitude and lower winter minima when compared to the "offline" simulations. Following that trend, leaf biomass stocks in SAF are showing higher variance in the "offline" coupled version of Madingley when compared to the "default" version. In UGA, the leaf biomass stocks of both the "default" and "offline" versions fluctuate only a little.

In the FIN, simulated carnivores and omnivores show similar biomass densities in the "offline" simulations, while omnivore biomass density exceeds carnivore biomass density in the "default" simulations. All other simulations show similar hierarchies in heterotroph biomass

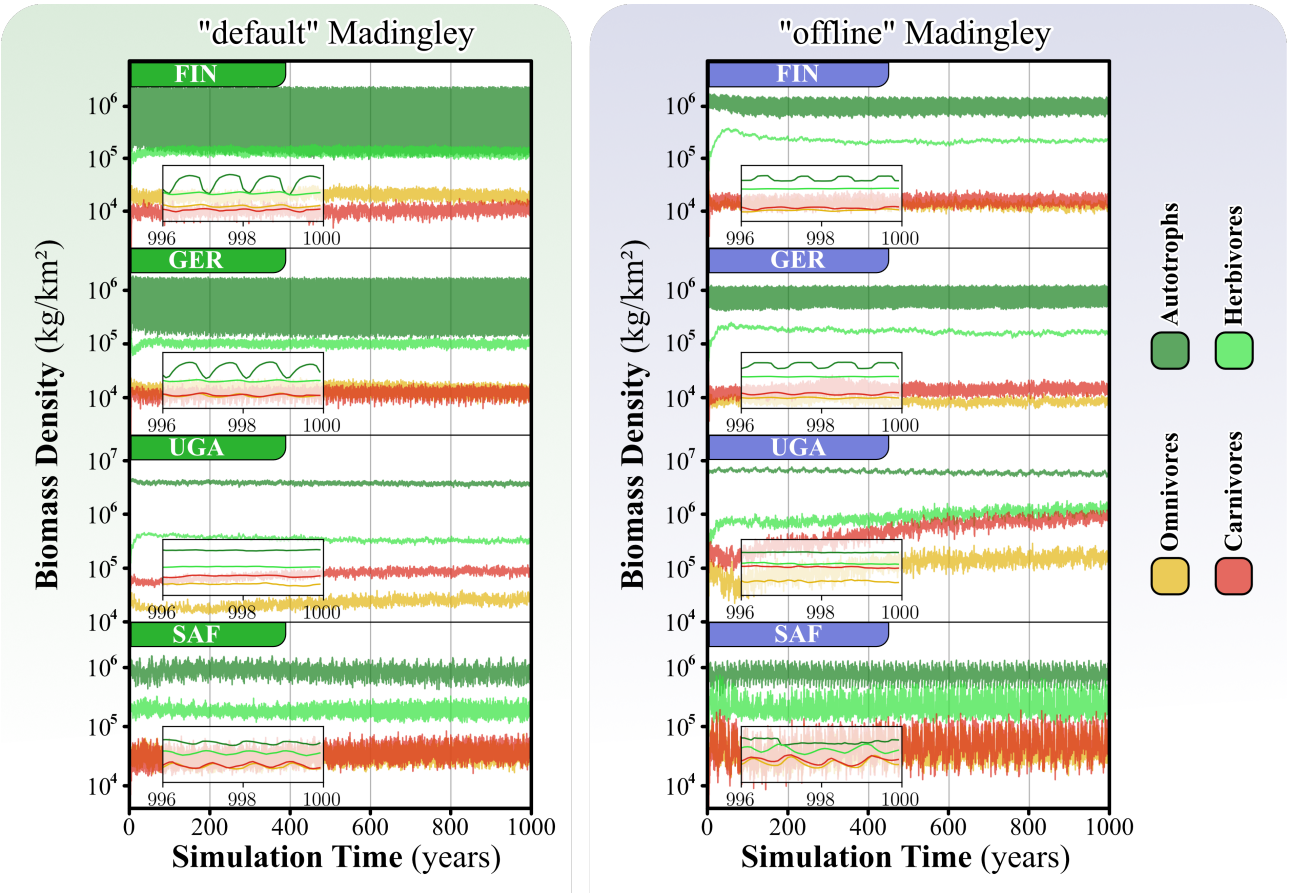

Figure 3.1 Long-term Analysis. Averages from 10 ensemble runs of wet biomass densities. The "offline" simulation on the right and the "default" simulations on the left. The zoomed insets are showing the last 4 years of the simulations to better visualise the annual fluctuations.

densities between the "default" and "offline" simulations. In all simulations, herbivores dominate heterotroph biomass densities.

3.1.2 Canopy Composition

As indicated already in Figure **3.1**, significant differences between LPJ-GUESS ("default") and the Miami Model (Madingley "default") emerge from the simulated vegetation composition. Figure **3.2** shows simulated autotrophic biomass split into the evergreen and deciduous stocks from both vegetation models. In the FIN and GER locations, the Miami Model simulates large seasonal fluctuations throughout the year for both evergreen and deciduous stocks. LPJ-GUESS simulates evergreen vegetation stocks that are much more stable throughout the year, while deciduous leaf biomass shows the expected seasonal fluctuations. Under sub-tropical and tropical climate conditions, LPJ-GUESS simulates substantially less deciduous leaf biomass than the Miami model.

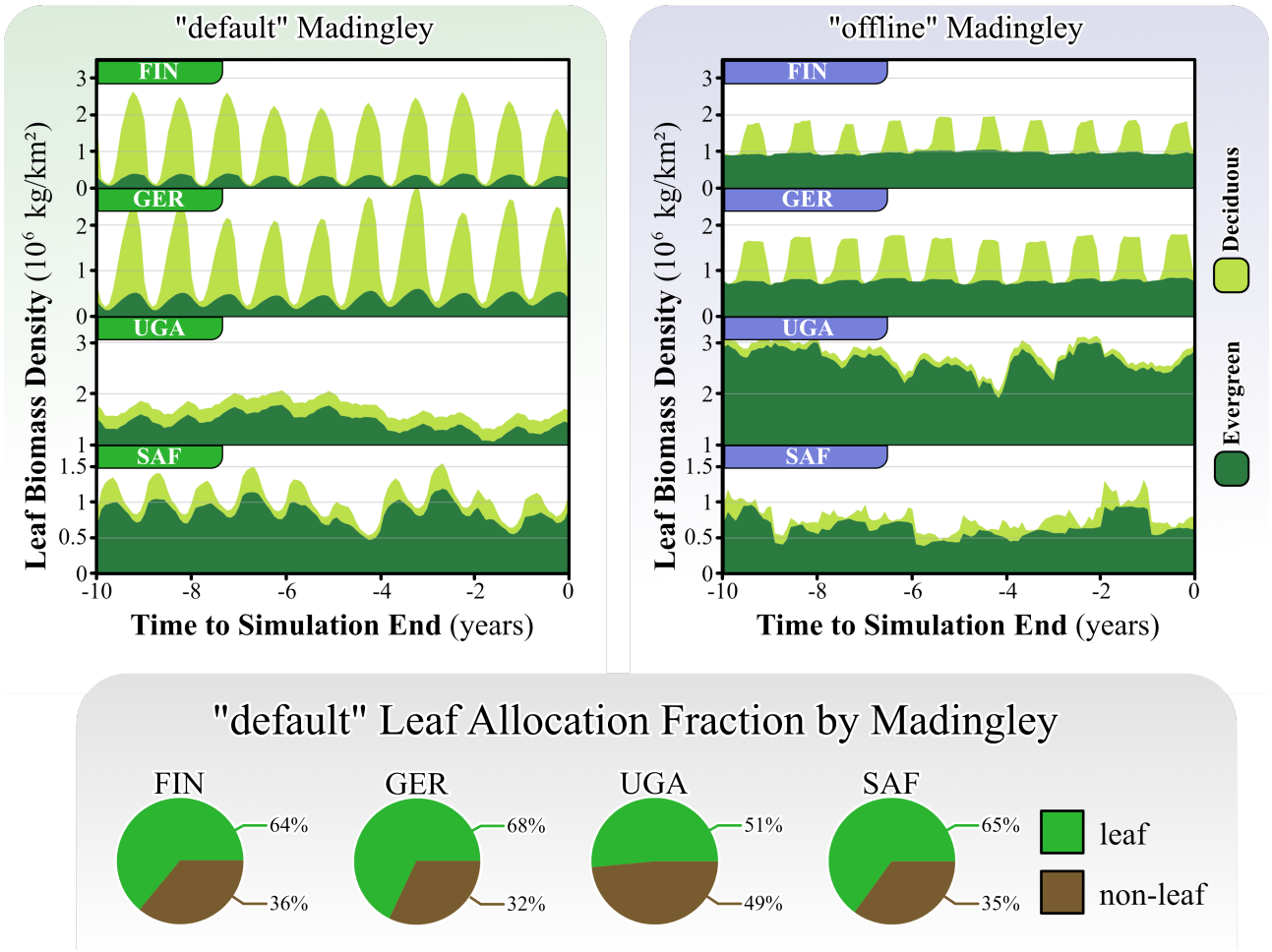

Figure 3.2 Evergreen and deciduous composition. Stacked plots of the vegetations total leaf biomass during 10 years of a simulation — split into light green evergreen and dark green deciduous compartments.

In SAF, variability in evergreen leaf biomass simulated by LPJ-GUESS is high and less regular, likely due to fire impact in these fire-prone environments. While "default" Madingley is parameterised to burn a fixed percentage of leaf biomass annually depending on climatic conditions, LPJ-GUESS uses the statistically-based fire model SIMFIRE-BLAZE, which simulates fire-frequencies, fire-intensities, fire-related fluxes and responses in vegetation (Launiainen et al. 2022; Rabin et al. 2017).

3.1.3 Community Level Analysis

All community-level simulations show differences between the "default" and "offline" simulations (Figures **3.3** and **3.4**). The average leaf biomass is smaller in the "offline" simulations for FIN (−16%), GER (−5%) and SAF (−15%) compared to the results from the "default" simulations. In UGA, LPJ-GUESS simulates 66% more average leaf biomass than the Miami model. The overall herbivore biomass in the "offline" simulations exceeds that of the "default" simulations

in every location (Figure **3.3**), most dominantly in UGA (+170%). Average carnivore biomass in the "offline" simulations is greater in FIN (+93%), SAF (+34%) and again most dominantly in UGA (+542%). Average omnivore biomass in the "offline" simulations is decreased in FIN (−39%) and GER (−51%) and is increased in UGA (+453%).

In FIN and GER, all biomass fluxes besides L→H, H→C and C→O show similar medians in both the "default" and "offline" simulations. In SAF, all fluxes show a slight increase of up to +20% in the "offline" simulations. In UGA, all fluxes show a significant increase of up to +500% in the "offline" simulations (Figure **3.4**).

In the "offline" simulations, the size distribution spectrum shows a tendency towards individuals with a higher abundance and lower biomasses, especially in FIN, GER and SAF (Figure **3.5**). In UGA, the high and low end of the body mass spectrum of endotherms show higher individual numbers in the "offline" simulations. Especially ectotherms show larger individual numbers at the lower end of the body mass spectrum.

Under boreal and temperate climate conditions, the "offline" coupling shows the largest increases in the number of endotherm cohorts. In contrast, at the tropical and sub-tropical sites, ectotherm cohort abundance is higher under LPJ-GUESS vegetation (Figure **3.5**). At all four sites, the "offline" coupling consistently results in larger cohort numbers of carnivore endotherms. In the "default" Madingley simulations at the FIN location, the whole functional group of carnivore endotherms disappear in the first years of the simulation without any chance for reestablishment afterwards. Herbivore endotherms are concentrated at the higher end of the body mass spectrum. In contrast, endothermic carnivores in FIN are present throughout the "offline" simulation, and herbivore endotherms populate a wider range of the body mass spectrum.

3.1.4 Individual Level Analysis

The individual-level analysis shows general similarities between the "default" and "offline" versions of Madingley for each location (Figure **3.6.A**). Growth rates are slightly elevated in the "offline" simulations. Most notable is an increased growth rate of the smallest individuals in SAF and UGA. Conversely, the lifespan of individuals that have body mass >100 g decreases in the "offline" simulations for all locations (Figure **3.6.B**), visible through an increased mortality rate for cohorts of these bigger individuals. This effect is most dominant in UGA. In FIN and SAF, endothermic cohorts need significantly less time to reach maturity state in the "offline" simulations (Figure **3.6.C**). Besides an increased growth rate and a shorter time to reach maturity, the shorter lifespan seems to be the dominant effect, leading to the cohorts having a reduced lifetime reproduction success rate in all "offline" simulations (Figure **3.6.D**).

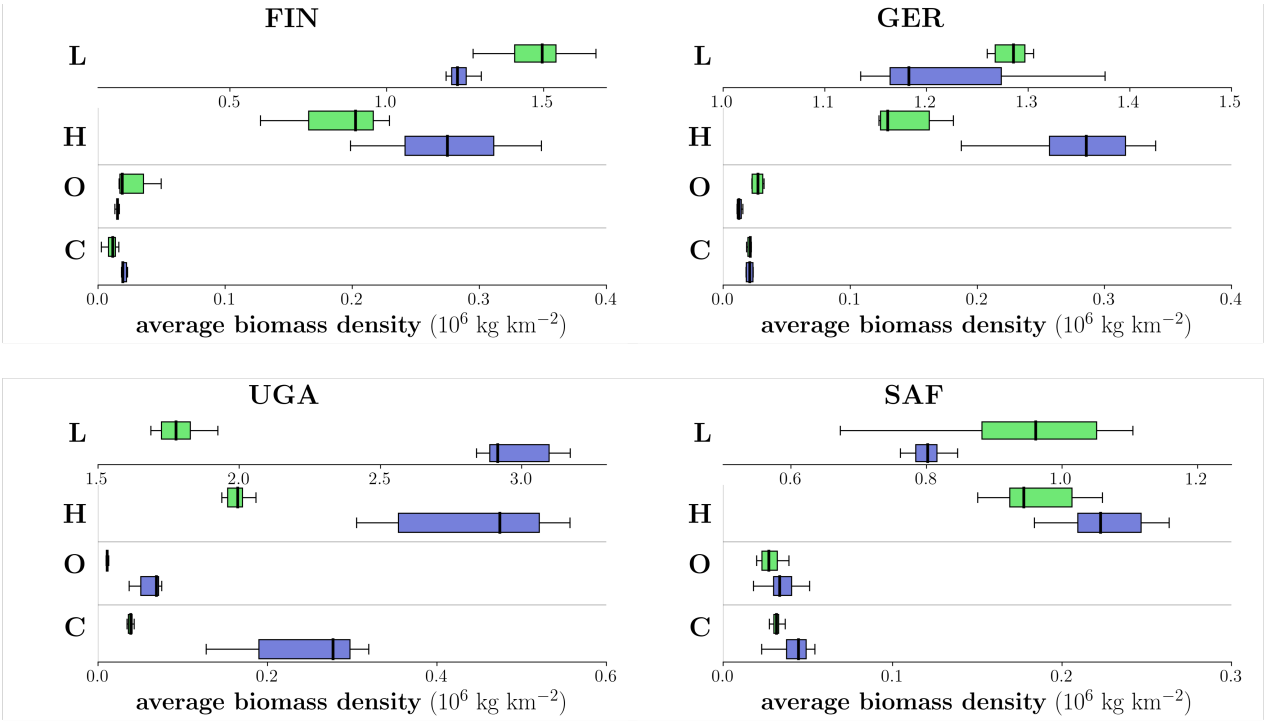

Figure 3.3 Pools of leaf (L), herbivores (H), omnivore (O) and carnivore (C) biomass densities, averaged over the last ten years of the simulations. Medians and deviations from the medians are calculated from eight ensemble simulations. Due to the greater magnitude of the leaf biomass, it is shown on a separate scale (same unit as the other pools). Green boxes indicate the data from the "default" simulations, blue boxes indicate the data from the "offline" simulations. For comparison between sites, note the different axes scale.

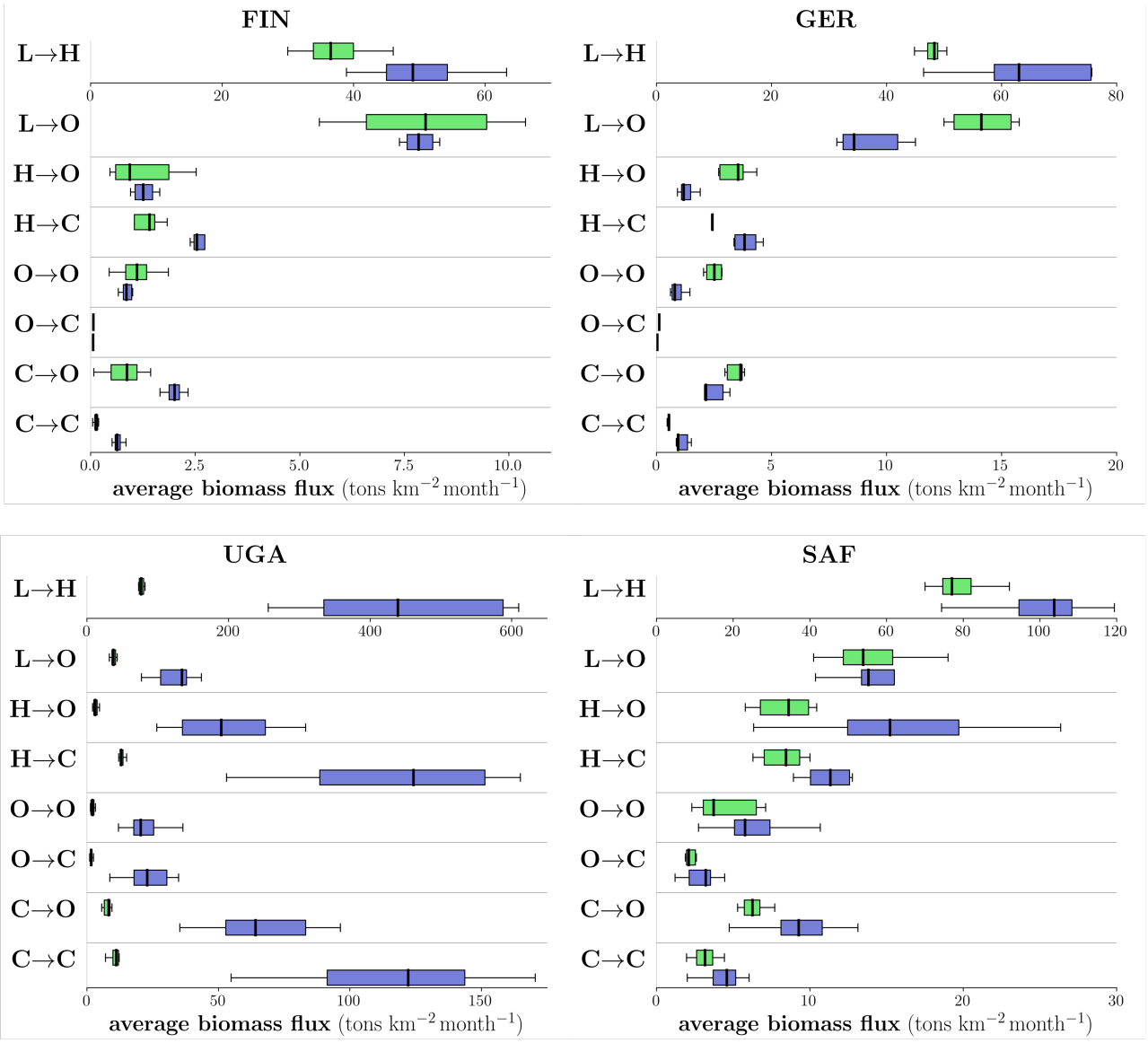

Figure 3.4 Biomass fluxes between leaf (L), herbivores (H), omnivores (O) and carnivores (C) averaged over the last ten years. Medians and deviations from the median are derived from eight ensemble simulations. Due to the greater magnitude of L→H flux, it is shown on a separate scale (same unit as the other fluxes). Green boxes indicate the data from the "default" simulations, blue boxes indicate the data from the "offline" simulations.

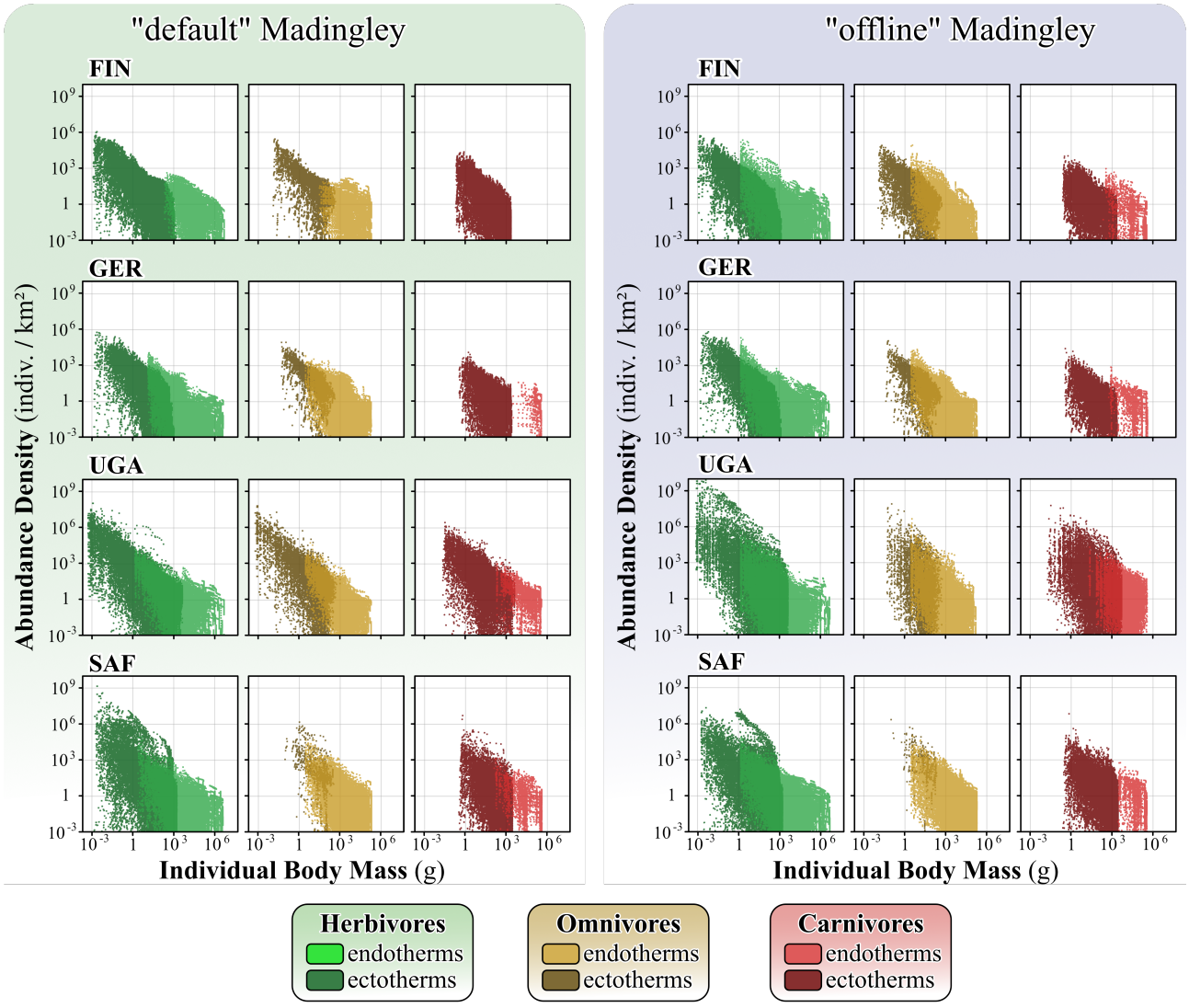

Figure 3.5 The emergent size distributions, showing every cohort state during the last year of one simulation. Each marker represents one cohort state. The lighter colours represent endotherm cohorts.

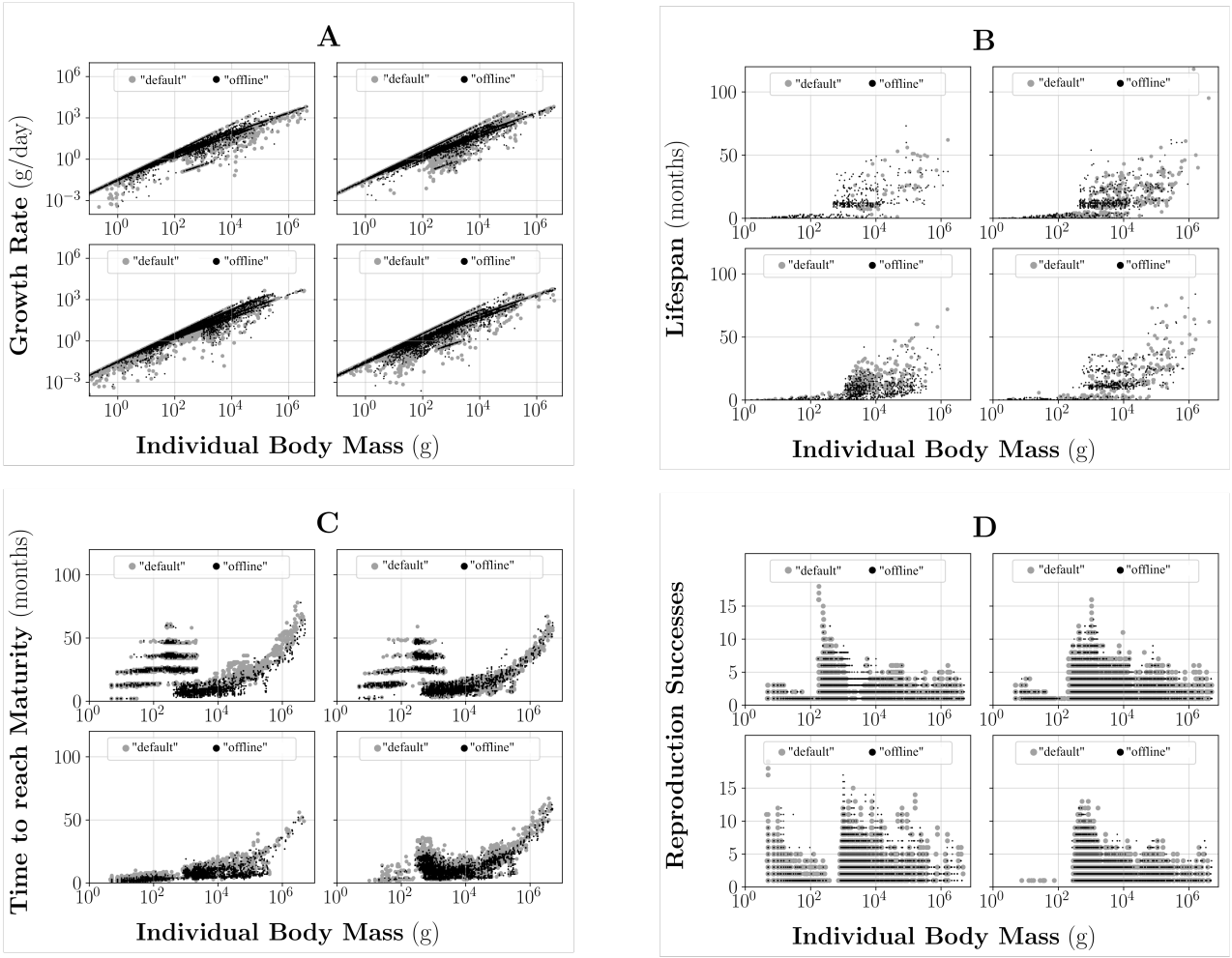

Figure 3.6 Individual Level Characteristics. Every dot represents the state of a cohort during the last year of a simulation. Grey dots represent cohorts from "default" setups, while black dots represent cohorts from the "offline" setup. (A) shows the individual growth rates. (B) shows the lifespan of the cohorts that have died (hence, the number of cohorts in B differs from the other graphs). (C) shows the time cohorts need to reach their adult body mass. (D) shows the cohort's lifetime reproduction successes.

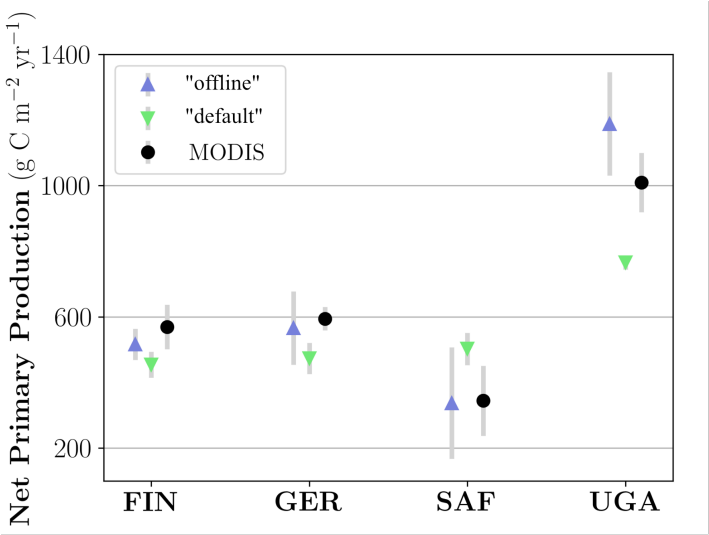

Figure 3.7 Comparing simulated NPP to MODIS data. Blue triangles represent the domain average for ”offline” simulations. Green triangles represent the domain average for ”default” simulations. Grey bars mark the range of the standard deviation. Black dots mark the area average derived from the MODIS dataset.

3.1.5 Evaluation

At all experiment locations, LPJ-GUESS predicts the NPP better than the Miami model when compared to the MODIS dataset (Figure **3.7**). The best LPJ-GUESS predictions were found in the FIN (−9%), GER (−5%) and SAF (−3%) setup, while the only larger difference was found in UGA (+17%). The Miami model shows a larger gap between predicted NPP and the data derived from the MODIS dataset (FIN −21%, GER −20%, SAF +45% and UGA−25%).

Beyond comparing the vegetation model outputs to the MODIS V6.1 dataset, we also made an assessment of whether the realism of the entire model system output was increased. According to Cebrian (2004), terrestrial ecosystems NPP is related to herbivore biomass and herbivore consumption by the following logarithmic power-laws:

$$\log(\text{biomass}) = -3.43 + 1.30 \cdot \log(\text{NPP}) \tag{3.1}$$

$$\log(\text{primary consumption}) = 0.24 + 0.82 \cdot \log(\text{NPP}) \tag{3.2}$$

We were able to determine similar shaped power-law relations from the “offline” simulations by applying a logarithmic fit for the last ten annual sums of herbivore biomass and consumption. We derived the following power-law relationships:

$$\log(\text{biomass}) = 0.90 + 0.31 \cdot \log(\text{NPP}) \tag{3.3}$$

$$\log(\text{primary consumption}) = 0.26 + 0.66 \cdot \log(\text{NPP}) \tag{3.4}$$

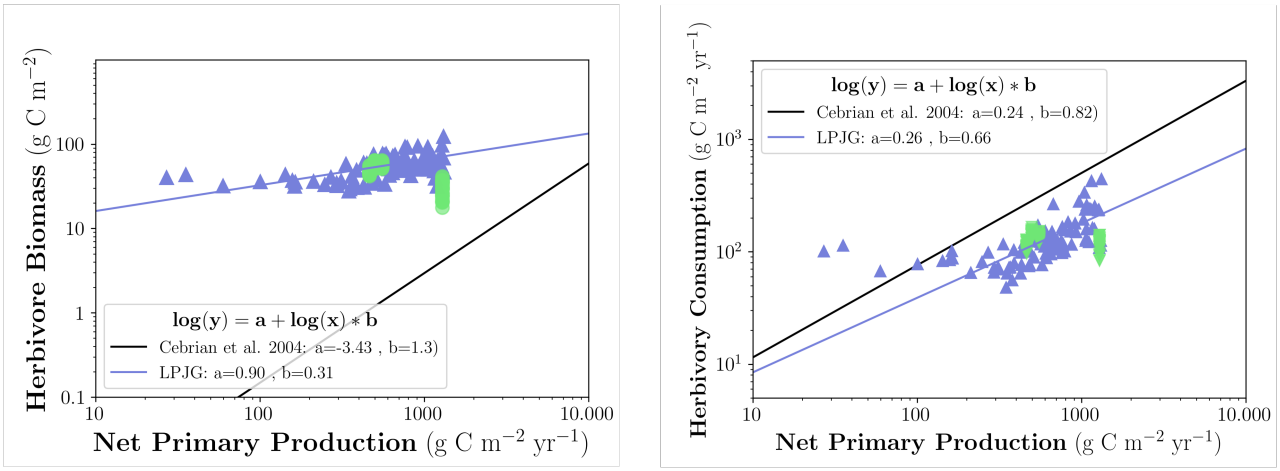

Figure 3.8 Power-law relationships. Blue triangles represent an annual sum during "offline" simulations. Green dots represent an annual sum during "default" simulations. For the "offline" version, herbivore biomass and herbivory consumption are related to NPP. There are no reasonable corresponding logarithmic fits for the "default" version. Note: this version of the Figure is a corrected version compared to the original published in Krause et al. (2022); see the corrigendum published Krause et al. (2022). The correction did not affect the point made, in that the "offline" simulation showed considerable improvement over "default"

These power-law relationships are shown in Figure **3.8**. Notable is the high herbivore biomass and herbivory consumption in SAF, which is the ecosystem with the lowest simulated productivity.

Since the Miami model predicts a smaller range of NPP throughout diverse ecosystems when compared to LPJ-GUESS, all data points for the "default" simulations are clustered in a narrow range. This renders a logarithmic fit for herbivore biomass and herbivory consumption unreasonable, so these are not provided here. However, it is worth noting that in the "default" simulations, both herbivore biomass and herbivory consumption consistently show lower values in ecosystems with slightly higher NPP, providing weak support for an inverse relationship in that model.

3.2 Discussion

The large differences between "default" and "offline" Madingley simulations show a complex interconnectivity of coupling-related effects throughout the experiments. To analyse their validity, we first explain the observed changes and the underlying processes. Secondly, we discuss the differences to the MODIS dataset and the power-laws derived by Cebrian (2004).

3.2.1 Development of the Animal Population

The Madingley model reaches a dynamic steady state with both versions. When such an equilibrium state is reached, cohort biomass is no longer increasing. The longer time needed in the "offline" UGA simulation is most likely caused by the much larger amount of edible leaf biomass simulated for this location in LPJ-GUESS compared with Miami. Cohorts of heterotrophs were initialised in the same way for all four locations. Their subsequent growth is, therefore, not only limited by food availability but also by climatic conditions and predation. UGAs warm climate lengthens the active time of ectotherms and thus increases their food uptake and metabolic cost. Therefore, LPJ-GUESS's larger UGA vegetation biomass supply funnels through to the higher trophic levels, which increases predation stress for the lower trophic levels. These interactions increase the growth limit of the cohorts and thus result in a longer period necessary to reach the model system's dynamic steady state. This effect appears to be most visible in enhancing herbivore and carnivore biomasses. Omnivores also responded to the changes in vegetation stocks, but not as much as the other groups, possibly because while omnivores have the ability to feed both from plants and other cohorts, they do so with a less efficient assimilation strategy.

In contrast to UGA, leaf biomass simulated by LPJ-GUESS is lower at the other three locations. Thus, the larger total herbivore biomass in all of the "offline" runs was unexpected. Since the reported leaf biomass data represents the stock state after the cohorts feed from it, one might argue that the reduced leaf biomass stock simply reflects a larger degree of herbivory. However, this seemingly simple explanation does not capture the complexity of the underlying processes that affect the development of emergent animal populations. In the following, we want to discuss the ecological responses to the "offline" coupling-related changes in total leaf biomass and varying climate conditions.

Total Leaf Biomass represents the primary modification to the "default" Madingley model. All observed differences between the model versions arise from changes in simulated vegetation dynamics. Compared to the "default" version, the "offline" version predicts greater leaf biomass availability as a food source during the cold season. This results in an increased biomass flux from autotrophs to herbivores over winter. The larger total cohort biomasses that correspond to the lower average leaf biomasses but higher minimum leaf biomasses (as computed in LPJ-GUESS compared to Miami) indicate that total cohort biomasses are more sensitive to the minimum leaf biomass. Such a relationship is plausible, as cohort growth limitations are more likely to occur during the cold season, particularly in boreal climates.

In the "offline" simulations, endotherms at the FIN location mature significantly faster than in the corresponding "default" simulations. This indicates that higher minimum leaf biomass enhances the flux of leaf biomass to herbivores on an individual level, enabling herbivores to

assimilate more biomass throughout the "offline" simulation and reach their adult body mass more quickly. A similar effect is observed in SAF, where LPJ-GUESS predicts a higher minimum leaf biomass pool than the Miami model. This is quite remarkable since the average leaf biomass in "offline" SAF is lower than in "default" SAF and explains how, despite the lower leaf biomass pool, the herbivore biomass pool can be higher in the "offline" simulation.

Besides UGA, LPJ-GUESS predicts a lower average annual leaf biomass than the Miami model. This decrease seemingly shifts the size distributions towards smaller individuals, most visible in the increased abundance of individuals lighter than 1 g (Figure **3.5**). This result is consistent with the increased number of cohorts going extinct in the "offline" simulations and their lower lifespans, which in turn reflects increased predation stress on the smaller individuals. In all "default" Madingley simulations, the larger total annual leaf biomass predicted by the Miami model supports cohorts of heavier individual body mass, which is consistent with the megafauna theory (Evans et al. 2012). However, the default Madingley version nonetheless overestimates the size of large herbivores by four to six times compared to field studies (Harfoot et al. 2014). It was also observed that the smaller the gap between the vegetation simulated by either LPJ-GUESS or Miami, the higher the herbivore biomass in the coupled run (compare "offline" GER and SAF). This indicates that a uniform increase in vegetation biomass without changing its evergreen/deciduous composition still enhances herbivore biomass.

Climatic conditions. Under colder conditions, animals are less active and thus have less time to fulfil their metabolic cost (Harfoot et al. 2014). While ectotherms become inactive below a certain temperature threshold, endotherms constantly need to be active under tropical and boreal conditions alike. Climatic conditions thus contribute to the cohorts' stress by enhancing the effect of calorific shortages. Figure **3.5** shows that the "offline" coupling leads to an increase in ectotherm herbivore abundance under warm climates (UGA and SAF). In these warm locations, the smallest individuals, which are typically ectotherms, show overall higher growth rates in the "offline" model version. Figure **3.6.B** supports this observation on an individual level, as low-weight ectotherms in the "default" version show a wide range of growth rates. This indicates that some ectothermic individuals are not reaching their maximum potential growth rate. Therefore, the amount of leaf biomass seems to be the limiting factor. In contrast, in the coupled "offline" version, the smallest individuals share similar growth rates.

Under colder climate conditions (FIN and GER), the abundance of ectotherm herbivores did not show significant changes due to the coupling. In these locations, the growth rates of similar individuals are not significantly enhanced by LPJ-GUESS vegetation input. We expect the climatic conditions to be the limiting factors in both the "default" and "offline" simulations.

These two examples have shown that climatic conditions can weaken or enhance the effect of changes in leaf biomass. As the most noticeable example, we want to highlight the extinction of carnivore endotherms in "default" simulations at the FIN location. During the first few

timesteps, the FIN endotherm herbivore population grows faster in the "offline" coupled version as a result of a higher minimum in leaf biomass during the cold season. This keeps the total biomass of herbivores large enough to feed endotherm carnivores in the "offline" simulations. In contrast, the reduced growth of FIN endotherm herbivores in the "default" version leads to the total herbivore biomass being too low to support a carnivore endotherm population. As a result, endothermic carnivores go extinct during the first few timesteps of the "default" simulations. After the first decades, the established FIN herbivore population grows without the top-down control of predation, and thus, their body mass size distribution shows fewer, heavier individuals than in the "offline" simulation. This effect of the absence of large carnivores in Madingley, leading to the non-regulated growth of the lower trophic levels, is consistent with observations (Brose et al. 2019; Elmhagen et al. 2010) and highlights the importance of representing all trophic levels in a simulation.

Overall, the individual-level characteristics only show minor differences when comparing the "default" and the "offline" versions of Madingley. However, we observe huge variations in the traits on a community level. This leads us to the conclusion that relatively small changes in individual processes can lead to substantial changes in the dynamics of a whole animal community. Minor differences on the individual level also indicate that Madingley still successfully predicts ecological processes for individuals and thus still produces reasonable assumptions for animal communities.

3.2.2 Comparison to External Sources

LPJ-GUESS consistently predicts NPP closer to empirical observations than the NPP predicted by the Miami model, which does not seem to fit well for temperature or precipitation extremes (very hot, very arid or very wet). In arid ecosystems such as SAF, LPJ-GUESS also includes wildfires in its simulations. While the Miami model predicts a lower NPP than LPJ-GUESS in FIN and GER, we see higher leaf biomass stocks in the "default" rather than in "offline" coupled simulations. This is caused by Madingley assuming that 64% (FIN) and 68% (GER) of the monthly available NPP is allocated towards leaves (see Figure **3.2**). LPJ-GUESS typically accounts for about 30% of the allocation towards leaves (De Kauwe et al. 2014).

The simulation-derived power-law for herbivore biomass to NPP is more consistent with empirical relationships in Madingley's "offline" version. Still, while the power-laws slope is similar, the magnitude of the simulated herbivore biomass is higher than seen in the empirical data from Cebrian (2004). Still, the Madingley model can, for the first time, predict similar kinds of power-laws as observable in nature, which is a major improvement of the model and lays the foundation for future model developments.

In the SAF location, both herbivore biomass and herbivory consumption are overestimated by the "offline" version when compared to the power-law relationships. We expect this to result from every cohort having access to 10% of the leaf biomass stock in Madingley. We have highlighted before that this assumption is a key limitation of the Madingley model. While the cohorts are limited by the accessible leaf biomass, they do not necessarily consume all of it but only try to fulfil their metabolic cost. In SAF, herbivores consume a higher portion of the standing stock due to the ecosystem's lower productivity. Such a high consumption of leaf biomass would, in reality, suppress future ecosystem productivity, which is disregarded in the "offline" coupled version of the model system.

3.2.3 Interpretation of previous Madingley publications

We have shown that Madingley's built-in NPP parameterisation by Miami only predicts a realistic NPP in one out of the four simulated locations. Even in European temperate forests, NPP is underestimated by 30%. In ecosystems with extremely low or high productivity, it is very likely that Miami has made a completely unrealistic NPP prediction. We have also shown that average NPP, high yearly fluctuations of evergreen and deciduous biomass, the vegetation biomass winter minima and the length of the growing season are very likely to affect the development of animal populations. In conclusion, we expect that previous publications have underestimated the abundance and growth rates of ectothermic animals in high or low-productivity ecosystems while also overestimating the cohorts' lifespan and reproduction cycles in all terrestrial ecosystems.

3.3 Summary

In this Chapter, we investigated how a more sophisticated vegetation model enhances simulations of animal populations. Specifically, we extracted leaf biomass data from the "default" version of LPJ-GUESS and utilised these leaf stocks as food resources for the animals in the "offline" version of Madingley.

Our findings demonstrate that animal populations are significantly influenced by this coupling due to the limited range of net primary productivity (NPP) predicted by Madingley's default vegetation model, compared to the broader spectrum of NPP simulated by LPJ-GUESS. We showed that general shifts in the animal population are likely driven not only by the total annual leaf mass but also by the winter minima in leaf mass and the climatic conditions. Power-law relationships for herbivory to NPP and herbivore biomass to NPP derived from both model versions revealed that only the "offline" model system simulates animal populations consistent with power-laws similar to those derived from empirical data.

This Chapter highlighted the potential of coupling the Madingley model with LPJ-GUESS. However, several limitations identified in this study highlight the need for incorporating feedback from herbivores to vegetation. In response, we developed the "online" coupled versions of LPJ-GUESS and Madingley. The experiments conducted with this "online" system are detailed in the following Chapter.

4 Modelling Herbivory Impacts on Vegetation Structure and Productivity

4.1 Results

In this Chapter, we focus on comparing the "default" version of LPJ-GUESS with its "online" coupled counterpart, where herbivory is introduced. First, we examine the effects of herbivory-induced damage on plant productivity, carbon assimilation, and the resulting shifts in canopy composition. Next, we explore the dynamic feedback between such herbivory damage and the animal population itself. This highlights the reciprocal impacts that both models enforce upon each other. Finally, we assess the performance of the "default" and "online" versions of LPJ-GUESS against empirical data and compare all three versions of Madingley against power-law relationships derived from empirical data.

4.1.1 Coupling Impacts on Plant Communities

The coupling impact on plant productivity and canopy composition is analysed by examining the aggregated response across the entire modelled domain and biome-specific responses at selected European (E1–E5) and African (A1–A5) sites. Comparisons are made between the uncoupled "offline" model state and a coupled "online" model state to evaluate the impact of the coupling on various metrics.

Productivity and Carbon Masses

Figure **4.1** shows the coupling-induced differences of simulated NPP on a grid cell level. Aggregated across the model domain, these changes are relatively minor when comparing results from LPJ-GUESS with herbivory (27.5 ± 1.4 Pg C) to those without herbivory (29.0 ± 1.4 Pg C). Herbivory, therefore, causes an overall reduction in NPP of 1.5 % Pg C (-5.2% ± 5.1%). However, substantial spatial variability is evident across the model domain. NPP generally increases in response to herbivory across most of the African continent but decreases in large parts of Europe.

The coupling responses in LPJ-GUESS are also reflected in changes to tree carbon mass. The effects of herbivory on total vegetation carbon are more pronounced than on NPP. Figure **4.2** shows this response across the model domain and provides a more detailed picture of the different PFTs at the ten selected sites. Across the model domain, vegetation carbon decreases by -9.7% (± 17.3%) in response to herbivory. The most significant reductions in vegetation carbon are found in the boreal regions, with, e.g., a decrease of -41.8% (site E4) and in savannas near grasslands, where vegetation carbon decreases by -37.5% (site A5). In northern Norway, however, there is a narrow expanse of boreal grassland that experiences a significant increase

in vegetation carbon. Besides this narrow expanse, the most prominent increases in vegetation carbon in response to herbivory are found in temperate mixed forests of central Europe (e.g., site E1, +3.9%).

Across the model domain, introducing herbivory leads to an average decrease in LAI of -9.0% (±10.1%), with the largest reductions occurring in boreal ecosystems. The spatial response of GPP closely mirrors the LAI response (Figure **4.1**). While the magnitude of changes at individual locations is more pronounced for GPP compared to LAI, the overall decline in GPP across the entire model domain is relatively modest, averaging -2.4% (±4.4%). Introducing herbivory to LPJ-GUESS results in a slight overall increase in evapotranspiration rates, averaging +0.2% (±4.2%). The most notable increases are observed in central Europe and tropical rainforest regions. At the individual sites, significant reductions in evapotranspiration were found of -6.5% at site E5 and -6.3% at site A5.

Canopy Composition

The changes in tree carbon mass arise not only from reductions in leaf carbon but also from alterations in PFT composition. Figure **4.3** shows each grid cell's dominant plant functional type, i.e. the PFT with the highest leaf area index, as well as the different PFTs contributions to the overall grid cell's LAI for the ten selected sites. We focus on three regions exhibiting the most notable responses. First, woody vegetation shifts towards vegetation dominated by C3 herbaceous PFTs in eastern Europe, represented by site E2. When exposed to herbivory, the contribution of C3 grass (C3G) to the total LAI increases markedly, from 6.1% without herbivory to 35.5%, making it the dominant PFT. This pattern is even more pronounced in the coldest ecosystems, represented by site E4. Here, the contribution of C3G to the total LAI rises sharply from 18.3% without herbivory to 50.9% with herbivory. Lastly, the area dominated by tropical broadleaf evergreen (TrBE) trees is found to expand into the subtropical regions, as represented by site A2. A similar effect is evident at the shores of Mozambique, where the dominant TrBE tree area expands from coastal zones into the inland regions.

Patterns of PFT dominance can also be associated with positive or negative vegetation carbon responses. In the boreal regions of northern Europe, large decreases in vegetation carbon in response to herbivory are observed in grid cells dominated by boreal needleleaf evergreen (BNE) trees. In contrast, central Europe, predominantly characterised by temperate broadleaf summergreen (TeBS) trees, exhibits an overall increase in vegetation carbon in response to herbivory. A comparable positive response is also evident in landscapes dominated by grassy PFTs, particularly the boreal grassland in northern Norway. African grassland ecosystems, dominated by C3G or C4 grass (C4G), also show an overall increase in vegetation carbon.

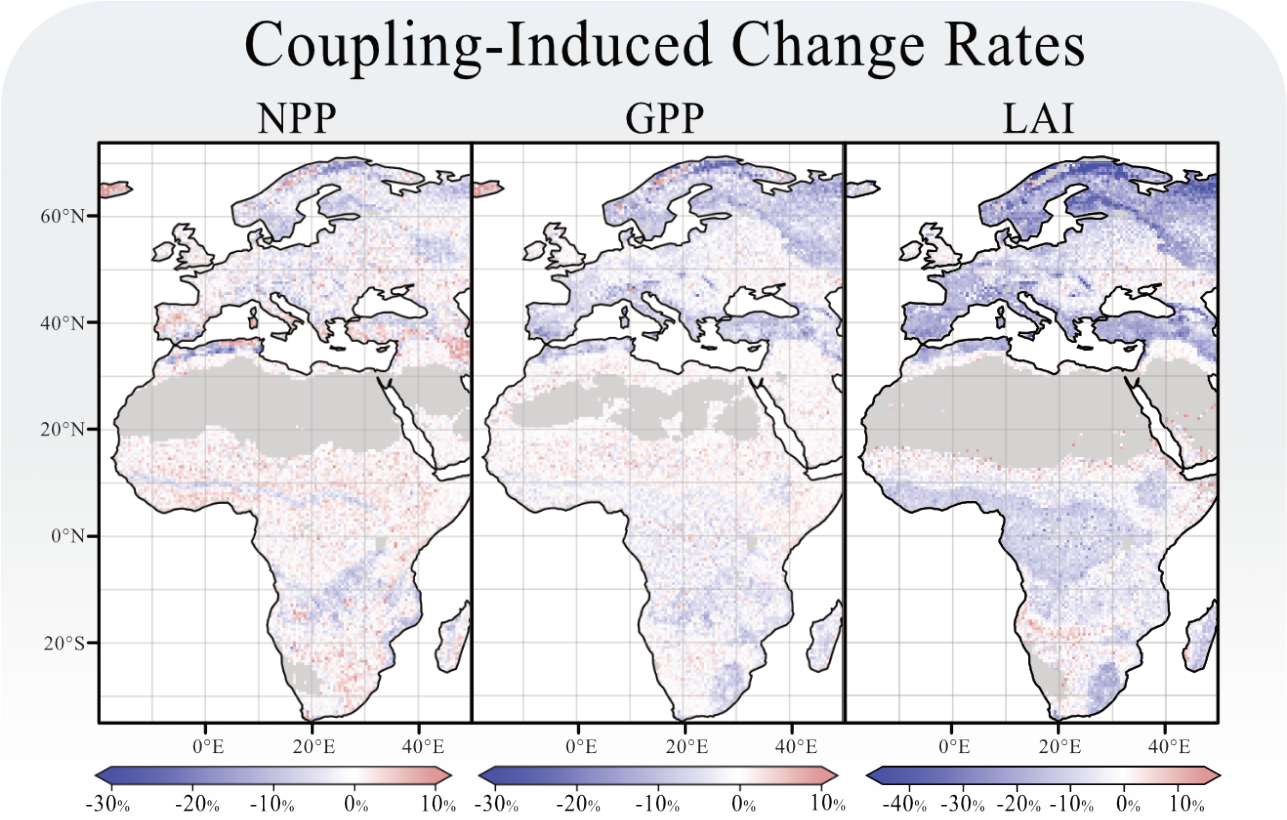

Figure 4.1 Coupling-related changes in grid cell's NPP, GPP and LAI. Each panel shows the percentage-wise difference between the "offline" and the "online" simulations. All figures were calculated based on the last 30 years of the simulations.

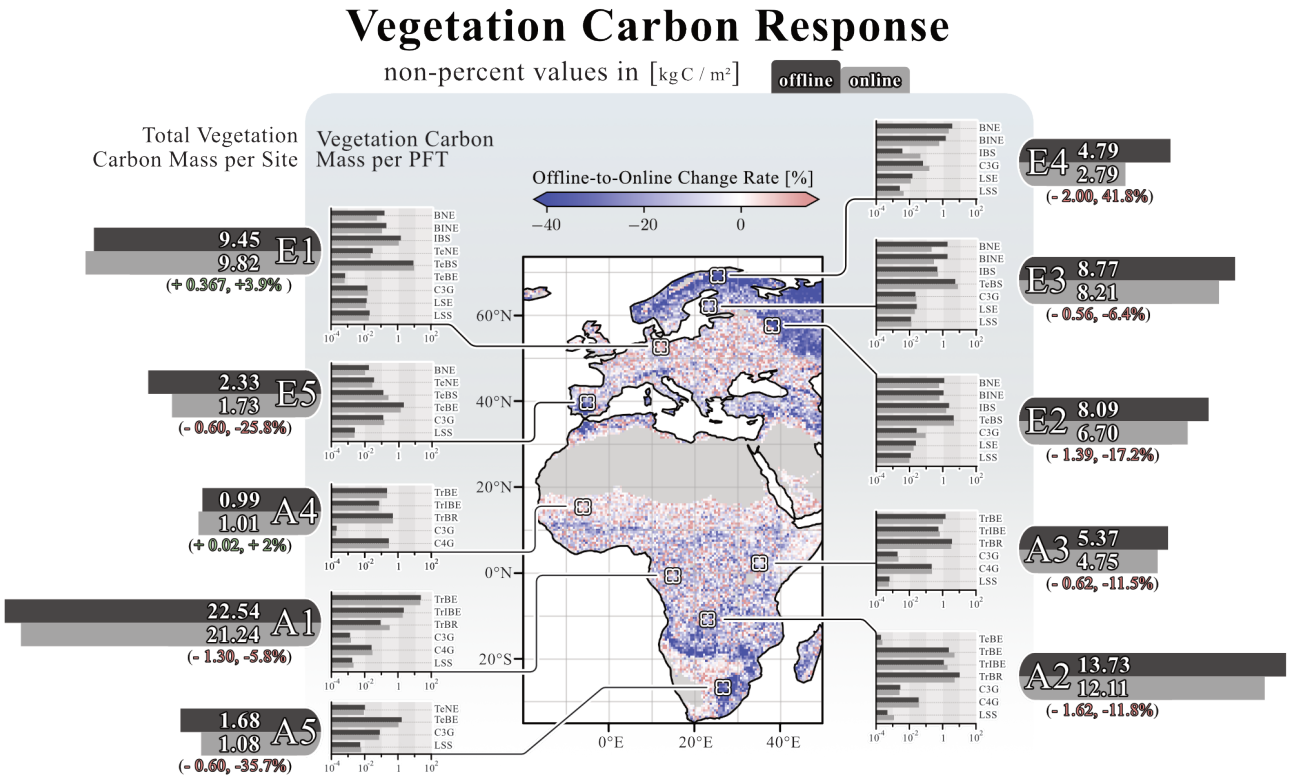

Figure 4.2 Coupling-related changes in vegetation carbon for the simulation domain. The map illustrates the percentage differences between the "offline" and "online" simulations per grid cell. Flanking the map on both sides are detailed vegetation carbon responses for the ten selected locations. The large horizontal bars next to the location tag represent the overall vegetation carbon response at that site, with its length corresponding to quantitative carbon levels. The smaller bars indicate the response of each PFT present at each location. Non-percent values of vegetation carbon are given in $\mathrm{kg\,C\,m^{-2}}$. The figure reflects data averaged over the final 30 years of the simulation.

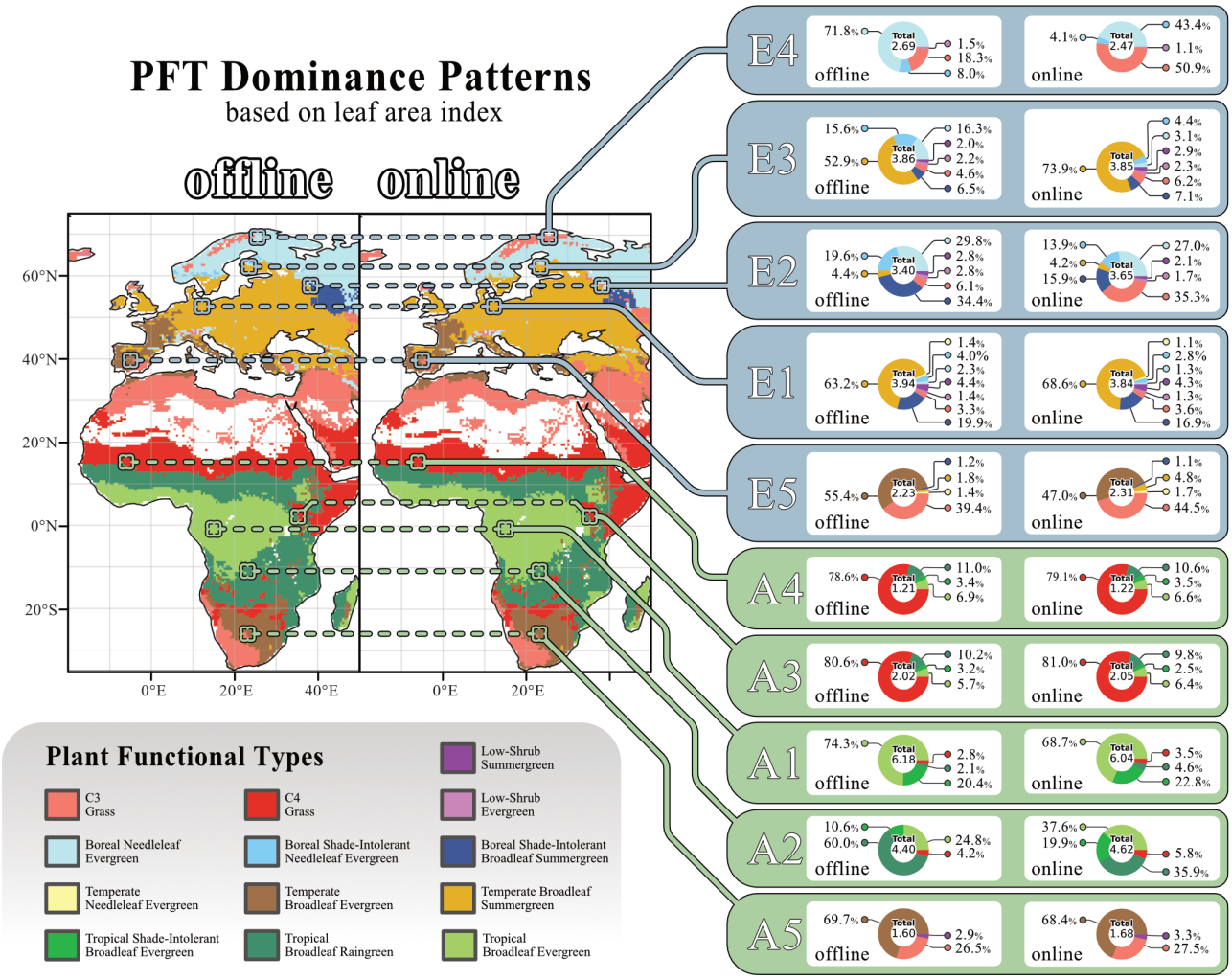

Figure 4.3 Coupling-related changes in grid cell's dominant PFT. The maps display the dominant PFT in each grid cell, determined by the PFT's LAI in the "offline" and "online" simulations. Only grid cells with a total LAI greater than 1 were included in the analysis. Flanking the maps, pie charts show the contributions of all PFTs to the total LAI for ten selected locations. The "offline" simulation results are presented on the left, while those from the "online" simulation are shown on the right. The figure reflects data averaged over the final 30 years of the simulations. PFT Colour coding is labelled underneath the figure.

4.1.2 Coupling Impacts on Animal Populations

Differences in simulated leaf, herbivore, omnivore and carnivore biomass densities are compared across three stages of model development (Figure **4.4**): "default" Madingley, which uses the Miami model for vegetation; "offline" Madingley, described in Chapter **2.4** and "online" Madingley detailed in Chapter **2.5**. In "online" LPJ-GUESS/Madingley, significant reductions are evident for herbivore (-58% ± 47%) and carnivore biomass densities (-59% ± 36%). Omnivore biomass density decreases to a lesser extent (-19%). These substantial declines stem from LPJ-GUESS simulating less leaf biomass available for consumption compared to "default" Madingley (-49% ± 32%). The high standard deviations are mostly caused by low-productivity regions adjacent to deserts, where "default" Madingley significantly overestimates annual NPP. Conversely, in areas where LPJ-GUESS simulates higher annual NPP than "default" Madingley, biomass densities of all animal groups increase.

(Figure **4.4**) also compares biomass densities for "default", "offline", and "online" Madingley based on the four sites investigated in Chapter **3**. For "offline" Madingley simulations, herbivore biomass increased at all four sites compared to "default" Madingley. In contrast, "online" Madingley shows lower herbivore biomass densities at all four sites compared to "default" Madingley. This reduction is especially pronounced at both European sites, where carnivore biomass densities are also significantly reduced in "online" Madingley. At the African sites, herbivore, omnivore and carnivore biomass densities in the "online" version are similar to those of "default" Madingley. However, "offline" Madingley simulates much higher biomass densities for all three groups.

Finally, (Figure **4.4**) shows biomass densities at three selected sites. The first site is located in the tropical rainforest, where LPJ-GUESS predicts the highest NPP. At this site, leaf and ATF biomass densities are similar between "default" and "online" Madingley. The second site is a grassland ecosystem adjacent to the Sahara Desert, where "online" Madingley simulates significantly lower leaf biomass densities (-71%) compared to 'default' Madingley. As a result, biomass densities for all AFTs are also significantly reduced, with the most notable decline in carnivores (-93%). The third site is located in Sweden, near the Baltic Sea, where "online" Madingley simulates higher leaf biomass densities (+17%) compared to "default" Madingley. This increase leads to higher omnivore biomass densities (+21%) and carnivore biomass densities (+34%), while herbivore biomass densities remain largely unchanged (-0.4%).

4.1.3 Evaluation

Outputs from the "default" and the "online" versions of LPJ-GUESS are compared to GPP derived from FLUXNET sites (Reichstein et al. 2007). Modelled monthly GPP fluxes are well within the standard deviation range of the measured GPP fluxes for both "default" and "online"

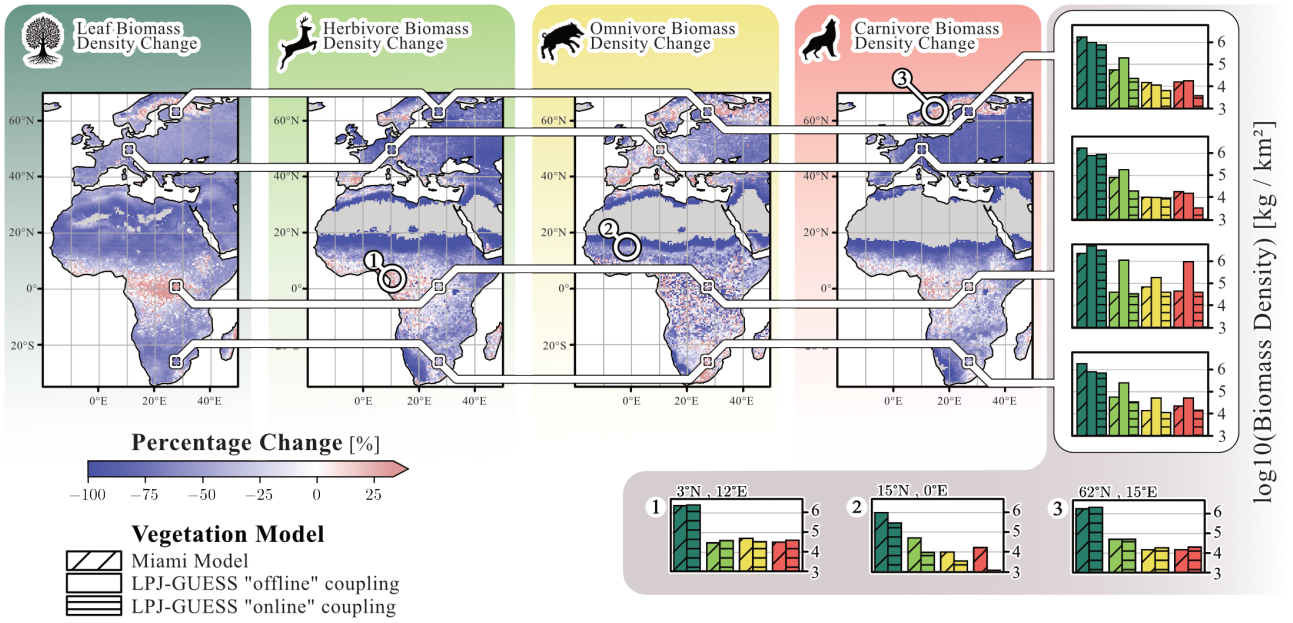

Figure 4.4 Coupling-related changes in AFT biomass densities. The four maps show differences in leaf, herbivore, omnivore, and carnivore biomass between the “default” version of Madingley and the “online” coupled version. Additionally, the figure shows a comparison of the ”default”, the ”offline” coupled (chapter 3) and the ”online” coupled Madingley versions at the four representative locations from Chapter 3. Finally, we selected 3 locations that exhibit the most significant differences in biomass density levels among herbivores, omnivores and carnivores between the “default” and “online” versions: (1) represents a tropical rainforest biome, (2) represents a hot arid grassland biome and (3) represents a boreal grassland biome. The figure reflects data averaged over the final 30 years of the simulation.

LPJ-GUESS (Figure **4.5**). However, in boreal Areas 1 and 2 (which correspond to boreal forests in Finland and Sweden), simulated GPP tends to be higher than GPP derived from the flux towers in these regions.

When examining evapotranspiration and GPP across the model domain, regression lines for "default" and "online" LPJ-GUESS show little deviation (Figure **4.6**). The "online" version appears to be simulating GPP estimates that are somewhat closer to the measured values, particularly in boreal ecosystem grid cells. The evapotranspiration regression lines show no significant differences between "default" and "online" LPJ-GUESS. However, a slightly reduced slope is observed, reflecting the minor overall decrease in evapotranspiration. The "default" version of LPJ-GUESS also demonstrates a tendency to overestimate LAI, especially in warm ecosystems such as those in southern Africa, where the satellite-derived LAI values range between 2 and 3, while simulated LAI is nearly doubled. While the "online" version also overestimates LAI compared to AVHRR-derived values, the discrepancy is less pronounced than in the "default" version (Figure **4.6**).

A general issue with the comparisons presented above is that we compare data derived from measurements that include human-influenced land covers with simulations of natural vegetation. For many variables such as GPP or NPP (and to some degree also LAI), croplands and forests do not necessarily differ hugely such that the comparison is qualitatively useful, in particular since the purpose is to demonstrate that the coupling with herbivory does not push the model into an unrealistic state.

For carbon mass, the products we use here are for forests only and also include managed forests Figure **4.7**. Overestimation of these data by our simulations is thus expected, as seen in particular in the comparison to Saatchi et al. (2011) for the forest vegetation carbon mass in Africa. For European forests, the dataset from Pugh et al. (2023), which attempts to be as close to an undisturbed state as possible, matches the modelled vegetation carbon best for both model versions. Compared to the non-cropland and non-pasture biomass (AGB) levels, based on the ESACCI from Santoro and Cartus (2021), the "default" and the "online" versions of LPJ-GUESS both show an overestimation in areas with low aboveground biomass and an underestimation in areas with high aboveground biomass.

Figure **4.8** compares herbivore biomass levels and herbivory consumption between the "default" and "online" versions of the Madingley model, illustrating the relationship between grid cell herbivore biomass density (and herbivory consumption) and grid cell NPP. In the "default" Madingley model, herbivore biomass exhibits minimal variation with grid cell NPP, in contrast to the "online" version. This results in a power-law relationship with a steeper slope for the "online" model, aligning more closely with the power-law derived by Cebrian (2004) compared to both the "default" and "offline" versions (Figure **4.8**). However, the general response of

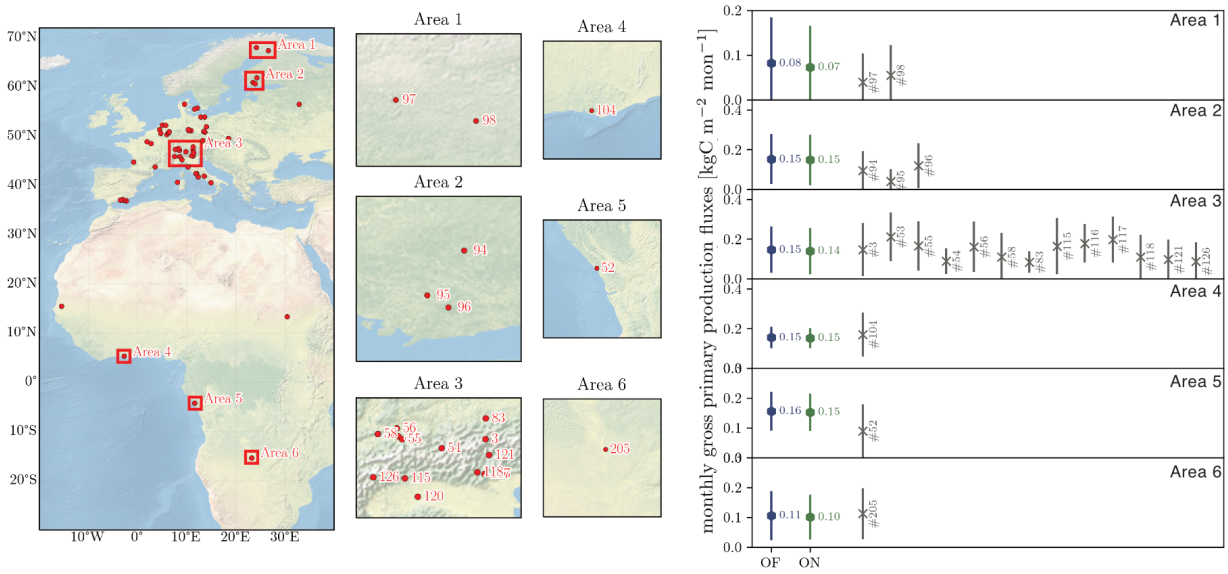

Figure 4.5 (Left) Distribution of FLUXNET eddy covariance measurement sites over the model domain with selected areas and station numbers. (Right) Comparison between "default" LPJ-GUESS (DF), the "online" simulation (ON) and the FLUXNET measurements with station number. The displayed GPP fluxes are monthly fluxes from the selected area which contains the FLUXNET sites. Simulated GPP are for the period 1994 to 2014. The time spans of the corresponding eddy flux data (within that same period is provided by the separate FLUXNET stations and can be found in Figure **2.8**. Background map "Shaded Relief and Water – large 3.2.0" by Natural Earth I (download under https://www.naturalearthdata.com/downloads/10m-natural-earth-1/10m-natural-earth-1-with-shaded-relief-and-water/).

herbivore biomass to underlying grid cell NPP is still overestimated by one order of magnitude for high-productive ecosystems and by two orders of magnitude for low-productive ecosystems.

Herbivory consumption rates in the "default" version also show little sensitivity to grid cell NPP. The "online" version, however, shows a power-law relationship with a steeper slope than those fitted against the "default" and "offline" versions. We previously demonstrated that "online" coupling reverses the increase in animal biomass observed with "offline" coupling (Figure **4.8**). However, this reversal does not affect the emergent power laws, as the underlying vegetation also undergoes significant reductions.

While the herbivore biomass to NPP relationship varies significantly across model versions, the herbivory consumption rate to NPP relationships for all versions are similar to the relationship described by Cebrian (2004).

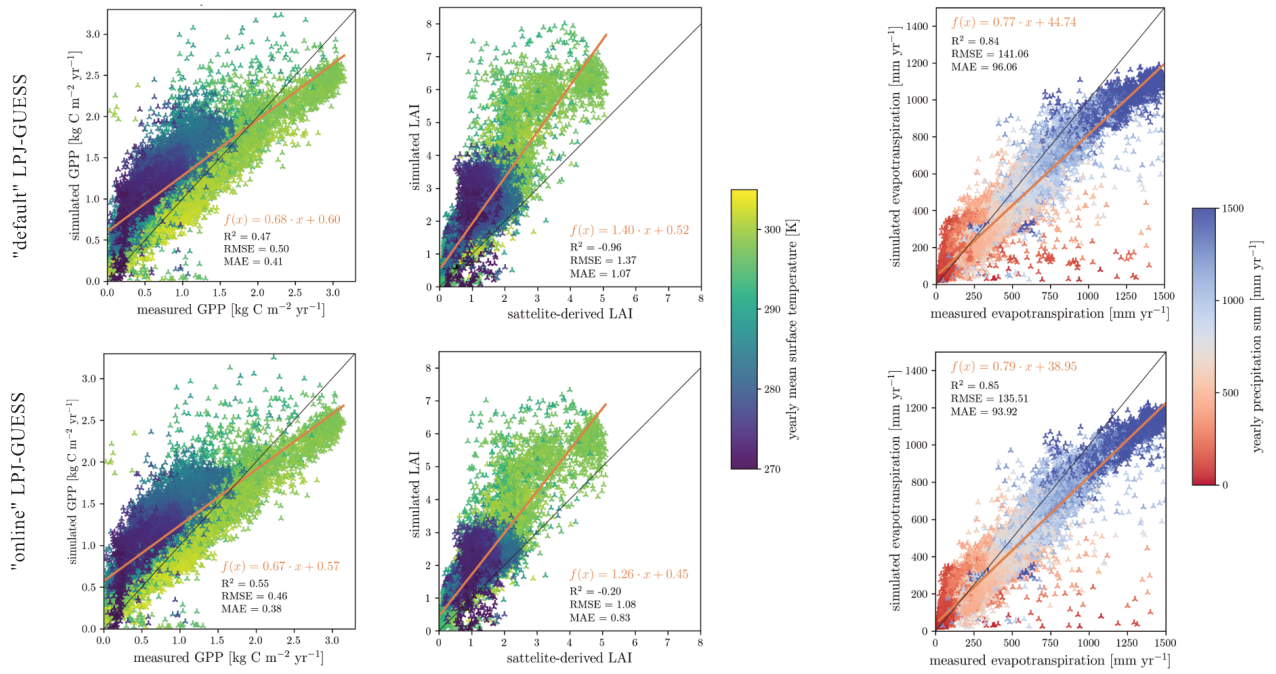

Figure 4.6 (Left) Linear fit of simulated and site-based estimated GPP from the FLUXCOM dataset (Tramontana et al. 2016). (Middle) Linear fit of simulated and measured LAI from the AVHRR dataset (Fang et al. 2019). (Right) Linear fit of simulated and measured evapotranspiration from the GLEAMv33a dataset (Miralles et al. 2011). All figures used model output between 1980-2014. Each marker shows the average of a grid cell over the 34-year timespan. The marker colours indicate the grid cell's yearly average near-surface temperature and precipitation sum.

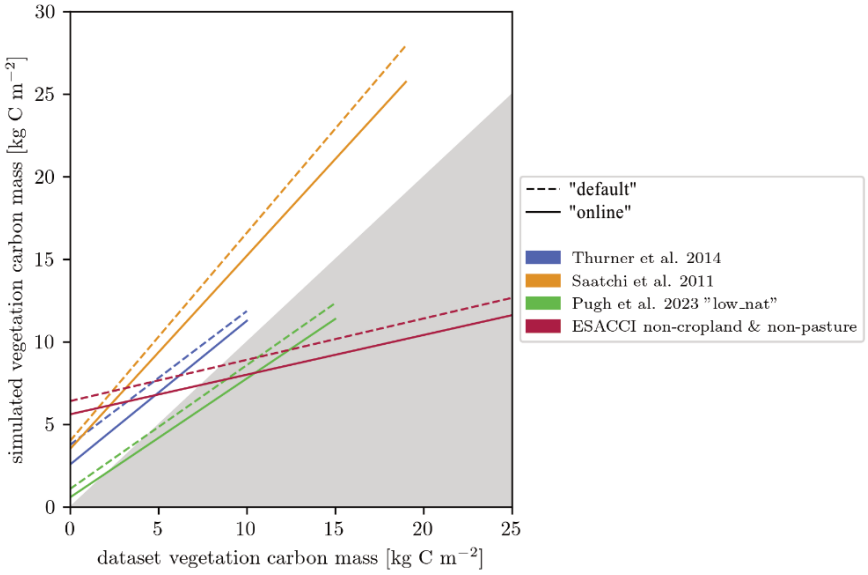

Figure 4.7 Linear fit of simulated and measured vegetation carbon mass for four datasets.

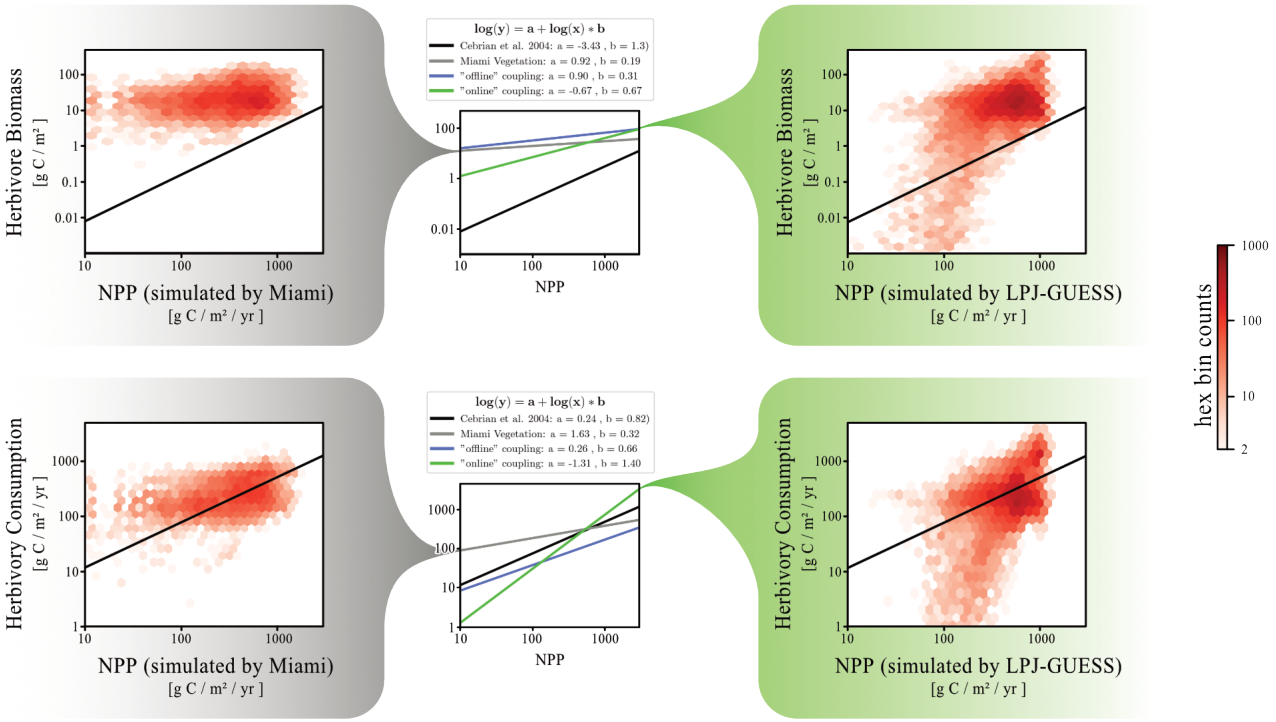

Figure 4.8 Power-law relationships between herbivore biomass and grid cell productivity, as well as herbivory consumptions and grid cell productivity. The red saturation of each hexagon represents the number of data points found in the model system that matches the NPP and the herbivore biomass (or herbivory consumption) of that hexagon's position in the grid. The left distributions show data from "default" Madingley (driven by the Miami model), while the right distributions show data from "online" Madingley. In the middle of the figure, power-law relationships are summarised for all three Madingley model versions. The black line in each plot displays the power-law derived by Cebrian (2004).

4.2 Discussion

The results presented in the previous chapter must be interpreted in the context of our simulations' limitations. We examine the coupling-induced impacts in our simulations alongside the technical processes underlying these outcomes. Next, we discuss the evaluation in light of excluding human activities from the model system and discuss how our simulations are expected to compare with real-world data.

4.2.1 About the Impacts of Animals on Modelled Vegetation

A high abundance of herbivores often reduces vegetation biomass (Dangal et al. 2017; Jia et al. 2018; Schmitz et al. 2014; Staver et al. 2021). This reduction, in principle, should also reduce canopy photosynthesis, although the effect may be partially compensated by more light reaching into the lower layer of the canopy. We, therefore, expected a reduction of plant biomass as a response to the herbivore introduction. While the effects across the modelled domains are small, spatial variation in the impacts is visible, indicating biome-specific dynamics. Nevertheless, the overall response shows a reduction in productivity, vegetation biomass, autotrophic respiration and LAI, as we expected.

The spatial patterns we found in our simulations show that under boreal climate conditions, the impact of leaf damage on photosynthesis may be more noticeable than in warmer climates. Boreal ecosystems are characterised by a shorter growth season with fewer days that allow high photosynthesis rates. When leaves are damaged by herbivory, this limitation becomes even more constraining. The reduced photosynthesis rates cannot be compensated by an increased light transfer to deeper canopy layers. Similar trends to shifts in canopy compositions were previously described in studies investigating general empirical relationships between herbivores and ecosystem productivity and structure: Schmitz et al. (2014) argued that in boreal ecosystems, leaf damage caused by moose can cause declines in CO_2 uptakes and storage directly by browsing on photosynthetic tissue and indirectly through suppressing of tree growth. In other boreal forests, moose were reported to lower primary productivity of tree species (Bonan 1992; Kielland and Bryant 1998; Schmitz et al. 2003). Another aspect of the herbivory response in central and northern Europe is that broadleaf summergreen PFTs are becoming more prominent. In reality, evergreen plants grow leaves that are less nutritious than leaves of deciduous plants, and animals choose their nutrition source depending on the nutrient content (Villalba and Provenza 2009). In contrast, animals modelled by the Madingley model attempt to meet their metabolic cost by consuming evergreen and deciduous plants without taking leaf C:N ratios into consideration. The impact observed through, e.g., moose selectively browsing on deciduous vegetation is not yet included. Still, our modelled responses broadly go in the right direction, although at the moment, we expect animals to over-prioritise evergreen vegetation in our coupled model system.

For the African continent, both LPJ-GUESS versions overestimate productivity, LAI, and vegetation carbon mass. Staver and Bond (2014) found that large browsers are likely to suppress tree establishment in savannas by damaging young trees. Releasing browsing pressure contrarily led to tree establishment. They also found that large grazer populations, especially wildebeest and impala, exert significant pressure on grassland ecosystems directly through biomass removal and indirectly via grazer-grass-fire interactions. The effects of grazers tempering wildfires by removing potential fuel are often described alongside the control over the amount of organic matter biomass and nutrients entering the soil pool (Schmitz et al. 2014). Pachzelt et al. (2015), who also used LPJ-GUESS in combination with a grazer-specific population model, found that a high grazer density asserts a substantial impact on grass biomass, tree biomass and burned area. Their herbivory-induced responses in vegetation mass are similar to the responses found in our simulations. The importance of grazers is also highlighted by Kiffner and Lee (2019), who showed that herbivore grass consumption can triple browse consumption, as reported in Lake Manyara Nation Park in Tanzania. However, the coupled model system so far does not differentiate herbivores into grazers and browsers.

4.2.2 Evaluation of the Coupled Model System

Human activities, including timber harvesting, livestock grazing, and the general disruption of natural trophic chains, are expected to influence the large-scale empirical datasets used in this evaluation, either directly or indirectly (Ripple et al. 2015; Wardle and Bardgett 2004). These impacts can lead to either increases or decreases in total biomass compared to the hypothetical human-free world, which we simulate in this chapter. In Africa, for instance, the human pressure on dry forests and savannas is high due to the dependence of people on savanna ecosystem goods and services like timber for construction, fuelwood and charcoal, land surface for livestock grazing and wildlife tourism (Osborne et al. 2018). Such pressure likely explains in part the model system's overestimation of the observed ecosystem's carbon stocks throughout the African continent. Conversely, forest management across the forested areas of Europe (which are dominated by northern temperate and boreal forests) may not lead to reductions in total biomass. Lindeskog et al. (2021) for instance found little difference in simulations of forest above-ground carbon with and without wood harvest in LPJ-GUESS. Erb et al. (2018) also found reductions in aboveground biomass stock in used tropical and subtropical forests and savannas that were substantially larger than reductions in used boreal forests - and also larger when compared to managed temperate forests, even though the differences were less pronounced.

Additionally, the significant impact of human activity on trophic chains complicates the comparison of our results, particularly when comparing results with and without trophic chains in an otherwise undisturbed vegetation. Large-scale ecosystem disruptions have included widespread reductions in apex predators such as lions, cougars, and wolves (Morris and Letnic

2017; Terborgh et al. 2001), cascading effects on large herbivore populations (Holdo et al. 2009), and the exclusion of smaller predators like foxes through fencing for livestock protection (Croll et al. 2005). Despite local variations, the long-standing scientific consensus holds that these disruptions to the trophic chain contribute to the overall degradation of worldwide ecosystems and impact global vegetation biomass (Estes et al. 2011). Our simulations exclude human activities such as forest management, land use, and direct alterations of the trophic chain. Consequently, when comparing our simulation results to empirical data, we expect an overestimation of forest vegetation carbon masses in both the "default" and the "online" versions of LPJ-GUESS.

Confidence in overall model performance is bolstered by the good fit against the estimates by Pugh et al. (2023), which were derived from areas with relatively little direct human impact. Still, these estimates themselves are strongly model-based and include simulations from LPJ-GUESS with an adjusted natural disturbance function compared to our model version. This methodological overlap likely contributes to the observed agreement. Furthermore, the estimates by Pugh et al. (2023) are approximately 30% lower than those reported by Thurner et al. (2014), who estimated low uncertainty regarding human influence in their dataset. Despite this discrepancy, the results from both Thurner et al. (2014) and Pugh et al. (2023) align closely with our simulation outputs.

Generally, vegetation datasets for Europe exhibit a better match with our simulation results than those for Africa. As mentioned above, the degradation of savanna biomes due to the impacts of human activity can have more drastic effects on total vegetation biomass when compared to forest management in European forests. This difference may help explain the stronger agreement between our simulations and European datasets.

The power-law relationships derived from simulations of the various Madingley model versions suggest that the "online" version best represents animal population responses to underlying vegetation productivity. We draw this conclusion since the "online" version's power-law slope aligns best with the empirical relationship reported by Cebrian (2004), whilst maintaining a realistic representation of herbivore consumption rates. However, a notable overestimation of herbivore biomass, as first highlighted in Figure 5 of Harfoot et al. (2014), remains evident.

Our study results show that including herbivory via the coupled model system still upholds Madingley's and LPJ-GUESS's ability to produce realistic biome plant species distributions, carbon fluxes and animal population distributions. Nevertheless, it is important to acknowledge that the empirical measurements underpinning these comparisons likely reflect human influence, which is not accounted for in the Madingley model. In the following, we address the limitations arising from the exclusion of these human impacts.

4.3 Summary

In this Chapter, we examined the impacts of herbivore feedback on vegetation dynamics simulated in LPJ-GUESS by comparing the "default" version of the model with the "online" coupled version. The "online" simulations, which incorporate bidirectional feedback between vegetation and herbivores, resulted in a domain-wide reduction of ecosystem net primary productivity (NPP) by -5%, leaf area index (LAI) by -9%, and vegetation carbon mass by -10%. These effects were most pronounced in the boreal domain, where vegetation carbon mass decreased by -42%.

We also analysed herbivore population dynamics by comparing the "default" and "online" versions of Madingley. The "online" version showed reduced biomass density across all functional groups, driven by an overestimation of NPP throughout most of the domain. However, in regions where LPJ-GUESS simulated high NPP, the "online" herbivore populations are similar to those of the "default" version.

Evaluation of output from both the "default" and the "online" version of LPJ-GUESS against remote sensing datasets and flux measurements highlighted that the coupled LPJ-GUESS/Madingley model preserves LPJ-GUESS's ability to predict realistic biome distributions and carbon pools. We also compared power-law relationships of herbivore population dynamics for all three different versions of the Madingley model and concluded that the "online" version surpasses both other versions in terms of representing similar power-laws derived from empirical data.

With the coupled model system in place, we are now in a position to explore different use cases of such a model system. One of those cases is presented in the following Chapter in the form of investigating the removal of large animals and ecosystem capabilities to recover from such removal.

5 The Effect of Large Animal Removal and Conservation under the Future of Climate Change

5.1 Results

In this Chapter, we investigate the impact of large animal removal on simulated vegetation. The analysis covers the isolated effect of large animal removal under constant climate conditions on both the simulated canopy composition and Madingley's remaining animal cohorts. Building upon that, we analyse simulation results with large animal removal and climate change affecting the model system simultaneously. Finally, we quantify to which extent large animal removal is reversible in our model system.

Notably, Madingley represents leaf biomass as wet matter ($\mathrm{kg\,km^{-2}}$), while LPJ-GUESS expresses leaf biomass as carbon mass ($\mathrm{kg\,C\,km^{-2}}$). Since leaf carbon mass is directly proportional to leaf wet matter, the change rates of both measures are identical. For simplicity, we are referring to leaf biomass in the following Chapter since we only present proportional changes.

5.1.1 Quantify the Isolated Effect of Large Animal Removal

Animal Biomass Densities

Figure **5.1** shows the response of overall AFT biomass density and the animals' size distribution during the last time step of the simulation under the 1850-1880 recycled climate conditions. Table **5.1** shows herbivore, carnivore, omnivore and leaf biomass responses to removing large herbivores or carnivores from the four experiment model domains.

Table 5.1 Average large herbivore and carnivore removal effects on biomass densities under constant climate and CO_2. The values reflect data over the final 30 years of the simulation.

Metric Affected	**Response to Herbivore Removal**	**Response to Carnivore Removal**	**Metric Affected**	**Response to Herbivore Removal**	**Response to Carnivore Removal**
Temperate Mixed Forest (**EU1**)			Boreal Evergreen Forest (**EU2**)		
Herbivore Biomass	-3.4%	-2.3%	Herbivore Biomass	-43.1%	+7.2%
Omnivore Biomass	-0.2%	+4.0%	Omnivore Biomass	+75.5%	-1.9%
Carnivore Biomass	-0.5%	-4.7%	Carnivore Biomass	-1.4%	-11.0%
Leaf Biomass	+0.7%	+0.5%	Leaf Biomass	+9.7%	-5.9%
Tropical Rainforest (**AF1**)			Moist Savanna (**AF2**)		
Herbivore Biomass	-55.8%	+149.3%	Herbivore Biomass	-57.1%	+141.2%
Omnivore Biomass	+23.2%	+101.0%	Omnivore Biomass	+7.2%	+76.8%
Carnivore Biomass	-7.1%	-1.8%	Carnivore Biomass	-4.8%	-10.4%
Leaf Biomass	+4.7%	-19.3%	Leaf Biomass	+6.1%	-19.2%

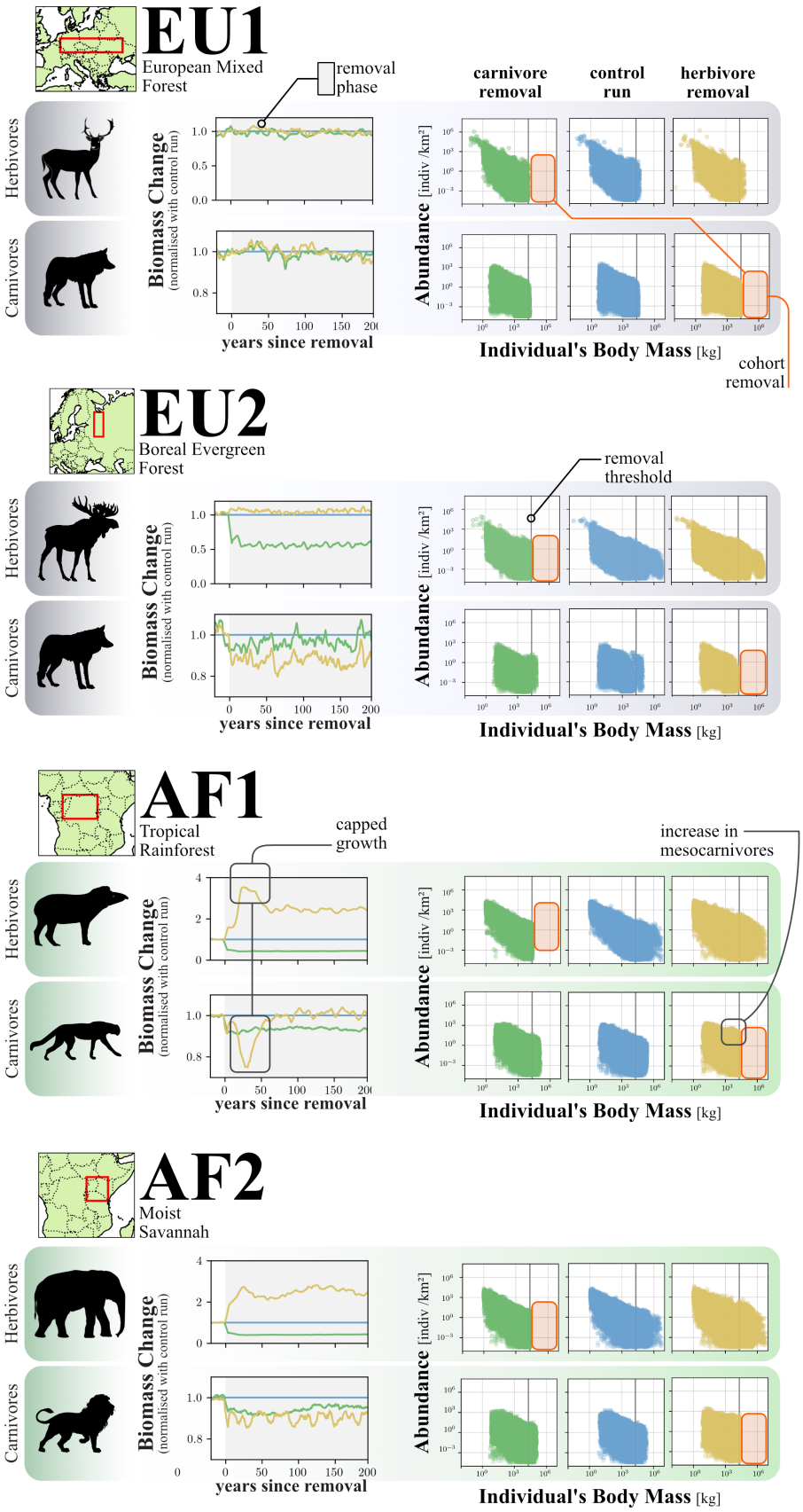

Figure 5.1 Animal population responses to cohort removal without the impact of climate change (applying re-cycled, detrended climate conditions) in the experiment's four locations. The left panels depict the domain-averaged biomass of herbivores and carnivores, normalized relative to the control simulation. A five-year moving average was used to smooth annual climate-driven fluctuations while preserving short-term responses, such as the rapid changes observed at the onset of cohort removal. The right panels show the size distribution of animal cohorts. Each point represents one cohort within a location domain during the final timestep of the simulation. Consistent colour coding is used throughout the figure: Blue indicates data from the control simulation without any cohort removal, green indicates data from a simulation where herbivores heavier than 21 kg were removed and yellow indicates data from a simulation where carnivores larger than 21kg have been removed. Grey background shading indicates the active removal window. In Af1, "capped growth" marks the feedback-driven growth cap of herbivores and omnivores following the removal of large carnivores. We also mark a typical hump shade that indicates an increase in mesocarnivores.

In the European mixed forest domain (EU1), the impact of large animal removal is negligible. Madingley simulates only a small population of animals with an adult body mass exceeding 21 kg. As a result, the removal affects only a limited number of individuals, leading to minimal observable differences between the control and removal panels in Figure **5.1**. In the **boreal evergreen forest** domain (EU2), removing large herbivores causes a -43% decline in overall herbivore biomass while elevating omnivore biomass by +76% (Table **5.1**). The predominantly evergreen vegetation assures that animals have a reasonable supply of nutrition during winter, which in Madingley supports a population of large herbivores to emerge, although ectothermic (small and mesoscale) herbivores struggle to reach high abundances. Omnivores benefit from herbivore removal because, in boreal environments where leaf biomass is the limiting resource, the removal of their primary competitor for this resource outweighs the potential loss of prey density. Removing carnivores from the simulation at the EU2 location only slightly elevates herbivore biomass since the release from predation affects mostly mesoscale herbivores and omnivores (not shown).

While the European animal population responds significantly only within the EU2 domain, primarily to large herbivore removal, the African animal population responds to the removal of both herbivores and carnivores, with the strongest response to the latter. Differences between the responses in Europe and Africa cannot be explained by the different evergreen-to-deciduous ratios of the model domains. In Madingley, feed quality so far is not yet accounted for, and evergreen and deciduous leaf biomass is treated equally valuable. In the African **tropical rainforest** domain (AF1), the removal of large herbivores leads to a substantial reduction in herbivore biomass (-56%) and a moderate decline in carnivore biomass (-7%) (Figure **5.1**). Conversely, omnivore biomass increases significantly (+23%), suggesting a compensatory dynamic within the food web. However, large omnivores cannot completely fill the herbivory consumption gap because they themselves are predators that depend on an abundance of large prey. While facing less competition regarding herbivory, omnivores also experience a shortage of prey after removing large herbivores. A new biomass equilibrium in AF1 is achieved relatively quickly, within approximately 10 years of herbivore removal.

In contrast, removing large carnivores from AF1 results in marked increases in herbivore (+149%) and omnivore (+101%) biomass (Table **5.1** and Figure **5.1**), aligning with previous findings by Hoeks et al. (2020). However, unlike Hoeks et al. (2020), our study reveals a pronounced transient response within the first 30 years of carnivore removal. During this period, herbivore (and omnivore, not shown) biomass overshoot their eventual equilibrium values, reaching peak increases of +254% (and +236%, respectively). Carnivore biomass exhibits an initial sharp decline (-25%), followed by a rapid recovery that ultimately stabilises at a small net decrease (-2%) (Figure **5.1** and Table **5.1**). We expect that the overshooting response observed in our experiment to be caused by the bidirectional feedback with the underlying vegetation;

the vegetation in Hoeks et al. (2020) was unaffected by herbivory damage, whereas herbivores in our simulations persistently damaged plants.

In the **moist savanna** domain (AF2), the removal of large herbivores decreases herbivore biomass (-57%) and carnivore biomass (-5%). Similar to AF1, omnivore biomass increases, but only by +7%. The removal of large carnivores from AF2 triggers an initial surge in herbivore biomass similar to AF1, but to a much lesser degree in the open vegetation structure of AF2 minimises pronounced overshooting. After an initial peak 25 years post-removal, herbivore biomass stabilises near the peak level, increasing by +141% (Table **5.1**). Omnivore biomass follows a similar trend but with a delay of approximately two years, peaking at +85% before stabilising at +77%. This temporal delay and the close relationship between herbivore and omnivore biomass suggest that large omnivores in AF2 are strongly controlled by large herbivore abundance. In the absence of large carnivores, large omnivores are the sole large predators in this system and play a critical role in regulating herbivore population growth.

The body sizes of the largest omnivores in African ecosystems remain unaffected by the removal of either large carnivores or herbivores. These ecosystems support omnivores up to the maximum body size predicted by the AFT (200kg) (see Table **5.2**). While the total biomass of omnivores increases in response to the removal, this increase is driven exclusively by a rise in their population abundance rather than by changes in individual body size.

Canopy Composition

Figure **5.2** shows the impact of the removal on the PFTs in the four model domains on green leaf biomass. In the European mixed forest (EU1), the low numbers of large mammals in the modelled animal population (Figure **5.1**) also result in leaf biomass responses being absent. In the European **boreal evergreen forest** (EU2), however, leaf biomass is reduced by -6% following the removal of large carnivores. By contrast, leaf biomass increases by +10% in response to herbivore removal, but no significant shifts are found in the PFT distribution. In the African model domains, changes in leaf biomass and PFT composition are visible after removing animals from the simulation. A lasting decline in leaf biomass follows the removal of large carnivores, which is much stronger compared to EU2. The increase in leaf biomass in response to herbivore removal is also visible, but in this case, it is less pronounced than in EU2.

In the **tropical rainforest** domain (AF1), we find an immediate drop in leaf biomass following the removal of large carnivores as herbivory increases. This reduction is most prominent for the dominant, relatively shade-tolerant tropical broadleaf evergreen (TrBE) trees. Similar to our findings in Chapter **4.1.1**, shade-intolerant tropical broadleaf evergreen trees are not impacted as strongly. This is partly due to the compensatory effect of increased light reaching the forest floor, combined with the low abundance of shade-intolerant species typical of ecosystems in the late stages of succession. In contrast to tree PFTs, the herbaceous understory benefits from removing large carnivores, which seems contradictory, given the larger pressure from herbivory.

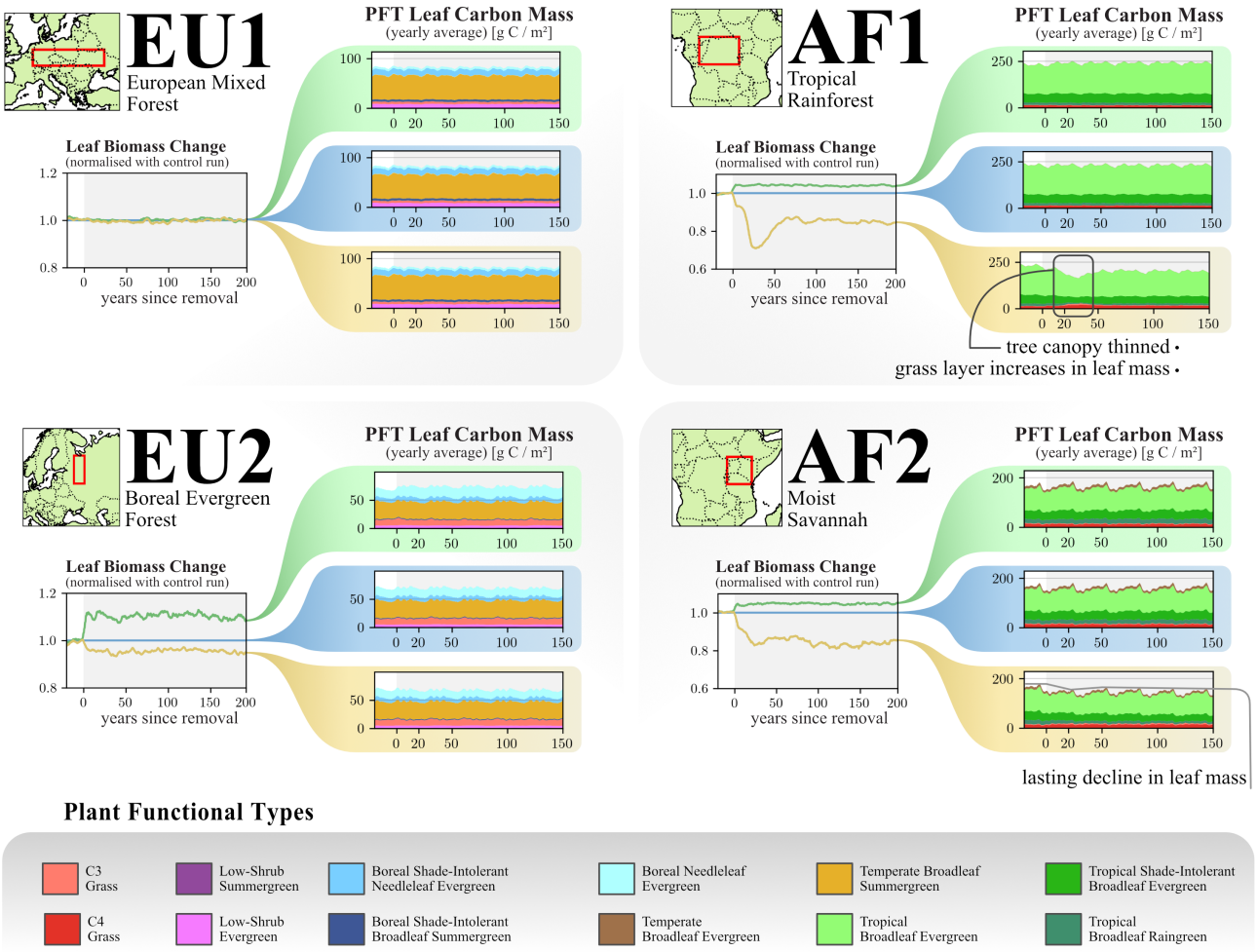

Figure 5.2 PFT leaf carbon mass responses to cohort removal without the impact of climate change (applying re-cycled, detrended climate) at the experiment's four locations. The left side of each panel depicts domain-averaged leaf biomass change in response to Madingley's herbivory, normalized relative to the control simulation. The right side of each panel presents a stacked time series of the different PFTs' annual average leaf (carbon) biomass. A five-year moving average is used to smooth annual climate-driven fluctuations while preserving short-term responses. Consistent colour coding is used throughout the figure: Blue indicates data from the control simulation without any cohort removal, green indicates data from a simulation where herbivores heavier than 21 kg were removed and yellow indicates data from a simulation where carnivores larger than 21kg were removed. PFT Colour coding is labelled underneath the figure. Grey background shading in the time series indicates the window in which the removal is active.

In the model system, more light reaching the ground doubles the leaf biomass of grasses in the tropical rainforest until about 50 years after the removal was applied (see Figure **5.2**), as more photosynthetic active radiation is available for herbaceous photosynthesis (not shown). In response to herbivore removal, an increase in total leaf biomass is visible but less pronounced than in EU2 (+5%). In the **moist savanna** domain (AF2), the long-term response to carnivore removal is comparable to AF1. However, transient effects are more prominent in AF1. Similarly, the response to large herbivore removal mirrors the herbivore removal response observed in AF1.

5.1.2 The Effects of Large Mammal Removal under Climate Change

Figure **5.3** illustrates the vegetation's response to cohort removal under climate change. The EU1 domain is excluded from this analysis due to the lack of response to simulated herbivore and carnivore removal (Figure **5.1** and **5.2**), as these response patterns did not change during the climate change experiment. In the absence of animal removal in the **boreal evergreen forest** domain (EU2), the leaf biomass of boreal needleleaf trees (BNE) increases during the first half of the 21st century (2005–2050). However, from 2050 onward, BNE leaf biomass declines under both climate change scenarios, likely due to warming temperatures. Rising temperatures in both scenarios gradually shift the EU2 domain towards a temperate mixed forest. This effect is more pronounced under the RCP 7.0 high-warming scenario than under the RCP 2.6 low-warming scenario. By the end of the control simulations, the abundance of large herbivore cohorts naturally decreases, particularly under RCP 7.0 (Figure **5.3**).

The removal of large herbivores in EU2 promotes the growth of BNE trees, especially from around 2000 onwards until approximately 2050. In contrast, the removal of large carnivores results in a reduction of BNE leaf biomass, which remains at near-constant levels from around 2000 until 2050. Beyond 2050, BNE leaf biomass decreases sharply also in the herbivore and carnivore removal experiments, converging to similar levels as in the control run by 2100. In all EU2 simulations under both RCP scenarios, the leaf biomass of temperate broadleaf summergreen (TeBS) trees increases steadily throughout the 1960–2100 period.

In the **tropical rainforest** domain (AF1), without the impact of large animal removal, the leaf biomass of tropical broadleaf evergreen (TrBE) trees increases steadily from 1950 onward. Under RCP 7.0, TrBE leaf biomass continues to rise consistently throughout the 21st century. In contrast, under RCP 2.6, TrBE leaf biomass stabilises around 2070. The leaf biomass of other PFTs remains constant throughout the simulation, making TrBE trees the sole contributors to the overall increase in leaf biomass. Notably, the total leaf biomass is higher under RCP 7.0, driven by a stronger CO_2 fertilisation effect compared to RCP 2.6.

The removal of large herbivores in AF1 slightly increases total leaf biomass under both RCP 2.6 and RCP 7.0 scenarios. A much more pronounced response occurs with the removal of large

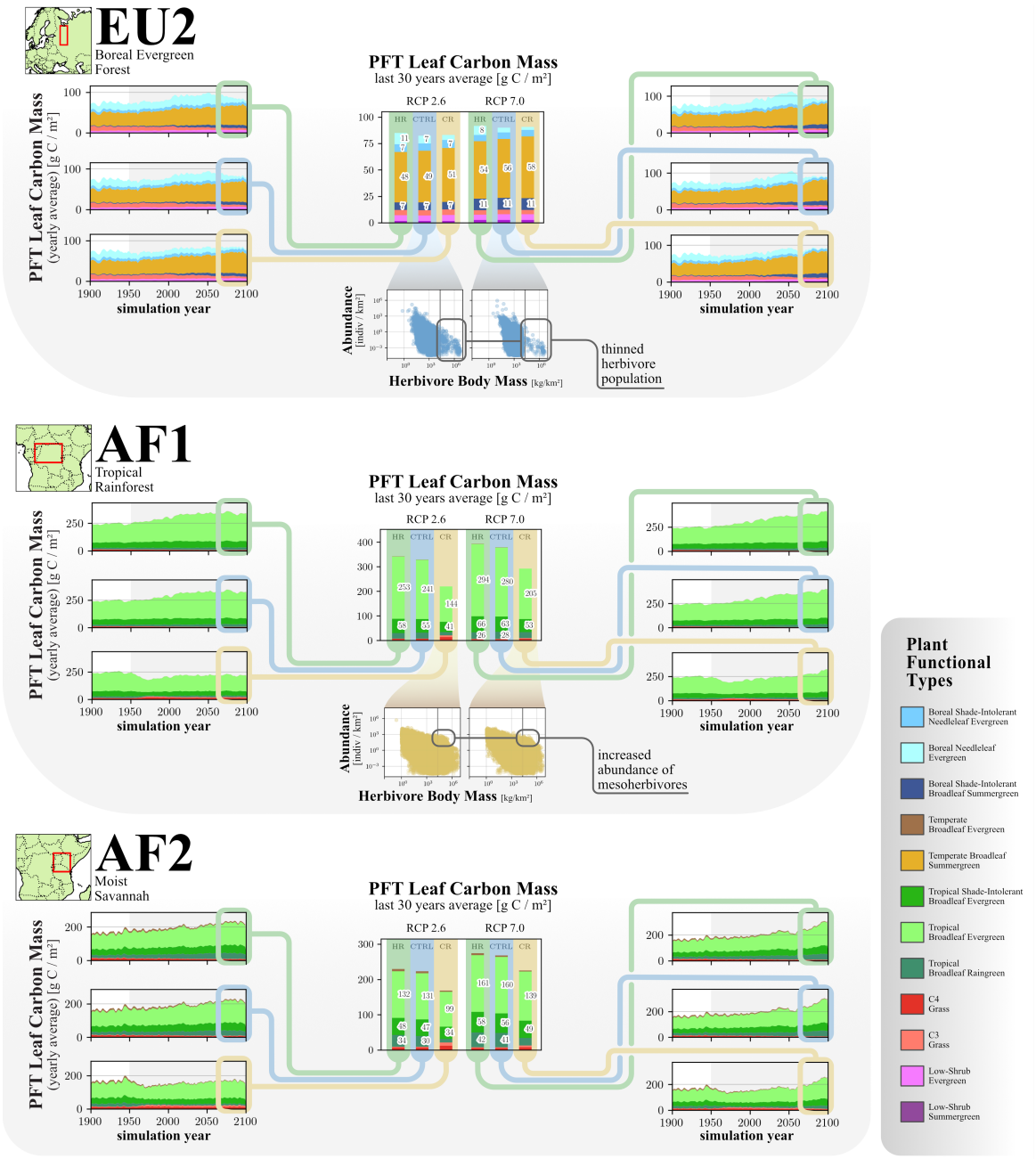

Figure 5.3 PFT leaf carbon mass responses to cohort removal under RCP 2.6 and 7.0 climate. The same locations are shown, as in Figure **5.2** , except for EU1, where removal impacts were minimal. Each panel shows stacked time series of the different PFTs' annual average leaf (carbon) biomass from 1900-2100. Timeseries to the left show simulations under RCP 2.6 climate, while those to the right show simulations under RCP 7.0 climate. A five-year moving average was used to smooth annual climate-driven fluctuations while preserving short-term responses. The last 30 years of each simulation are averaged and summarised in the middle of each panel. Notable shifts in herbivore populations are presented underneath this summary (for the control simulation in EU2 and the carnivore removal case in AF1). AF2 shows similar shifts in animal population as AF1 (not shown). Consistent colour coding is used throughout the figure: Blue timelines and background shading indicate data from the control simulation without any cohort removal, green indicates data from a simulation where herbivores heavier than 21 kg were removed and yellow indicates data from a simulation where carnivores larger than 21 kg have been removed. Grey background shading in the time series indicates the window in which the removal is active. PFT Colour coding is labelled next to the figure.

carnivores. The immediate impact on canopy composition closely resembles the response to large carnivore removal in the absence of climate change (Figure **5.2**), marked by a sharp decline in TrBE leaf biomass and a corresponding increase in C4 grass biomass. Under RCP 2.6, total leaf biomass increases after the initial decline and stabilises after 2010. Large carnivore removal in AF1 promotes the abundance of herbivores (and also omnivores) weighing between 20 to 100 kg, which likely causes the absent (RCP 2.6) and smaller (RCP7.0) leaf biomass increase compared to the control run.

In the **moist savanna** domain (AF2), overall leaf biomass response to climate change is similar to AF1. Under both scenarios, leaf biomass of temperate broadleaf trees - absent in AF1 - declines throughout the simulation due to the expansion of tropical climate zones. The removal of large herbivores or carnivores leads to responses similar to those in AF1.

5.1.3 Reverting the Effects of Animal Removal

Figure **5.4** shows the effect of lifting the otherwise consecutive large carnivore or herbivore removal after 100 years in a simulation without climate change, using AF2 as an example region. After ending the removal of large animals, the size spectrums of the different AFTs recover over time. Table **5.2** shows the recovery rates of the endothermic animal size spectrums. When the removal of large herbivores ends, overall herbivore biomass increases slowly until the end of the simulation period. Reinstating the full spectrum of herbivore body masses (i.e. achieving equilibrium biomass) would likely take centuries since large herbivores are overall substantially heavier than carnivores. Two hundred years after stopping removal, the heaviest herbivore found in the model domain weighs 89 kg instead of 5 t in the undisturbed state. Thus, the upper end of the herbivore size spectrum grew 68 kg in 200 years, recovering only 1.4% of the equilibrium size spectrum.

Prior to carnivore removal, the largest carnivore found in the model domain weighs 209 kg. Two hundred years after ending the removal, the largest carnivore living in the model domain weighs 113 kg, reflecting a recovery of 49% of their undisturbed size spectrum. By contrast, two hundred years after ending the large carnivore removal, the herbivore biomass is more or less similar to the undisturbed (pre-removal) state. While the increase in herbivore biomass following carnivore removal is exclusively driven by an increase in the abundance of large herbivores, the subsequent decrease after the removal ends reflects not only a corresponding reduction in large herbivore abundance but also a decline in the maximum body mass of herbivores (Table **5.2**). Omnivore biomass levels closely track herbivore biomass trends both during and after the removal of large carnivores. After lifting the removal, the abundance of large and mesoscale omnivores declines, eventually returning to levels simulated prior to the disturbance.

Table 5.2 Recovery potential of different AFTs in the moist Savanna biome after ending large herbivore or carnivore removal. The table presents data for endothermic herbivores, omnivores, and carnivores, detailing the weight of the heaviest individual, the average weight of the 10 heaviest individuals, and the average weight of the 95th percentile of individuals. Animal weights are reported for three singular timesteps during the simulations: the undisturbed equilibrium state prior to removal (pre-removal phase), the equilibrium state with the removal employed (removal phase), and the recovering state 200 years after the removal ended (post-removal phase).

AFTs Analysed	**Simulation State**	**Top 1**	**⌀ Top 10**	**⌀ Top 5%**
	Moist Savanna (**AF2**) under herbivore removal			
Herbivores	pre-removal phase	5.000 kg	4.396 kg	364 kg
	end of removal phase	21 kg	21 kg	21 kg
	post-removal phase	89 kg	78 kg	52 kg
Omnivores	pre-removal phase	200 kg	200 kg	112 kg
	end of removal phase	200 kg	200 kg	113 kg
	post-removal phase	200 kg	200 kg	118 kg
Carnivores	pre-removal phase	205 kg	178 kg	99 kg
	end of removal phase	88 kg	84 kg	63 kg
	post-removal phase	174 kg	173 kg	104 kg
	Moist Savanna (**AF2**) under carnivore removal			
Herbivores	pre-removal phase	5.000 kg	4.396 kg	351 kg
	end of removal phase	5.000 kg	4.666 kg	427 kg
	post-removal phase	4.345 kg	3.744 kg	299 kg
Omnivores	pre-removal phase	200 kg	200 kg	115 kg
	end of removal phase	200 kg	200 kg	157 kg
	post-removal phase	200 kg	200 kg	111 kg
Carnivores	pre-removal phase	209 kg	186 kg	92 kg
	end of removal phase	21 kg	21 kg	21 kg
	post-removal phase	113 kg	109 kg	78 kg

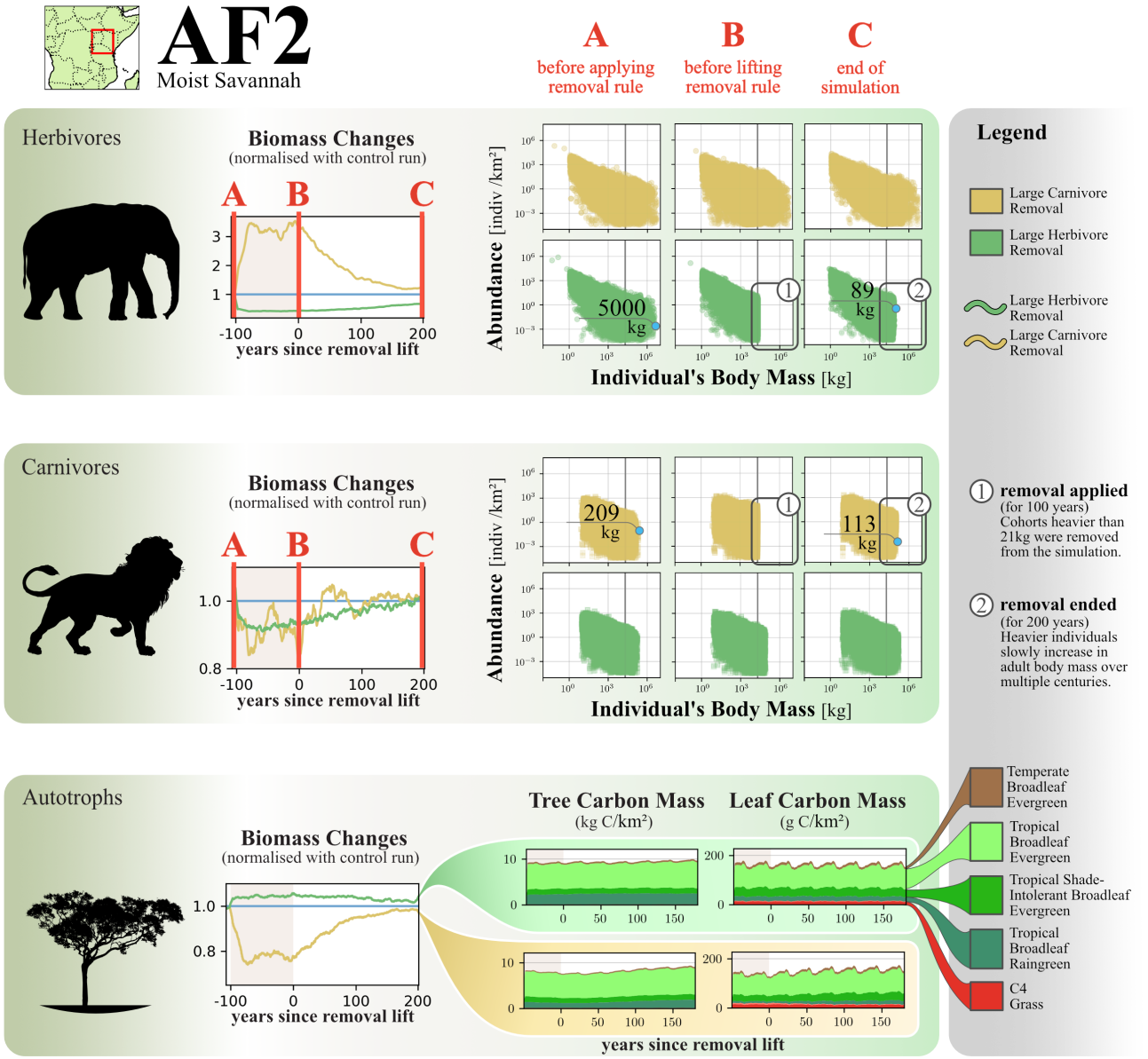

Figure 5.4 The AF2 ecosystem's recovery potential after ending the removal (in the absence of climate change). The figure shows responses in three trophic-specific levels (herbivores, carnivores, autotrophs). The left side of each panel depicts the domain-averaged biomass of herbivores (carnivores, autotrophs) normalized relative to the control simulation. The right side of the herbivore and carnivore panel shows the size distribution of animal cohorts at three different simulation stages. Each point represents one cohort within a location domain during the final timestep of the simulation. (A) shows animal size distributions under undisturbed conditions. (B) shows animal size distributions after 100 years of consecutive animal removal. (C) shows animal size distributions after 200 years of recovery. The right side of the autotroph panels shows a stacked time series of the different PFTs' annual average leaf and tree (carbon) masses. A five-year moving average smooths annual climate-driven fluctuations while preserving short-term responses. Consistent colour coding is used throughout the figure: Green indicates data from a simulation where herbivores heavier than 21 kg were removed, and yellow indicates data from a simulation where carnivores larger than 21kg have been removed. Red background shading indicates the window in which the removal is active. PFT Colour coding is labelled next to the figure.

The overall leaf biomass decreases only slowly after ending the removal of large herbivores. After 200 years, leaf biomass levels have hardly changed and are still elevated compared to an undisturbed state. The response of vegetation to carnivore removal and its subsequent reversal is more pronounced. When large carnivores do not act as predators to herbivores, leaf biomass is substantially reduced (Figure **5.4**). As carnivore biomass increases after ending their removal, herbivore biomass decreases, resulting in a steady increase in leaf biomass towards its undisturbed levels at the end of the simulation period.

Figure **5.5** illustrates the changes in herbivore biomass levels when the removal of large herbivores is only applied partially. Compared to simulations where large herbivores were removed across the entire model domain, herbivore biomass recovers significantly faster after the removal ends. In cases of complete removal, only half of the herbivore biomass recovers within 200 years. In contrast, when large herbivores survive in some parts of the model domain, full herbivore biomass recovery occurs within just 20 years. Moreover, herbivore biomass temporarily overshoots its pre-removal levels before stabilising to similar levels as before the intervention, achieving this equilibrium within 100 years. The Figure also shows the spatial distribution of the maximum weight of individual herbivores found in each grid cell. After reallowing large herbivores in the central area of the model domain, the rapid repopulation of large herbivores in this region becomes evident as they migrate from regions where they weren't removed.

5.2 Discussion

The impacts of large animal removal must be interpreted within the context of two significant limitations in the model. First, the absence of large animals in EU1, which led to the exclusion of said location from further analysis, and second, the unrealistic presence of extremely heavy animals in the tropical rainforest. After addressing these effects, we will analyse the isolated impacts of large animal removal and explore the combined effects of this removal under two different climate change scenarios. Finally, we will consider the implications derived from the ecosystem-recovery experiment.

The Absence of Large Animals in EU1

The removal of large mammals significantly alters the modelled vegetation dynamics in three of the four study domains; however, domain EU1 showed limited response to the cohort removal, which can be explained by the interaction of two critical effects. First, herbivore growth is sensitive to leaf biomass' winter minima, more so than the leaf biomass annual average (see Chapter **3.2.1**). The high seasonality in boreal and temperate environments leads to lower herbivore growth rates compared to ecosystems with more consistent calorific supplies throughout the year. Lowered growth rates extend the time that an individual needs to reach maturity. A prolonged youth also exposes juveniles to predation over a longer period, leading to an overall

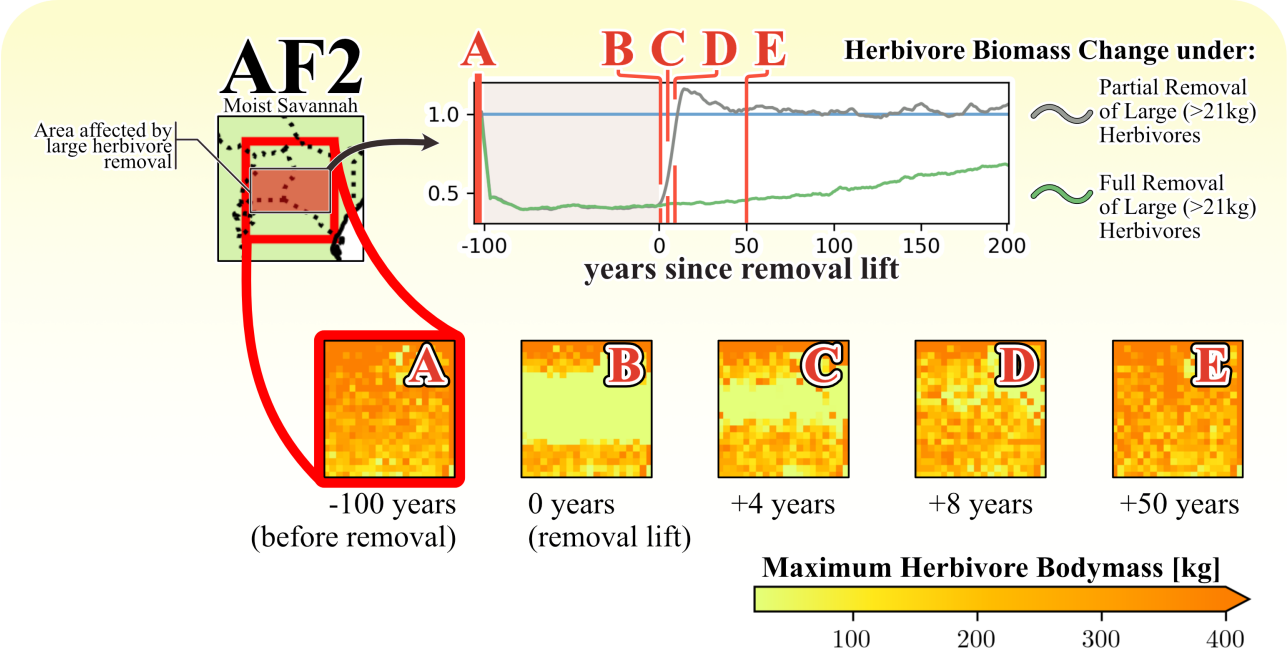

Figure 5.5 The AF2 ecosystem's recovery potential after ending the (partial) removal of large herbivores (in the absence of climate change). The time series depicts the average herbivore biomass in the central domain of the larger AF2 region. All timelines are normalized relative to the control simulation. The green timeline shows herbivore biomass recovery for the simulation, where large herbivores were removed from the entire model domain, similar to the experiment shown in 5.1.1. The grey timeline shows herbivore biomass recovery from the simulation, where large herbivores were exclusively removed from a central corridor of the model domain. Red background shading in the time series indicates the window in which the removal is active. A five-year moving average was used to smooth annual climate-driven fluctuations while preserving short-term responses. For each grid cell, the largest herbivore inhabiting it is identified. Spatial representations of maximum herbivore biomass across grid cells are arranged for five different stages of the simulations.

reduced reproduction success rate. This disadvantage counteracts the inherent advantage large animals usually have over smaller ones and puts them at a competitive disadvantage.

A second reason for the observation in EU1 lies in the coupled model's structure. Only one-third of herbivory damage every year is applied to evergreen vegetation, while the full extent of damage affects deciduous vegetation (see Chapter **2.5**). This method was chosen to avoid simulating unrealistically large herbivory damage in evergreen PFTs. Thereby, the feedback structure also allows evergreen-dominated ecosystems (like EU2) to sustain larger herbivore populations than deciduous forests with a similar leaf biomass stock (like EU1). As a deciduous forest with high seasonality in leaf biomass, EU1 represents a competitional disadvantage for large herbivores and omnivores and, by extension, large carnivores reliant on such prey.

Overestimation of the Maximum Animal Size in the Tropical Rainforest
In our simulations, the largest animals are found in ecosystems with the highest leaf biomass supply. However, this outcome is unrealistic, as we would expect larger animals to thrive in the savannas (AF2) rather than in the rainforests (AF1). This discrepancy between simulation and reality is likely caused by the absence of a vertical feeding structure in Madingley. Unlike in the simulations—where all leaf biomass is equally accessible to large animals—in actual rainforests, the majority of leaf biomass is located in the canopy, far out of reach for ground-dwelling large animals.

5.2.1 The Isolated Effect of Animal Removal

Large Herbivore Removal
Based on the results presented in Chapter 4, we anticipate that large herbivore removal results in a shift in vegetation composition, favouring woody biomass - i.e. a reversal of effects that also seem to be supported by paleo-vegetation reconstructions (Pearce et al. 2023). At the EU2 location, the removal of large herbivores results in a slight shift towards a larger proportion of woody leaf biomass, as C3 grass leaf biomass is reduced by -7% (not shown), while overall leaf biomass increases by 10%. In the African model domains, a comparable but less pronounced shift is observed with an increase in overall leaf biomass (+6% AF1) at the expense of leaf biomass from herbaceous PFTs (-5% C3 + C4 grasses, not shown).

Empirical animal removal experiments of a scale that allow for comparing our model results to observations are relatively scarce. However, studies in African savannas have demonstrated that herbivore exclusion typically leads to reductions in both tree and grass abundance (-30% and -57%, respectively in a synthesis by Staver et al. (2021). These experiments differ in their setup (i.e. the size of herbivores excluded), and impacts also depend on the type of herbivory (mixed feeding, predominantly grazing, predominantly browsing). However, a common response is that in the absence of herbivores, vegetation shifts towards woody cover (e.g., Levick et al.

2009; Kibet et al. 2021; Back et al. in review). Such trends are consistent with other reports of browsers suppressing tree growth (Barnes 2002; Sharam et al. 2006; Staver et al. 2009; Staver and Bond 2014) and simultaneously releasing grasses. Staver et al. (2021) comment on how previous modelling of herbivore impacts on leaf biomass in African savannas is substantially lower compared to observations – and our results consistently follow this pattern. For good reasons: The coupled LPJ-GUESS/Madingley model system does not simulate specific grazer AFTs to offset this release. Instead, all animals can access grass and tree leaf biomass. Notably, herbaceous PFTs can allocate a greater portion of their NPP to leaf tissue growth as they don't have to maintain woody plant compartments, allowing them to compensate more effectively for herbivory damage than trees. This is a substantial competitive advantage of herbaceous PFTs over woody PFTs.

The proportion of herbivore biomass removed at any experimental location does not result in a corresponding increase in leaf biomass (see Table **5.1**). This discrepancy originates from multiple animal functional types competing for leaves as food. In all locations (excluding EU1), large herbivore removal elevates omnivore biomass. However, the magnitude of this response is not uniform across all model domains. It is largest in EU2 (+76%), whereas in both African domains, omnivore biomass increases are less pronounced (23% in AF1 and 7% in AF2). This phenomenon is explained by the underlying competition between herbivores and omnivores. Omnivores have a lower efficiency at assimilating consumed leaf biomass (68%) compared to herbivores (80%). Cold and sparsely vegetated environments, especially with strong seasonal climate, can further enhance this competitive disadvantage. Omnivores living under these conditions have growth rates that are mainly controlled by leaf biomass supply and hence relatively gain when competition with herbivores is released. In contrast, omnivores living in warmer climates or in ecosystems with much denser vegetation do not face regular calorific shortages. Their growth is mainly controlled by predation pressure. Given that similar magnitudes of herbivore removal do not elevate omnivore biomasses in Africa as significantly as in Europe, we cannot expect a uniform or proportional response of the vegetation's leaf biomass to the removal of large herbivores. However, omnivores and smaller herbivores cannot fill the ecological niche large herbivores inhabit and compensate for their removal. This result is consistent with (Pringle et al. 2023), who argued that large herbivore species are not functionally redundant.

In Chapter **4**, we observed a shift in the balance between raingreen and evergreen woody biomass. However, the presence or absence of large herbivores alone did not significantly alter this response, suggesting that critical processes are missing in the current model setup (see Chapter **6.2**).

Large Carnivore Removal

In contrast to the large herbivores, large carnivores only comprise 15% of the o%erall modelled carnivore biomass. However, the effect of removing these carnivores should not be underestimated

due to their lower share of overall animal biomass. Adult carnivores not only control the population of adult herbivores but also place significant pressure on juveniles of larger herbivores. The offspring of large carnivores compete with adult carnivores of a similar size class for prey. Our results show that removing large carnivores from the simulations decreases the stability of emergent model-wide biomass levels, which is consistent with previous studies (Hoeks et al. 2020; Miller et al. 2001; Ripple et al. 2014; Van Valkenburgh et al. 2016). However, key differences exist between our large carnivore removal experiment and the one conducted by Hoeks et al. (2020). While our study does not include biomes that precisely match those of Hustai Nuruu or Yosemite National Parks, the temperate coniferous and mixed forests of Białowieża National Park correspond to the temperate mixed forest in our EU1 simulations. In these simulations, the emergent animal-vegetation feedback results in low biomass of large animals at the EU1 site, which consequently minimises the impact of carnivore removal. In contrast, Hoeks et al. (2020) reported the second-highest response to large carnivore removal in Białowieża National Park.

In our AF2 simulations, large carnivore removal led to a significant increase in herbivore biomass (+141%). By comparison, Hoeks et al. (2020) reported a much larger increase (+407%) in their corresponding experiment in Serengeti National Park. We expect that these differences originate from missing feedback between animals and vegetation in the framework used by Hoeks et al. (2020). As detailed in Chapter 4, incorporating such feedback significantly reduces overall animal biomass levels by limiting growth rates. This dynamic likely explains why herbivores in Hoeks et al. (2020) were able to assimilate more biomass following large carnivore removal, as their framework does not account for vegetation-mediated constraints on herbivore growth.

In all model domains, we find fluctuations in herbivore biomass following a similar pattern in the wake of carnivore removal. Immediately after removing large carnivores, predation pressure is released from large herbivores. In the following simulation years, the population of large herbivores and omnivores surges. The magnitude of this surge is determined by whether their growth was previously controlled by carnivores or the amount of feed supply. In AF1 and AF2, where pre-removal growth was controlled by predatory pressure, herbivore and omnivore biomass increases are stronger than in EU2, where pre-removal growth was primarily controlled by nutritional supply.

With the removal of large carnivores, herbivores and omnivores increasingly cause significant damage to the vegetation. After 20 to 30 years, the vegetation can no longer sustain their expanding population. As a result, starvation drives a decline in herbivore and omnivore abundance. Herbivores tend to suffer more from starvation, as omnivores are able to adapt to food shortages. Simultaneously, mesopredators experience a surge due to reduced competition (with juveniles of larger carnivores) and the increased availability of prey in the form of juvenile herbivores and omnivores. These dynamics collectively lead to a pronounced rebound effect, significantly reducing the biomass of herbivores and omnivores. This rebound effect is most

pronounced in AF1, where the rich tropical rainforest vegetation promotes the highest growth rates for large herbivores and omnivores, as feeding access is no constraint by, e.g. accounting for a vertical vegetation structure. However, the rebound effect in AF1 is delayed (compared to AF2) because the abundant leaf biomass sustains population growth for a longer period. Following the rebound effect, vegetation begins to recover as herbivory pressure decreases. In both AF2 and EU2, the recovering vegetation again supports increases in herbivore and omnivore biomass. In AF2, a second rebound effect occurs, though it is weaker than the first.

Overall, the removal of carnivores causes significant damage to PFT leaves by promoting herbivory pressure, which underlines the findings of Beschta and Ripple (2009) who indicated major impacts on woody vegetation following the removal of large predators. The following decline in leaf biomass triggers a long-term decrease in whole tree growth and carbon storage, pointing to potential impacts on ecosystem carbon storage. This result is consistent with Schmitz et al. (2014), who argued that animals have the potential to cause regional ecosystems to shift from being net CO_2 sinks to sources or vice versa. Shade-intolerant or shrubby PFTs are less affected by the increased defoliation, as they benefit from enhanced light availability. Consistent with the conceptual relationship between herbivory pressure and grass growth found in herbivore removal experiments (Staver et al. 2021), increased herbivory pressure (through removing predators) further promotes the growth of herbaceous PFTs at the expense of woody PFTs.

5.2.2 Animal Removal under the Effect of Climate Change

The removal of large animals does not affect ecosystems uniformly, particularly under the influence of climate change. In the boreal evergreen forests of Europe (EU2), our simulations indicate that removing either large carnivores or herbivores leads to minimal long-term impacts on vegetation by the end of the century. Both scenarios show short-term effects, such as increased growth of boreal needleleaf trees following herbivore removal and their suppressed growth with carnivore removal. However, these changes diminish as the simulation progresses. Despite Madingley not explicitly accounting for browsing, this short-term pattern aligns with field reports, such as moose suppressing their preferred browse-species' (Scots pine) growth in boreal forests, even in forests dominated by Norway spruce (Edenius et al. 2002). Such a strong relationship between moose density and Scots pine damage is also evident in Swedish national forest inventory data (Angelstam et al. 2000). These transient differences are visible under both low-warming (RCP 2.6) and high-warming (RCP 7.0) scenarios. However, these effects are overshadowed by broader ecosystem changes driven by climate change towards the end of the simulation, with a concurrent shift in animal populations favouring smaller species. The ecological transition towards lighter individuals reduces the overall influence of large animal removal, rendering their absence less impactful in the evolving ecosystem. Our findings underscore that in EU2, the effects of climate change far exceed the influence of altering

animal populations, highlighting the dominant role of climatic factors in shaping ecosystem dynamics.

In the African regions, the influence of large animal removal persists under climate change but varies in magnitude. The effect of large herbivore removal is measurable, but the removal of large carnivores has a far greater impact. In fact, the magnitude of the effects of large carnivore removal is comparable to the CO_2 fertilisation effect. Hooper et al. (2012) have argued that the impact of animals on ecosystems is as large as other (abiotic) drivers of global environmental change. However, given the many processes still absent both in LPJ-GUESS (drought and heat mortality, herbivore-wildfire interactions, insect outbreaks, …) and Madingley (C:N:P stoichiometry, soil-animal biota, …), it is too early to interpret our results in the light of the synthesis presented by Hooper et al. (2012).

5.2.3 Reversibility of Modelled Disturbances

Beschta and Ripple (2009) documented the recovery of woody vegetation following the reintroduction of previously extirpated grey wolves into Yellowstone National Park. Although Yellowstone represents a very different ecosystem, the reversibility of large carnivore removal observed by Beschta and Ripple (2009) aligns with findings from our simulations in that leaf biomass recovers fully from the removal of carnivores – whereas leaf biomass after herbivores are allowed to recover remains slightly elevated. In the absence of carnivores, the herbivore size spectrum is controlled by population dynamics and competition with omnivores. Such dynamics indicate that large carnivore removal triggers complex interactions in the food chain that are not easily reversible. These results are consistent with Andriuzzi (2025), who recently reported that carnivore reintroduction alone could not restore ecosystems to their prior stable state and highlighted that reintroducing carnivores is no quick fix to restore ecosystems.

Large herbivores are also reported to be difficult to replace functionally by Pringle et al. (2023). In our simulations, large herbivores' full recovery takes longer when compared to carnivores because herbivores can potentially achieve much higher maximum body masses — a pattern observed across diverse ecosystems. Moreover, we found that the rate of recovery in maximum body mass for large herbivores after their removal ends is significantly slower than that of carnivores. In the coupled Madingley/LPJ-GUESS model system, this slower growth rate is caused by an increased abundance of competitors for resources. The large omnivore abundance in the herbivore removal experiment provides feed competition for herbivores. In addition, juvenile herbivores increase prey availability, compensating for the negative effects of competition. Together with the potential for higher maximum bodymass of large herbivores, recovering their removal would take many centuries in the model system.

In a simulation where large animals are completely wiped out across the whole model domain, the recovery of large animals depends solely on incremental evolutionary growth and encroachment. However, preserving large animals outside the removal-affected areas significantly accelerates their reestablishment once the removal regime ends. This underscores the critical importance of protecting large animal species. If these species go extinct, it may take centuries for natural evolution to produce substitutes, while repopulation through migration can populate ecological niches much more quickly. This concern is particularly urgent, as approximately 60% of wild large herbivores are threatened by extinction (Ripple et al. 2015).

5.3 Summary

In this Chapter, we studied the impact of large animal removal on both the underlying vegetation and the remaining animal population. The removal of large herbivores evidently led to an increase in leaf biomass in boreal biomes (+10%), tropical rainforests (+5%) and moist savannas (+6%). Conversely, removing large carnivores reduced leaf biomass in boreal biomes (-11%), tropical rainforests (-19%) and moist savannas (-19%).

When these effects are compounded by climate change scenarios, general ecosystem shifts caused by climate change overshadowed the effects of large animal removal in the boreal model domain. However, in the African model domains, the suppressing effect of large carnivore removal on productivity proved to be of a similar magnitude as the enhancing effects of CO_2 fertilisation.

Simulations of animal population and ecosystem recovery revealed that the whole system requires centuries to recover from the complete removal of large animals. Ecosystem recovery occurs more rapidly when large animal populations are preserved in unaffected areas. Even though numerous fundamental processes are missing in how vegetation-animal interactions are represented in the current version of the Madingley/LPJ-GUESS model set-up, these results support the critical role of conserving animal biodiversity in the face of climate change.

6 General Conclusion and Outlook

This thesis studied the impacts of introducing animal effects to process-based vegetation modelling. The following paragraphs aim to summarise the key findings of this thesis, reiterate major technical limitations that led to uncertainties, and propose possible future model development.

6.1 Answers to the underlying research questions

6.1.1 Do process-based simulations of natural vegetation improve the realism of animal populations modelled by the Madingley Model?

The findings of this thesis demonstrate that incorporating vegetation modelled by a DGVM significantly improves the realism of simulated animal populations. By elevating herbivore biomass and autotroph consumption in response to underlying vegetation productivity for different versions of the coupled model system, we can show that each successive version exhibits increasingly realistic power-law relationships compared to its predecessors. Additionally, the coupling reveals critical sensitivities in the modelled animal populations, such as the severity of the winter minima in overall leaf biomass supply.

Overall, this thesis underscores the limitations of the original Madingley model due to its simplistic inherent vegetation model. When coupled with a sophisticated vegetation model, larger heterogeneity within modelled animal populations is evident, as well as dynamic feedback between vegetation and animals. However, evaluating results from the Madingley model is challenging due to the lack of large-scale, general datasets on animal biomass and abundance. The limited availability of such datasets has restricted the evaluation of simulated animal populations to emergent power-law relationships, such as those derived by Cebrian (2004). Furthermore, the absence of specific animal species within the Madingley framework complicates evaluation, as most reports on animal-vegetation interactions focus on specific species. Additionally, these interactions are often dependent on local environmental conditions (Wilmers and Schmitz 2016).

6.1.2 How do multi-trophic food chains impact ecosystem productivity, and which feedback can be found between herbivores and the underlying vegetation layer?

Modelled ecosystem productivity is influenced directly by herbivory and indirectly by the top-down effects of predators. Introducing herbivory to LPJ-GUESS leads to a reduction in productivity (-5%), equating to a reduction in annual NPP of 1.5 Pg C across Europe and Africa. The trend of this response is consistent with previous studies (Dangal et al. 2017; Jia et al. 2018; Staver et al. 2021). Our analysis indicates that this trend is consistent across most

biomes, though the magnitude of the impact varies significantly. Biomes with sparser vegetation experience a greater relative impact from herbivory damage.

Although the Madingley model is neither designed nor equipped to resolve the effects of individual animal species, the responses found qualitatively correspond to observations (e.g., Angelstam et al. 2000; Edenius et al. 2002). This does not suggest that Madingley can be expected to potentially resolve dynamics at the species level.

6.1.3 How does the absence of large mammalian herbivores or carnivores alter the vegetation cover, and how do different future climate scenarios affect the impacts found?

This thesis highlights the impact of large animals on ecosystem state and functioning for both herbivores and carnivores alike. The effects of removing such animals are complex and vary in magnitude depending on the surrounding ecosystem conditions. Removing large herbivores results in a +10% increase in vegetation leaf biomass in boreal ecosystems, +5% in tropical ecosystems, and +6% in savanna ecosystems. Conversely, the removal of large carnivores decreases vegetation leaf biomass by -19% in tropical and savanna ecosystems and by -11% in boreal ecosystems.

The model system shows vital dynamics between all functional groups when parts of the trophic pyramid are removed. Omnivores, being highly adaptive, tend to proliferate in the absence of either carnivores or herbivores, partially occupying the ecological niches left behind. However, their ability to functionally substitute for large herbivores is limited, and long-term ecosystem imbalances persist. These findings align with Pringle et al. (2023), who argued that large herbivore species are not functionally redundant.

The removal of animals can impact ecosystems, but these impacts interact with impacts of climate change. In boreal ecosystems, shifts in plant species composition due to climate change can potentially outweigh the effects of removing large animals from such an ecosystem. Contributing to this are the effects of climate change on the animal population itself. In Madingley, warmer climates result in lighter but more abundant animals compared to colder climates. In contrast, in African ecosystems, the removal of large carnivores has a comparable impact on simulated vegetation biomass as climate change itself, regardless of whether a low-warming (RCP 2.6) or high-warming (RCP 7.0) scenario is considered.

Our simulations highlight the urgent need for global efforts to protect large animals. Ecosystems from which large animals have been previously removed recover significantly faster when populations of large animals remain intact in adjacent, protected areas. This urgency is further emphasised since approximately 60% of the large herbivore species are facing extinction today (Ripple et al. 2015).

6.2 Limitations

Like all ecosystem models, the model system described in this thesis also faces limitations due to the technical representation of processes. These limitations are described throughout the thesis; the following paragraphs summarise the most relevant ones.

6.2.1 Human Impact

As elaborated in Chapter **4.2.2**, the coupled model system currently simulates a human-free world. This limitation complicates the translation of model results to real-world implications and hinders effective evaluation, as human influence significantly impacts the majority of Earth's surface.

6.2.2 Parameterisation of leaf damage to evergreen PFTs

In the model system, evergreen plants retain leaf damage longer than deciduous plants due to their annual leaf biomass regrowth being limited to one-third. While evergreen plants, in reality, do invest more in long-lived leaves compared to deciduous plants, they also invest more in defence mechanisms to protect these valuable leaves (Coley and Aide 1991). The absence of such defence mechanisms in the model leads to an overestimation of herbivore consumption of evergreen leaves.

6.2.3 Preferential Feeding

Herbivores in the Madingley model lack the ability to differentiate between plant types. The Madingley model assumes that herbivore cohorts and leaf biomass are well-mixed within a grid cell, with each herbivore cohort having access to 10% of the leaf biomass from each plant individual. While this assumption produces somewhat realistic overall biomass levels for herbivores and plants, it introduces several issues:

First, as mentioned above, modelled herbivores over-prioritise evergreen leaves due to both the parameterisation of evergreen leaf turnover and the lower nutritional value of evergreen leaves compared to deciduous ones. In reality, herbivores preferentially consume deciduous leaves when given a choice (Silva et al. 2015). Second, as noted in Chapter **2.2.3**, the uniform accessibility of 10% of leaf biomass disregards the higher vertical reach of smaller animals, placing larger animals at an advantage.

Moreover, the lack of preferential feeding, together with the absence of a dedicated grass stock, prevents distinctions between grazers and browsers. This limitation is particularly significant in African ecosystems, where grazer-fire interactions strongly influence vegetation dynamics (Holdo

et al. 2009). With only evergreen and deciduous vegetation stocks available for consumption, the current model version cannot capture these complex interactions.

6.3 Future work

As discussed above, the model system - especially the Madingley model - needs to be further improved to represent key ecological processes. In the following paragraphs, I will describe the most pressing and potentially promising future developments of the model system.

6.3.1 Preferential Feeding

A major branch of current model development is the implementation of nitrogen in the Madingley model. The tracking of nitrogen throughout the animal's lifetime enables feedback of animal faeces and carcasses with both soil and vegetation processes, as well as a nutrition-based selection between leaf biomass stocks. By these means, the currently omitted but often reported acceleration of the nutrient cycle through herbivores (Enquist et al. 2020; Wilmers and Schmitz 2016) can be quantified. A manuscript for the first "offline" coupled version of Madingley-N is currently being prepared in the group of Almut Arneth, by Jan-Moritz Kupisch and with also my contributions.

6.3.2 Sub-annual carbon allocation in LPJ-GUESS

Another major development branch is the daily allocation of carbon towards plant compartments, which will allow us to better simulate aub-annual growth processes in LPJ-GUESS. Such an allocation will partially remove the disadvantage evergreen trees have when recovering from leaf damage.

6.3.3 Diversifying Madingley's Vegetation Stocks

A version of Madingley with more than two vegetation stocks is currently being developed. That version will qualify the coupled model system for a multitude of possible experiments.

For instance, a differentiation between grazers and browsers can be implemented by adding a third stock, which is linked to the leaf biomass of C3 and C4 grasses of LPJ-GUESS. Such a grass stock can be exclusively accessible to a new herbivore functional group. Herbivores, in general, can be specialists through stock-dependent herbivory assimilation efficiencies. Such an approach would cover grazers being able to browse when in need and vice-versa. However, such an implementation would also increase the number of AFTs significantly, thus leading to an increased computational cost.

Building upon a grazer-browser implementation, such a model version can also lay the groundwork for the implementation of domestic herbivore herds. Such herds can be parameterised as a cohort of a special functional group with exclusive access pasture leaf biomass simulated by LPJ-GUESS in conjunction with its land use module. This development branch could play a pivotal role in further integrating the Madingley model into the LandSyMM framework.

6.3.4 Soil Processes

The current version of Madingley does not simulate detritivores. Alongside the implementation of animal litter production with an animal-specific C:N ratio, it would be beneficial to include animal contributions to heterotrophic decomposition.

6.4 Final remarks

The impacts of animals on the carbon cycle have been disregarded for a long time, especially in ecosystem modelling. The traditional view that animals contribute little to ecological processes due to their low overall biomass is challenged by a rapidly growing body of literature, as by the results of this thesis. However, global animal biodiversity is facing historic declines, adding to the urgency of understanding the complex interconnections between animals and vegetation. This thesis highlights the possibility of combining both process-based dynamic vegetation modelling and animal population modelling and evolving ecosystem modelling towards a more holistic approach. It also confirms the vulnerability of large animals and underlines the urgency to protect animal biodiversity.

Acknowledgement

At the end of my thesis I would like to thank all those countless people who made this work possible over the last couple of years. In particular, I want to thank the following people:

First of all, I am fortunate to be part of the working group of my supervisor Almut Arneth, who spent countless hours on the success of this thesis despite her numerous other duties. Almut, thank you so much for your guidance, knowledge, inspiration, humour and patience. I am especially thankful for the support during the Covid-19 pandemic that kept me on track when it was easier to be consumed by the chaos surrounding us. I would not have been able to finish this thesis without your support. Thanks for being such a great supervisor!

I am also very thankful for my co-advisor Peter Anthoni for never hesitating to help me with the LPJ-GUESS model code, for his countless technical explanations and writing suggestions, and his help developing the coupled model system.

The same is true for Mike Harfoot, who – despite being involved in numerous other scientific endeavours – always helped me with technical and logical questions regarding the Madingley model code.

I also want to thank my other co-advisors, Mark Rounsevell and Calum Brown, who helped me conceptualise the coupling link in regular meetings.

I want to give special thanks to the other members of the LEMG group at KIT/IMK-IFU, particularly the "Upstairs Office," which never shied away from heated discussions. I have always valued the supportive and friendly work environment.

Furthermore, I am grateful to Thomas Hickler for reviewing this thesis.

Finally, I want to thank my friends and parents for their unlimited support and company, especially during the tough times of Covid-19 and during the final hours of writing this thesis. Special thanks go to my partner, Nina, who always knew the right words to catch me when I was falling.

My work was supported by the Helmholz Foundation Impulse and Networking, Germany fund and the Helmholz ATMO programme, Germany.

Statement on AI Assistance

In this thesis, I used OpenAI's ChatGPT v4 and Grammarly v1.100.2.0 to assist with text rephrasing and linguistic refinement. The AI tool was employed exclusively to improve the clarity and coherence of an original manuscript, while the core intellectual content, analysis, and conclusions remain entirely my own. Subsequently, the text was critically reviewed and further edited. All use of AI adhered to ethical guidelines and institutional policies regarding the use of technology in academic work.

References

Allen, C. D., Breshears, D. D., and McDowell, N. G. (2015) "On Underestimation of Global Vulnerability to Tree Mortality and Forest Die-off from Hotter Drought in the Anthropocene"
In: Ecosphere, Vol. 6.8, art129.
DOI: 10.1890/ES15-00203.1

Andriuzzi, W. (2025) "Lasting Effects of Losing Large Carnivores"
In: Nature Ecology & Evolution, Vol. 9.1, pp. 3–3.
DOI: 10.1038/s41559-024-02609-z

Angelstam, P., Wikberg, P.-E., Danilov, P., Faber, W., and Nygren, K. (2000) "Effects of Moose Density on Timber Quality and Biodiversity Restoration in Sweden, Finland, and Russian Karelia"
In: Alces, Vol. 36, pp. 133–145

Arneth, A. et al. (2017) "Historical Carbon Dioxide Emissions Caused by Land-Use Changes Are Possibly Larger than Assumed"
In: Nature Geoscience, Vol. 10.2, pp. 79–84.
DOI: 10.1038/ngeo2882

Arneth, A. et al. (2020) "Post-2020 Biodiversity Targets Need to Embrace Climate Change"
In: Proceedings of the National Academy of Sciences, Vol. 117.49, pp. 30882–30891.
DOI: 10.1073/pnas.2009584117

Back, H., Arneth, A., Perez-Postigo, I., and Geitner, C. (in review) "Analysing the Impact of Large Mammal Herbivores on Vegetation Structure in Eastern African Savannas Combining High Spatial Resolution Multispectral Remote Sensing Data and Field Observations"
In: -, Vol. -

Bar-On, Y. M., Phillips, R., and Milo, R. (2018) "The Biomass Distribution on Earth"
In: Proceedings of the National Academy of Sciences, Vol. 115.25, p. 6506.
DOI: 10.1073/pnas.1711842115

Barnes, M. (2002) "Effects of Large Herbivores and Fire on the Regeneration of Acacia Erioloba Woodlands in Chobe National Park, Botswana"
In: African Journal of Ecology, Vol. 39, pp. 340–350.
DOI: 10.1046/j.1365-2028.2001.00325.x

Bayer, A. D. et al. (2017) "Uncertainties in the Land-Use Flux Resulting from Land-Use Change Reconstructions and Gross Land Transitions"
In: Earth System Dynamics, Vol. 8.1, pp. 91–111.
DOI: 10.5194/esd-8-91-2017

Beringer, T., Lucht, W., and Schaphoff, S. (2011) "Bioenergy Production Potential of Global Biomass Plantations under Environmental and Agricultural Constraints: Bioenergy Production Potential of Global Biomass Plantations"
In: GCB Bioenergy, Vol. 3.4, pp. 299–312.
DOI: 10.1111/j.1757-1707.2010.01088.x

Berzaghi, F. et al. (2019) "Carbon Stocks in Central African Forests Enhanced by Elephant Disturbance"
In: Nature Geoscience, Vol. 12.
DOI: 10.1038/s41561-019-0395-6

Beschta, R. L. and Ripple, W. J. (2009) "Large Predators and Trophic Cascades in Terrestrial Ecosystems of the Western United States"
In: Biological Conservation, Vol. 142.11, pp. 2401–2414.
DOI: 10.1016/j.biocon.2009.06.015

Bonan, G. B. (1992) "Soil Temperature as an Ecological Factor in Boreal Forests". From:A Systems Analysis of the Global Boreal Forest. 1st ed., pp. 126–143
Publisher: Cambridge University Press. Ed. by H. H. Shugart, R. Leemans, and G. B. Bonan . ISBN: 978-0-521-40546-1 978-0-521-61973-8 978-0-511-56548-9

Bondeau, A. et al. (2007) "Modelling the Role of Agriculture for the 20th Century Global Terrestrial Carbon Balance"
In: Global Change Biology, Vol. 13.3, pp. 679–706.
DOI: 10.1111/j.1365-2486.2006.01305.x

Brose, U. et al. (2019) "Predator Traits Determine Food-Web Architecture across Ecosystems"
In: Nature Ecology & Evolution, Vol. 3.6, pp. 919–927.
DOI: 10.1038/s41559-019-0899-x

Bugmann, H. (2001) "A Review of Forest Gap Models"
In: Climatic Change, Vol. 51.3, pp. 259–305.
DOI: 10.1023/A:1012525626267

Carbone, C., Mace, G. M., Roberts, S. C., and Macdonald, D. W. (1999) "Energetic Constraints on the Diet of Terrestrial Carnivores"
In: Nature, Vol. 402.6759, pp. 286–288.
DOI: 10.1038/46266

Cardinale, B. J. et al. (2011) "The Functional Role of Producer Diversity in Ecosystems"
In: American Journal of Botany, Vol. 98.3, pp. 572–592.
DOI: 10.3732/ajb.1000364

Cardinale, B. J. et al. (2012) "Biodiversity Loss and Its Impact on Humanity"
In: Nature, Vol. 486.7401, pp. 59–67.
DOI: 10.1038/nature11148

Cebrian, J. (2004) "Role of First-Order Consumers in Ecosystem Carbon Flow: Carbon Flow through First-Order Consumers"
In: Ecology Letters, Vol. 7.3, pp. 232–240.
DOI: 10.1111/j.1461-0248.2004.00574.x

Coley, P. and Aide, T. M. (1991) "Comparison of Herbivory and Plant Defenses in Temperate and Tropical Broad-Leaf Forests"
In: Plant-animal Interactions: Evolutionary Ecology in Tropical and Temperate Regions, Vol. Pp. 25–49

Collatz, G., Ball, J., Grivet, C., and Berry, J. A. (1991) "Physiological and Environmental Regulation of Stomatal Conductance, Photosynthesis and Transpiration: A Model That Includes a Laminar Boundary Layer"
In: Agricultural and Forest Meteorology, Vol. 54.2, pp. 107–136.
DOI: 10.1016/0168-1923(91)90002-8

Collier, N. et al. (2018) "The International Land Model Benchmarking (ILAMB) System: Design, Theory, and Implementation"
In: Journal of Advances in Modeling Earth Systems, Vol. 10.11, pp. 2731–2754.
DOI: 10.1029/2018MS001354

Croll, D. A., Maron, J. L., Estes, J. A., Danner, E. M., and Byrd, G. V. (2005) "Introduced Predators Transform Subarctic Islands from Grassland to Tundra"
In: Science, Vol. 307.5717, pp. 1959–1961.
DOI: 10.1126/science.1108485

Dangal, S. R. S. et al. (2017) "Integrating Herbivore Population Dynamics Into a Global Land Biosphere Model: Plugging Animals Into the Earth System"
In: Journal of Advances in Modeling Earth Systems, Vol. 9.8, pp. 2920–2945.
DOI: 10.1002/2016MS000904

De Kauwe, M. et al. (2014) "Where Does the Carbon Go? A Model-Data Intercomparison of Vegetation Carbon Allocation and Turnover Processes at Two Temperate Forest Free-Air CO 2 Enrichment Sites"
In: The New phytologist, Vol. 203.
DOI: 10.1111/nph.12847

Edenius, L., Bergman, M., Ericsson, G., and Danell, K. (2002) "The Role of Moose as a Disturbance Factor in Managed Boreal Forests"
In: Silva Fennica, Vol. 36.1.
DOI: 10.14214/sf.550

Elmhagen, B., Ludwig, G., Rushton, S. P., Helle, P., and Lindén, H. (2010) "Top Predators, Mesopredators and Their Prey: Interference Ecosystems along Bioclimatic Productivity Gradients"
In: Journal of Animal Ecology, Vol. 79.4, pp. 785–794.
DOI: 10.1111/j.1365-2656.2010.01678.x

Enquist, B. J., Abraham, A. J., Harfoot, M. B. J., Malhi, Y., and Doughty, C. E. (2020) "The Megabiota Are Disproportionately Important for Biosphere Functioning"
In: Nature Communications, Vol. 11.1, p. 699.
DOI: 10.1038/s41467-020-14369-y

Erb, K.-H. et al. (2018) "Unexpectedly Large Impact of Forest Management and Grazing on Global Vegetation Biomass"
In: Nature, Vol. 553.7686, pp. 73–76.
DOI: 10.1038/nature25138

Estes, J. A. et al. (2011) "Trophic Downgrading of Planet Earth"
In: Science, Vol. 333.6040, pp. 301–306.
DOI: 10.1126/science.1205106

Evans, A. R. et al. (2012) "The Maximum Rate of Mammal Evolution"
In: Proceedings of the National Academy of Sciences of the United States of America, Vol. 109.11, pp. 4187–4190.
DOI: 10.1073/pnas.1120774109. PMID: 22308461

Fang, H., Baret, F., Plummer, S., and Schaepman-Strub, G. (2019) "An Overview of Global Leaf Area Index (LAI): Methods, Products, Validation, and Applications"
In: Reviews of Geophysics, Vol. 57.3, pp. 739–799.
DOI: 10.1029/2018RG000608

Gutjahr, O. et al. (2019) "Max Planck Institute Earth System Model (MPI-ESM1.2) for the High-Resolution Model Intercomparison Project (HighResMIP)"
In: Geosci. Model Dev. Vol. 12.7, pp. 3241–3281.
DOI: 10.5194/gmd-12-3241-2019

Harfoot, M. et al. (2014) "Emergent Global Patterns of Ecosystem Structure and Function from a Mechanistic General Ecosystem Model"
In: PLoS Biology, Vol. 12.4. Ed. by M. Loreau, e1001841–e1001841.
DOI: 10.1371/journal.pbio.1001841

Harris, I. C. (2020) CRU JRA v2.1: A Forcings Dataset of Gridded Land Surface Blend of Climatic Research Unit (CRU) and Japanese Reanalysis (JRA) Data. Jan.1901 - Dec.2019
Publisher:
Centre for Environmental Data Analysis.
DOI: 10.2151/jmsj.2015-001

Hatfield, J. L. and Dold, C. (2019) "Chapter 1 - Photosynthesis in the Solar Corridor System". From:The Solar Corridor Crop System, pp. 1–33
Publisher: Academic Press. Ed. by C. L. Deichman and R. J. Kremer
. ISBN: 978-0-12-814792-4

Hickler, T., Prentice, I., Smith, B., Sykes, M., and Zaehle, S. (2006) "Implementing Plant Hydraulic Architecture within the LPJ Dynamic Global Vegetation Model"
In: Global Ecology and Biogeography, Vol. 15, pp. 567–577.
DOI: 10.1111/j.1466-8238.2006.00254.x

Hoeks, S. et al. (2020) "Mechanistic Insights into the Role of Large Carnivores for Ecosystem Structure and Functioning"
In: Ecography, Vol. 43.12, pp. 1752–1763.
DOI: 10.1111/ecog.05191

Hoeks, S. et al. (2021) "MadingleyR: An R Package for Mechanistic Ecosystem Modelling"
In: Global Ecology and Biogeography, Vol. 30.9. Ed. by A. Bates, pp. 1922–1933.
DOI: 10.1111/geb.13354

Holdo, R. M. et al. (2009) "A Disease-Mediated Trophic Cascade in the Serengeti and Its Implications for Ecosystem C"
In: PLoS Biology, Vol. 7.9. Ed. by G. M. Mace, Article e1000210–Article e1000210.
DOI: 10.1371/journal.pbio.1000210

Hooper, D. U. et al. (2012) "A Global Synthesis Reveals Biodiversity Loss as a Major Driver of Ecosystem Change"
In: Nature, Vol. 486, pp. 105–109.
DOI: 10.1038/nature11118

Huang, S., Titus, S. J., and Wiens, D. P. (1992) "Comparison of Nonlinear Height–Diameter Functions for Major Alberta Tree Species"
In: Canadian Journal of Forest Research, Vol. 22.9, pp. 1297–1304.
DOI: 10.1139/x92-172

Jägermeyr, J. et al. (2015) "Water Savings Potentials of Irrigation Systems: Global Simulation of Processes and Linkages"
In: Hydrology and Earth System Sciences, Vol. 19.7, pp. 3073–3091.
DOI: 10.5194/hess-19-3073-2015

Jia, S. et al. (2018) "Global Signal of Top-down Control of Terrestrial Plant Communities by Herbivores"
In: Proceedings of the National Academy of Sciences, Vol. 115.24, p. 6237.
DOI: 10.1073/pnas.1707984115

Kattge, J. et al. (2011) "TRY - A Global Database of Plant Traits"
In: Global Change Biology, Vol. 17.9, pp. 2905–2935.
DOI: 10.1111/j.1365-2486.2011.02451.x

Kautz, M., Anthoni, P., Meddens, A. J. H., Pugh, T. A. M., and Arneth, A. (2018) "Simulating the Recent Impacts of Multiple Biotic Disturbances on Forest Carbon Cycling across the United States"
In: Global Change Biology, Vol. 24.5, pp. 2079–2092.
DOI: 10.1111/gcb.13974

Kibet, S., Nyangito, M., MacOpiyo, L., and Kenfack, D. (2021) "Savanna Woody Plants Responses to Mammalian Herbivory and Implications for Management of Livestock–Wildlife Landscape"
In: Ecological Solutions and Evidence, Vol. 2.3, e12083.
DOI: 10.1002/2688-8319.12083

Kielland, K. and Bryant, J. P. (1998) "Moose Herbivory in Taiga: Effects on Biogeochemistry and Vegetation Dynamics in Primary Succession"
In: Oikos, Vol. 82.2, pp. 377–383.
DOI: 10.2307/3546979. JSTOR: 3546979

Kiffner, C. and Lee, D. E. (2019) "Population Dynamics of Browsing and Grazing Ungulates in the Anthropocene". From:The Ecology of Browsing and Grazing II. Vol. 239, pp. 155–179 Publisher: Springer International Publishing. Ed. by I. J. Gordon and H. H. T. Prins . ISBN: 978-3-030-25864-1 978-3-030-25865-8

Krause, J. et al. (2022) "How More Sophisticated Leaf Biomass Simulations Can Increase the Realism of Modelled Animal Populations"
In: Ecological Modelling, Vol. 471, p. 110061.
DOI: 10.1016/j.ecolmodel.2022.110061

– (2024) "Corrigendum to "How More Sophisticated Leaf Biomass Simulations Can Increase the Realism of Modelled Animal Populations" [Ecological Modelling 471 (2022) 110061]"
In: Ecological Modelling, Vol. 492, p. 110706.
DOI: 10.1016/j.ecolmodel.2024.110706

Lange, S. and Büchner, M. (2021) ISIMIP3b Bias-Adjusted Atmospheric Climate Input Data V1.1
Publisher:
ISIMIP Repository.
DOI: 10.48364/ISIMIP.842396.1

Launiainen, S. et al. (2022) "Does Growing Atmospheric CO2 Explain Increasing Carbon Sink in a Boreal Coniferous Forest?"
In: Global Change Biology, Vol.
DOI: 10.1111/gcb.16117

Levick, S. R., Asner, G. P., Kennedy-Bowdoin, T., and Knapp, D. E. (2009) "The Relative Influence of Fire and Herbivory on Savanna Three-Dimensional Vegetation Structure"
In: Biological Conservation, Vol. 142.8, pp. 1693–1700.
DOI: 10.1016/j.biocon.2009.03.004

Levis, S., Hartman, M. D., and Bonan, G. B. (2014) "The Community Land Model Underestimates Land-Use CO2 Emissions by Neglecting Soil Disturbance from Cultivation"
In: Geoscientific Model Development, Vol. 7.2, pp. 613–620.
DOI: 10.5194/gmd-7-613-2014

Levis, S. et al. (2012) "Interactive Crop Management in the Community Earth System Model (CESM1): Seasonal Influences on Land–Atmosphere Fluxes"
In: Journal of Climate, Vol. 25.14, pp. 4839–4859.
DOI: 10.1175/JCLI-D-11-00446.1

Lieth, H. (1975) "Modeling the Primary Productivity of the World". From:Primary Productivity of the Biosphere, pp. 237–263
Publisher: Springer Berlin Heidelberg. Ed. by H. Lieth and R. H. Whittaker
. ISBN: 978-3-642-80913-2

Lindeskog, M., Lagergren, F., Smith, B., and Rammig, A. (2021) "Accounting for Forest Management in the Estimation of Forest Carbon Balance Using the Dynamic Vegetation Model LPJ-GUESS (v4.0, R9333): Implementation and Evaluation of Simulations for Europe"
In: Geosci. Model Dev. Discuss. Vol. 2021, pp. 1–42.
DOI: 10.5194/gmd-2020-440

Lindeskog, M. et al. (2013) "Implications of Accounting for Land Use in Simulations of Ecosystem Carbon Cycling in Africa"
In: Earth System Dynamics, Vol. 4.2, pp. 385–407.
DOI: 10.5194/esd-4-385-2013

Malhi, Y. et al. (2016) "Megafauna and Ecosystem Function from the Pleistocene to the Anthropocene"
In: Proceedings of the National Academy of Sciences, Vol. 113.4, pp. 838–846.
DOI: 10.1073/pnas.1502540113

Malhi, Y. et al. (2022) "The Role of Large Wild Animals in Climate Change Mitigation and Adaptation"
In: Current Biology, Vol. 32.4, R181–R196.
DOI: 10.1016/j.cub.2022.01.041

Mayer, D. (2017) "Potentials and Side-Effects of Herbaceous Biomass Plantations for Climate Change Mitigation"
Universität Hamburg

McDowell, N. et al. (2002) "The Relationship between Tree Height and Leaf Area: Sapwood Area Ratio"
In: Oecologia, Vol. 132.1, pp. 12–20.
DOI: 10.1007/s00442-002-0904-x

Meinshausen, M. et al. (2017) "Historical Greenhouse Gas Concentrations for Climate Modelling (CMIP6)"
In: Geosci. Model Dev. Vol. 10.5, pp. 2057–2116.
DOI: 10.5194/gmd-10-2057-2017

Miller, B. et al. (2001) "The Importance of Large Carnivores to Healthy Ecosystems"
In: Endangered Species Update, Vol. 18

Miralles, D. G. et al. (2011) "Global Land-Surface Evaporation Estimated from Satellite-Based Observations"
In: Hydrology and Earth System Sciences, Vol. 15.2, pp. 453–469.
DOI: 10.5194/hess-15-453-2011

Morris, T. and Letnic, M. (2017) "Removal of an Apex Predator Initiates a Trophic Cascade That Extends from Herbivores to Vegetation and the Soil Nutrient Pool"
In: Proceedings of the Royal Society B: Biological Sciences, Vol. 284.1854, p. 20170111.
DOI: 10.1098/rspb.2017.0111

Newbold, T., Tittensor, D. P., Harfoot, M. B. J., Scharlemann, J. P. W., and Purves, D. W. (2020) "Non-Linear Changes in Modelled Terrestrial Ecosystems Subjected to Perturbations"
In: Scientific Reports, Vol. 10.1, p. 14051.
DOI: 10.1038/s41598-020-70960-9

Olin, S. et al. (2015a) "Modelling the Response of Yields and Tissue C : N to Changes in Atmospheric CO2 and N Management in the Main Wheat Regions of Western Europe"
In: Biogeosciences, Vol. 12.8, pp. 2489–2515.
DOI: 10.5194/bg-12-2489-2015

Olin, S. et al. (2015b) "Soil Carbon Management in Large-Scale Earth System Modelling: Implications for Crop Yields and Nitrogen Leaching"
In: Earth System Dynamics, Vol. 6.2, pp. 745–768.
DOI: 10.5194/esd-6-745-2015

Osborne, C. P. et al. (2018) "Human Impacts in African Savannas Are Mediated by Plant Functional Traits"
In: New Phytologist, Vol. 220.1, pp. 10–24.
DOI: 10.1111/nph.15236

Pachzelt, A., Forrest, M., Rammig, A., Higgins, S., and Hickler, T. (2015) "Potential Impact of Large Ungulate Grazers on African Vegetation, Carbon Storage and Fire Regimes: Grazer Impacts on African Savannas"
In: Global Ecology and Biogeography, Vol. 24.
DOI: 10.1111/geb.12313

Pacifici, M. et al. (2015) "Assessing Species Vulnerability to Climate Change"
In: Nature Climate Change, Vol. 5.3, pp. 215–225.
DOI: 10.1038/nclimate2448

Pearce, E. A. et al. (2023) "Substantial Light Woodland and Open Vegetation Characterized the Temperate Forest Biome before Homo Sapiens"
In: Science Advances, Vol. 9.45, eadi9135.
DOI: 10.1126/sciadv.adi9135

Prentice, I. C. et al. (2004) "Dynamic Global Vegetation Modeling: Quantifying Terrestrial Ecosystem Responses to Large-Scale Environmental Change". From:Terrestrial Ecosystems in a Changing World, pp. 175–192
Publisher: Springer Berlin Heidelberg
. ISBN: 978-3-540-32729-5

Pringle, R. M. et al. (2023) "Impacts of Large Herbivores on Terrestrial Ecosystems"
In: Current Biology, Vol. 33.11, R584–R610.
DOI: 10.1016/j.cub.2023.04.024

Pugh, T. A. M. et al. (2015) "Simulated Carbon Emissions from Land-Use Change Are Substantially Enhanced by Accounting for Agricultural Management"
In: Environmental Research Letters, Vol. 10.12, p. 124008.
DOI: 10.1088/1748-9326/10/12/124008

Pugh, T. A. M. et al. (2023) "The Anthropogenic Imprint on Temperate and Boreal Forest Demography and Carbon Turnover"
In: Global Ecology and Biogeography, Vol.
DOI: 10.1111/geb.13773

Rabin, S. S. et al. (2017) "The Fire Modeling Intercomparison Project (FireMIP), Phase 1: Experimental and Analytical Protocols with Detailed Model Descriptions"
In: Geosci. Model Dev. Vol. 10.3, pp. 1175–1197.
DOI: 10.5194/gmd-10-1175-2017

Reichstein, M. et al. (2007) "Determinants of Terrestrial Ecosystem Carbon Balance Inferred from European Eddy Covariance Flux Sites"
In: Geophysical Research Letters, Vol. 34.1.
DOI: 10.1029/2006GL027880

Riggs, R. A. et al. (2015) "Biomass and Fire Dynamics in a Temperate Forest-Grassland Mosaic: Integrating Multi-Species Herbivory, Climate, and Fire with the FireBGCv2/GrazeBGC System"
In: Ecological Modelling, Vol. 296, pp. 57–78.
DOI: 10.1016/j.ecolmodel.2014.10.013

Ripple, W. J. et al. (2014) "Status and Ecological Effects of the World's Largest Carnivores"
In: Science, Vol. 343.6167, p. 1241484.
DOI: 10.1126/science.1241484

Ripple, W. J. et al. (2015) "Collapse of the World's Largest Herbivores"
In: Science Advances, Vol. 1.4, e1400103.
DOI: 10.1126/sciadv.1400103

Rolinski, S. et al. (2017) "Modeling Vegetation and Carbon Dynamics of Managed Grasslands at the Global Scale with LPJmL 3.6"
In: Geoscientific Model Development Discussions, Vol. Pp. 1–32.
DOI: 10.5194/gmd-2017-26

Running, S. and Zhao, M. (2021) MODIS/Terra Net Primary Production Gap-Filled Yearly L4 Global 500m SIN Grid V061. 2021
Publisher:
NASA EOSDIS Land Processes Distributed Active Archive Center.
DOI: 10.5067/MODIS/MOD17A3HGF.061

Saatchi, S. S. et al. (2011) "Benchmark Map of Forest Carbon Stocks in Tropical Regions across Three Continents"
In: Proceedings of the National Academy of Sciences, Vol. 108.24, pp. 9899–9904.
DOI: 10.1073/pnas.1019576108

Santoro, M. and Cartus, O. (2021) ESA Biomass Climate Change Initiative (Biomass_cci): Global Datasets of Forest above-Ground Biomass for the Years 2010, 2017 and 2018, V3 application/xml
Publisher: NERC EDS Centre for Environmental Data Analysis.
DOI: 10.5285/5F331C418E9F4935B8EB1B836F8A91B8

Schmitz, O. J., Post, E., Burns, C. E., and Johnston, K. M. (2003) "Ecosystem Responses to Global Climate Change: Moving Beyond Color Mapping"
In: BioScience, Vol. 53.12, pp. 1199–1205.
DOI: 10.1641/0006-3568(2003)053[1199:ERTGCC]2.0.CO;2

Schmitz, O. J. et al. (2014) "Animating the Carbon Cycle"
In: Ecosystems, Vol. 17.2, pp. 344–359.
DOI: 10.1007/s10021-013-9715-7

Schmitz, O. J. et al. (2018) "Animals and the Zoogeochemistry of the Carbon Cycle"
In: Science, Vol. 362.6419, eaar3213–eaar3213.
DOI: 10.1126/science.aar3213

Sharam, G., Sinclair, A. R. E., and Turkington, R. (2006) "Establishment of Broad-leaved Thickets in Serengeti, Tanzania: The Influence of Fire, Browsers, Grass Competition, and Elephants[1]"
In: Biotropica, Vol. 38.5, pp. 599–605.
DOI: 10.1111/j.1744-7429.2006.00195.x

Shevliakova, E. et al. (2009) "Carbon Cycling under 300 Years of Land Use Change: Importance of the Secondary Vegetation Sink"
In: Global Biogeochemical Cycles, Vol. 23.2, 2007GB003176.
DOI: 10.1029/2007GB003176

Silva, J., Espírito-Santo, M., and Morais, H. (2015) "Leaf Traits and Herbivory on Deciduous and Evergreen Trees in a Tropical Dry Forest"
In: Basic and Applied Ecology, Vol. 16.
DOI: 10.1016/j.baae.2015.02.005

Smith, B. et al. (2014) "Implications of Incorporating N Cycling and N Limitations on Primary Production in an Individual-Based Dynamic Vegetation Model"
In: Biogeosciences, Vol. 11.7, pp. 2027–2054.
DOI: 10.5194/bg-11-2027-2014

Smith, M. J., Purves, D. W., Vanderwel, M. C., Lyutsarev, V., and Emmott, S. (2013) "The Climate Dependence of the Terrestrial Carbon Cycle, Including Parameter and Structural Uncertainties"
In: Biogeosciences, Vol. 10.1, pp. 583–606.
DOI: 10.5194/bg-10-583-2013

Sobral, M. et al. (2017) "Mammal Diversity Influences the Carbon Cycle through Trophic Interactions in the Amazon"
In: Nature Ecology & Evolution, Vol. 1.11, pp. 1670–1676.
DOI: 10.1038/s41559-017-0334-0

Staver, A. C., Bond, W. J., Stock, W. D., Van Rensburg, S. J., and Waldram, M. S. (2009) "Browsing and Fire Interact to Suppress Tree Density in an African Savanna"
In: Ecological Applications, Vol. 19.7, pp. 1909–1919.
DOI: 10.1890/08-1907.1

Staver, A. C., Abraham, J. O., Hempson, G. P., Karp, A. T., and Faith, J. T. (2021) "The Past, Present, and Future of Herbivore Impacts on Savanna Vegetation"
In: Journal of Ecology, Vol. 109.8, pp. 2804–2822.
DOI: 10.1111/1365-2745.13685

Staver, A. C. and Bond, W. J. (2014) "Is There a 'Browse Trap'? Dynamics of Herbivore Impacts on Trees and Grasses in an African Savanna"
In: Journal of Ecology, Vol. 102, pp. 595–602.
DOI: 10.1111/1365-2745.12230

Stocker, B. D., Feissli, F., Strassmann, K. M., Spahni, R., and Joos, F. (2014) "Past and Future Carbon Fluxes from Land Use Change, Shifting Cultivation and Wood Harvest"
In: Tellus B: Chemical and Physical Meteorology, Vol. 66.1, p. 23188.
DOI: 10.3402/tellusb.v66.23188

Terborgh, J. et al. (2001) "Ecological Meltdown in Predator-Free Forest Fragments"
In: Science, Vol. 294.5548, pp. 1923–1926.
DOI: 10.1126/science.1064397

Thurner, M. et al. (2014) "Carbon Stock and Density of Northern Boreal and Temperate Forests"
In: Global Ecology and Biogeography, Vol. 23.3, pp. 297–310.
DOI: 10.1111/geb.12125

Tramontana, G. et al. (2016) "Predicting Carbon Dioxide and Energy Fluxes across Global FLUXNET Sites with Regression Algorithms"
In: Biogeosciences, Vol. 13.14, pp. 4291–4313.
DOI: 10.5194/bg-13-4291-2016

Trepel, J. et al. (2024) "Meta-Analysis Shows That Wild Large Herbivores Shape Ecosystem Properties and Promote Spatial Heterogeneity"
In: Nature Ecology & Evolution, Vol.
DOI: 10.1038/s41559-024-02327-6

Van Valkenburgh, B., Hayward, M. W., Ripple, W. J., Meloro, C., and Roth, V. L. (2016) "The Impact of Large Terrestrial Carnivores on Pleistocene Ecosystems"
In: Proceedings of the National Academy of Sciences, Vol. 113.4, pp. 862–867.
DOI: 10.1073/pnas.1502554112

Villalba, J. J. and Provenza, F. D. (2009) "Learning and Dietary Choice in Herbivores"
In: Rangeland Ecology & Management, Vol. 62.5, pp. 399–406.
DOI: 10.2111/08-076.1

Wardle, D. A. and Bardgett, R. D. (2004) "Human-Induced Changes in Large Herbivorous Mammal Density: The Consequences for Decomposers"
In: Frontiers in Ecology and the Environment, Vol. 2.3, pp. 145–153.
DOI: 10.2307/3868240. JSTOR: 3868240

Wårlind, D., Smith, B., Hickler, T., and Arneth, A. (2014) "Nitrogen Feedbacks Increase Future Terrestrial Ecosystem Carbon Uptake in an Individual-Based Dynamic Vegetation Model"
In: Biogeosciences, Vol. 11.21, pp. 6131–6146.
DOI: 10.5194/bg-11-6131-2014

Wilkenskjeld, S., Kloster, S., Pongratz, J., Raddatz, T., and Reick, C. H. (2014) "Comparing the Influence of Net and Gross Anthropogenic Land-Use and Land-Cover Changes on the Carbon Cycle in the MPI-ESM"
In: Biogeosciences, Vol. 11.17, pp. 4817–4828.
DOI: 10.5194/bg-11-4817-2014

Wilmers, C. C. and Schmitz, O. J. (2016) "Effects of Gray Wolf-Induced Trophic Cascades on Ecosystem Carbon Cycling"
In: Ecosphere, Vol. 7.10, Article e01501–Article e01501.
DOI: 10.1002/ecs2.1501

Wramneby, A., Smith, B., Zaehle, S., and Sykes, M. (2008) "Parameter Uncertainties in the Modelling of Vegetation Dynamics—Effects on Tree Community Structure and Ecosystem Functioning in European Forest Biomes"
In: Ecological Modelling, Vol. 216, pp. 277–290.
DOI: 10.1016/j.ecolmodel.2008.04.013

Appendix

The original published paper and the Corrigendum are attached in the following.

Ecological Modelling 471 (2022) 110061

Contents lists available at ScienceDirect

Ecological Modelling

journal homepage: www.elsevier.com/locate/ecolmodel

How more sophisticated leaf biomass simulations can increase the realism of modelled animal populations

Jens Krause [a,*], Mike Harfoot [b], Selwyn Hoeks [c], Peter Anthoni [a], Calum Brown [a], Mark Rounsevell [a], Almut Arneth [a]

[a] KIT-Campus Alpin, Institute of Meteorology and Climate Research (IMK-IFU), Garmisch-Partenkirchen, Germany
[b] UN Environment Programme World Conservation Monitoring Center, Cambridge, United Kingdom
[c] Department of Environmental Science, Radboud University Nijmegen, Netherlands

ARTICLE INFO

Keywords:
Modelling animal populations in terrestrial ecosystem
Advances/refinement in methods for ecological modelling

ABSTRACT

Animal biodiversity, and its key roles in ecosystem state and functioning, is facing critical challenges in the wake of anthropogenic activities. It is urgently necessary to improve understanding of the interconnections between animals and the vegetation within ecosystems. Process-based modelling has shown to be a mighty tool in making assessments on ecological processes. We assess the effect of different vegetation models on simulated animal biodiversity by replacing the vegetation module within Madingley, a multi-trophic model of functional diversity with LPJ-GUESS, a dynamic global vegetation model. We compare the output metrics of the model system to Madingley's default version for four ecosystem types around the globe and analyse whether the realism of the simulation results increased as a result of the coupling between Madingley and LPJ-GUESS. Simulated animal populations react to the coupling by shifting towards smaller individuals with a higher abundance. General shifts in body mass and animal distributions can be traced back to ecological processes, allowing in-depth analysis of heterotrophic responses to changes in leaf biomass. We also derive power-law relationships for herbivory to NPP and herbivore biomass to NPP and conclude that the coupled model system simulates animal populations that follow reasonable power-laws which are similar to power-laws derived from empirical data. Our results indicate that developing process-based model systems is a viable way to assess multi-trophic interconnections between animal populations and the ecosystems vegetation.

1. Introduction

Animals can play a key role in controlling the state and function of all terrestrial ecosystems (Schmitz et al., 2014, 2018). By consuming autotrophic biomass, herbivory enhances light transfer into plant canopies and affects net carbon assimilation. Cascading trophic effects triggered by top predators or the largest herbivores propagate through food webs, regulating levels of herbivory and affecting soil carbon and nitrogen cycling through excreta and dead bodies (Schmitz et al., 2014). However, anthropogenic activities such as habitat modification, harvesting and, increasingly, anthropogenic climate change are driving large declines in biodiversity (Cardinale et al., 2012; Pacifici et al., 2015; Arneth et al., 2020). Therefore, a better understanding of how changes and losses of plant and animal functional diversity will affect ecosystem functioning is needed from the perspective of both an ecosystems role for both climate change mitigation and climate change adaptation. However, the diverse mixture of species and the interconnectivity in food webs makes quantifying the link between ecosystem biogeochemical cycling and an ecosystems functional diversity a challenge (Schmitz et al., 2018).

Animals comprise lower total biomass overall compared to plants (Bar-On et al., 2018) which could easily result in the assumption that animals play a relatively minor role in terrestrial ecosystem carbon cycling. But this view is being challenged by an increasing body of literature. For instance, for eastern Africa (Holdo et al., 2009) extrapolated impacts of strongly reduced wildebeest numbers due to the rinderpest into the future, and hypothesised that major future wildebeest die-offs might lead to a significant increase in grass biomass, leading to changes in fire regimes and a potential shift of ecosystems into a net carbon source. Hooper et al. (2012) suggested that the absence or presence of herbivores and carnivores within an ecosystem can lead to similar magnitude impacts as caused by other environmental change drivers such as global warming, enhanced CO2 or nitrogen pollution. Wilmers and Schmitz (2016) estimated, based on measurements, that wolves

* Corresponding author.
E-mail address: jens.krause@kit.edu (J. Krause).

https://doi.org/10.1016/j.ecolmodel.2022.110061
Received 25 October 2021; Received in revised form 19 June 2022; Accepted 21 June 2022
Available online 2 July 2022

preying upon moose in Northern American boreal forests enhance net primary productivity (NPP) and net ecosystem carbon uptake by up to 30% by decreasing moose CO2 respiration and increasing growth of deciduous trees, due to releasing herbivory pressure. Sobral et al. (2017) carried out an analysis based on observations in the Amazonian region which showed animal diversity influencing the carbon cycle directly via metabolism and indirectly via seed dispersal and altering the vegetations species composition. Nevertheless, so far studies and extrapolations of their results that seek to link animal impacts to ecosystem biogeochemical cycles are typically limited by their temporal or spatial scale (Holdo et al., 2009; Staver and Bond, 2014; Sobral et al., 2017) or focus on a few distinct animal species (Schmitz et al., 2018; Nichols et al., 2016) so limiting the general applicability of their conclusion.

Process-based models can help to overcome observation limitations and improve our knowledge about the complex interactions within ecosystems by expanding the scope to the whole ecosystem. A few model studies have started to explore the role of animals. Berzaghi et al. (2019) included elephant disturbances into an ecosystem demography model and showed that the resulting reduction in tree stem density altered competition for light and water and actually enhanced above-ground biomass. Pachzelt et al. (2015) coupled a physiological grazer population model with a dynamic vegetation model and identified NPP and the length of the dry season as the main determinants of grazer population size in African savannah ecosystems. They found that the presence or absence of grazers substantially impacts the standing grass and tree vegetation biomass, as well as the area vulnerable to burning. Dangal et al. (2017) coupled a herbivore population dynamics model with a dynamic land ecosystem model and were able to preproduce observed herbivore populations for livestock species. The presence of these herbivores reduced the NPP in all nine modelled regions while revealing a vulnerability of herbivores to climate extremes.

While these studies contribute important information to the understanding of animals' roles in ecosystem functioning, they also focus on distinct animal species or species classes and neglect complexities such as the top-down control predators impose on herbivores and omnivores and thus food-webs in ecosystems. The Madingley model (Harfoot et al., 2014) adopts a different approach, linking fluxes of biomasses between above-ground autotrophs and heterotrophs by modelling the fundamental processes affecting the ecology of these organisms. Trophic structures in the modelled ecosystems emerge from the representation of individual and community level biological processes, and interactions between organisms and their environment. Madingley has been shown to reproduce patterns and functional processes in animal populations and has been used to model terrestrial and marine ecosystems (Harfoot et al., 2014; Enquist et al., 2020) and to analyse complex food chains (Hoeks et al., 2020). At present, the vegetation, which drives herbivory, is modelled by an empirical carbon cycling model (Smith et al., 2013), in which primary production is determined by the Miami Model (Lieth, 1975). However, the Miami Model does not capture important dynamics such as interannual variability and trends in vegetation composition and productivity introduced by weather, climate change, carbon–nitrogen interactions and changes in atmospheric CO2, which modern dynamic vegetation models do. This limits Madingleys applicability to explore future global environmental change impacts on ecosystem functional diversity.

Here, we couple Madingley to the advanced dynamic global vegetation model (DGVM) LPJ-GUESS to test how more complex vegetation dynamics affects characteristics of simulated animal populations. The work presented here is the first step towards creating a fully coupled multi-trophic model of functional diversity which combines the advantages of complex process-based vegetation and animal modelling, allowing comprehensive assessment of animal-vegetation feedbacks in ecosystems.

2. Methods

2.1. The Madingley model

Madingley represents herbivores, omnivores and carnivores of all size classes, from very large to very small. The heterotrophs are organised into functional groups according to a set of categorical functional traits related to feeding modes, metabolic pathways, reproduction and movement. The model is defined at the level of individual organisms. To avoid impractical computational requirements, within each functional group, individuals are grouped together into cohorts, in which all individuals possess the same set of categorical traits plus identical continuous traits defining their juvenile, adult and current body mass and age. These continuous traits vary across cohorts which share a functional group. Cohorts of individuals undergo a set of ecological processes: metabolism, predation, feeding, reproduction and mortality (Harfoot et al., 2014). Dividing the model domain into distinct grid cells makes it possible for cohorts to disperse between those grid cells. The lowest levels of the heterotrophic pyramid, the herbivores, are feeding upon evergreen and deciduous leaf biomass stocks simulated by the carbon cycle model of Smith et al. (2013). While the deciduous stock is showing seasonal availability, herbivores assimilate relatively more biomass when compared to the same amount of evergreen leaf biomass being consumed. Evergreen and deciduous stock therefore represent a trade-off between food availability and food quality. At higher trophic levels, carnivores prey upon other animal cohorts, with a prey size preference. Omnivores feed from the leaf biomass stocks and heterotroph cohorts alike but are less effective doing so, due to a lower assimilation rate for both herbivory and carnivory. These feeding processes are limited to the stocks and cohorts of the respective grid cell. Herbivory is not uniform (e.g, different types of herbivores access different amounts and types of leaf biomass in an ecosystem), processes that are currently not yet captured in Madingley. As a conservative assumption (implemented in Madingley as $\phi_{herb,f} = 0.1$, Table 6 in Harfoot et al. (2014)), the total biomass consumed is thus limited to 10% of the gridcells leaf-biomass stock.

The growth of individuals is handled as the difference between their nutrition uptake and metabolic cost. Once an individual reaches its maturity, it starts accumulating its nutrition uptake towards reproduction. For this study, we adopted and modified the latest version of the model described by Hoeks et al. (2020).

So far, the leaf biomass stocks, which apply a bottom-up control on the simulated trophic pyramid, are modelled by the carbon cycle model of Smith et al. (2013), which includes the Miami Model by Lieth (1975). The Miami Model predicts the total annual net primary production (NPP) based on the yearly mean temperature and total precipitation sum in the following way:

$$NPP_{(T,p)} = min\left(\frac{0.916645}{1 + exp(0.23747 - 0.006 \cdot T)}, \frac{0.916645}{1 - exp(0.00118 \cdot p)}\right) \quad (1)$$

In Madingley, the annual simulated NPP is converted to wet matter, which animals consume, via an estimate of 9.813 $g_{wetmatter}/gC$ (Kattge et al., 2011). The annual values are then split into monthly fractions using a seasonality factor. Leaf mortality and carbon partitioning to leaves is also parameterised through temperature related factors. The resulting monthly wet matter leaf increment is divided between evergreen and deciduous vegetation according to the fraction of the year prone to frost in the specific grid cell.

2.2. Forcing Madingley with LPJ-GUESS vegetation data

LPJ-GUESS is a biogeochemical dynamic global vegetation model that combines the advantages of a global macroscopic nutrient cycle and carbon assimilation model with the advantages of an individual-based growth model (Smith et al., 2014; Wårlind et al., 2014). Plant individuals are represented by age-cohorts, which share key ecological

Table 1
Plant functional types in LPJ-GUESS with evergreen or deciduous leaf biomass. Summergreen, raingreen and grassy PFTs, are accounted towards Madingley's deciduous stock.

PFT-ID	Climate type	Lifeform	Leaf physiognomy	Phenology	Light behaviour
BNE	Boreal	Tree	Needle-leaved	Evergreen	Shade tolerant
BINE	Boreal	Tree	Needle-leaved	Evergreen	Shade intolerant
TeNE	Temperate	Tree	Needle-leaved	Evergreen	Shade tolerant
TeBE	Temperate	Tree	Broadleaved	Evergreen	Shade tolerant
TrBE	Tropical	Tree	Broadleaved	Evergreen	Shade tolerant
TrIBE	Tropical	Tree	Broadleaved	Evergreen	Shade intolerant
BLSE	Boreal	Low Shrub	Needle-leaved	Evergreen	Shade intolerant
BNS	Boreal	Tree	Needle-leaved	Summergreen	Shade intolerant
IBS	Boreal	Tree	Broadleaved	Summergreen	Shade intolerant
TeBS	Temperate	Tree	Broadleaved	Summergreen	Shade tolerant
TrBR	Tropical	Tree	Broadleaved	Raingreen	Shade intolerant
BLSS	Boreal	Low Shrub	Broadleaved	Summergreen	Shade intolerant
C3G	All	Grass	C3 grass	Cold season or yearlong	
C4G	All	Grass	C4 grass	Warm season	

properties and traits, categorising them into plant functional types (PFTs) distinguished by their bioclimatic preferences, photosynthesis pathways and growth strategies. Plant cohorts compete for nitrogen, light, water and space. Annual processes, like biomass allocation, leaf, root and sapwood turnover, disturbances or mortality are simulated at the beginning of a year. Short-term processes like soil hydrology, stomata regulation, photosynthesis, plant respiration, decomposition and phenology are simulated on a daily basis. The overall accuracy of the modelled processes and interactions has been evaluated extensively (Hickler et al., 2006; Wramneby et al., 2008; Lindeskog et al., 2021; Smith et al., 2014) and has shown LPJ-GUESSs skills in capturing large-scale vegetation patterns and vegetation dynamics. LPJ-GUESSs physiological vegetation process representation goes far beyond Madingleys current approach to estimate the biomass of deciduous and evergreen leave.

LPJ-GUESS requires multiple years of climate data to ensure sufficient variability for computing the models stochastics, interannual disturbances and for the model spin-up. For our purposes here, we chose to cycle the CRUJRA v2.1 climatology (Harris, 2020) based on the years 1950 to 1979. This approach allows us to compare vegetation simulated with LPJ-GUESS and Miami, since Miami was parameterised based on empirical data available during the 1960s. We cycled atmospheric CO2 concentrations ranging from 311 to 335 ppm during the LPJ-GUESS simulations. Since the CRUJRA dataset has a 6-h resolution, we used daily postprocessing methods (supplementary information S1).

LPJ-GUESS simulates 12 woody and 2 grassy plant functional types, which were converted, based on their phenology, into the evergreen and deciduous leaf-biomass stocks that are available for herbivory in Madingley (Table 1). Since LPJ-GUESS is running on a daily timestep, we account leaf biomass from all PFT cohorts during every timestep and produce a monthly average of the total evergreen and deciduous leaf biomass per grid cell. We then pass this information to Madingley using a file-transfer method and replace Madingleys parameterised autotroph stocks during every timestep. Fig. 1 shows a simplified technical blueprint to illustrate how we realised the coupling of the two models.

The latest version of Madingley (Hoeks et al., 2020) cycles a single year of environmental input data throughout the simulation. Climate does not only affect the vegetation, but also the animals metabolism due to its ecto- and endothermic thermoregulation method. To ensure that the animals in Madingley are exposed to the same climate used for the vegetation prediction in LPJ-GUESS, we expanded the length of Madingleys environmental forcing from the single-year cycle to a 30-year time series. We used the same CRUJRA v2.1 climate data but due to Madingleys monthly timestep, we needed to process the data monthly (supplementary information S1).

Both model setups represent a solid and stable version of the model. The computational time necessary to carry out a single simulation did not change noticeably when coupling Madingley with LPJ-GUESS.

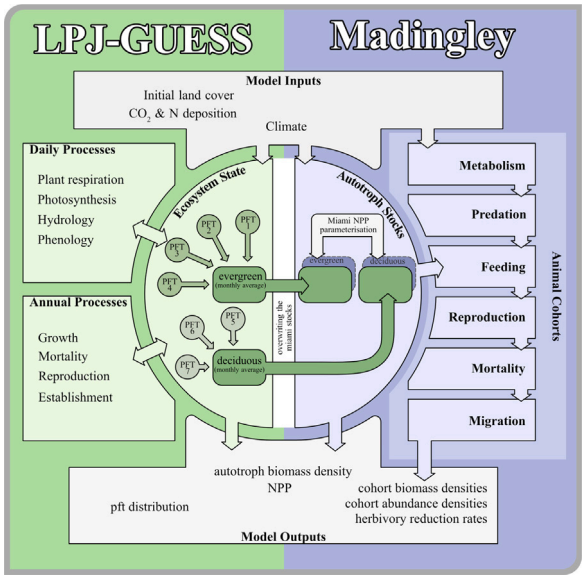

Fig. 1. Technical coupling illustration.

The additional time needed to precompile the LPJ-GUESS is small in comparison to the average Madingley runtime. Thus, we did not increase the computational cost for a single run significantly. However, the Madingley simulations with the C++ version are quite time and memory-consuming so we decided to carry out smaller scale simulations at different locations instead of a continental or global run. Other recent studies with Madingley followed a similar approach (Newbold et al., 2020) or used a coarser grid for their simulations (Hoeks et al., 2020).

2.3. Madingley simulation setup

We compared Madingley output simulated with its standard Miami-based vegetation with simulations in which, at the beginning of each timestep, the leaf biomass was replaced by the modelled leaf biomass from LPJ-GUESS, summed up for deciduous and evergreen pfts. Four experiments are presented here to test how LPJ-GUESS vs. Miami vegetation affects model stability, community structures and individual traits. To investigate how ecosystem productivity and climatic conditions affect the coupling responses, we performed simulations for four locations representing three different types of forest ecosystems and one savanna ecosystem (Table 2). Each location was resolved by a grid of three-by-three cells, spanning a 1.5° latitude by 1.5° longitude model domain with a resolution of 0.5° in each direction. Both Madingley

Table 2
Description coordinates of the four experiment locations.

Simulation tag	Vegetation model	Longitude range	Latitude range	Ecosystem type
Hyytiälä (Finland)				
FIN M-M FIN M-LPJG	Miami Model LPJ-GUESS	24°E–25°E (0.5° resolution)	61°N–62°N	Boreal Coniferous Forest
Waldstein (Germany)				
GER M-M GER M-LPJG	Miami Model LPJ-GUESS	11°E–12°E (0.5° resolution)	50°N–51°N	Temperate Mixed Forest
Lake Mburo Nat. Park (Southern Uganda)				
UGA M-M UGA M-LPJG	Miami Model LPJ-GUESS	28°E–29°E (0.5° resolution)	0°N–1°N	Tropical Rainforest
Pretoria (South Africa)				
SAF M-M SAF M-LPJG	Miami Model LPJ-GUESS	28°E–29°E (0.5° resolution)	26°S–25°S	Subtropical Savanna

Table 3
Animal functional groups in Madingley and their corresponding key ecological traits.

Feeding mode	Reproductive strategy	Thermoregulation strategy	Min. body mass [g]	Max. body mass [g]	Herbivory assimilation efficiency	Carnivory assimilation efficiency
Herbivore	Iteroparity	Endotherm	1.5	5 000 000	0.8	0.0
Omnivore	Iteroparity	Endotherm	3	200 000	0.65	0.65
Carnivore	Iteroparity	Endotherm	3	400 000	0.0	0.8
Herbivore	Iteroparity	Ectotherm	0.0004	10	0.8	0.0
Omnivore	Iteroparity	Ecotherm	0.0004	20	0.65	0.65
Carnivore	Iteroparity	Ecotherm	0.0008	20	0.0	0.8
Herbivore	Semelparity	Ecotherm	0.0004	1000	0.8	0.0
Omnivore	Semelparity	Ecotherm	0.0004	2000	0.65	0.8
Carnivore	Semelparity	Ecotherm	0.0008	2000	0.0	0.65

and LPJ-GUESS run on a 0.5 resolution, so we did not need to up- or downscale any of the exchanged data.

In all four studies, we compared both setups, Madingley+Miami-Model (M-M) and Madingley+LPJ-GUESS (M-LPJG) and check what effects our coupling implies on the model system.

All simulations include the same animal functional group definitions. These groups are distinguished by their feeding mode, their reproductive strategy and their thermoregulation strategy (Table 3). Each grid cell was initialised with 100 cohorts of each functional group with initial body masses that are drawn randomly from the cohorts juvenile and adult body mass. During a simulation, cohorts die out or are newly created in response to predation, mortality and reproduction. The total number of cohorts that are allowed to coexist in one grid cell is limited to 1000.

For all experiments, we carried out runs at each of the four locations from Table 2. All the data extracted from the model were collected at the end of each timestep and thus represent the state of the ecosystem after all ecological processes have been executed. This is true for all animal functional groups and autotroph stocks alike.

In the first experiment, we ran an ensemble of ten long-term simulations to investigate the development of leaf biomass and heterotrophic functional-group dynamics. Each simulation covered 1000 years of simulation time. The objective here was to test whether Madingleys model dynamics reaches equilibrium conditions with LPJ-GUESSs, as well as with Miamis vegetation input. When a simulation reaches a state where aggregated biomass densities of both autotroph stocks and heterotroph cohorts are not trending up or downwards anymore, we assume the model system has reached its dynamic equilibrium stage.

For the second experiment, we compared the canopy compositions of the simulated vegetation from both LPJ-GUESS and the Miami Model. The objective here was to visualise the differences between the two vegetation models. Since these differences are the key drivers for all coupling-related changes, understanding them is essential for the interpretation of all other experiments.

In our third experiment, we focussed on how the coupling alters the basic shape of the trophic pyramid and how it affects the animal population on a community level as a whole. To do so, we investigated the biomass pools of the trophic pyramid and the fluxes between those pools. We used an ensemble of ten simulations to capture stochastic variation within the pools. Shifts in leaf biomass density are likely to affect the size distribution of animals as a result of the bottom-up regulation of autotrophs in the trophic pyramid, so we also compared the emergent size distribution of cohorts driven by the two vegetation models.

After investigating the effects of our coupling on the community level, our fourth experiment focussed on the effects on an individual level by taking a closer look at power-law relationships between individual body mass and growth rate per timestep, days needed to reach maturity, lifespan and lifetime reproduction successes.

The simulations for the third and fourth experiments differ in terms of simulation length due to the longer time needed for the UGA setup to reach its dynamic equilibrium (as found in experiment 1). The UGA simulations covered 600 years of simulation time, while all other setups covered 250 years of simulation time. We extracted detailed information on cohort characteristics during the last year of every simulation. A table with all setup descriptions and the most relevant output for each experimental setup can be found in the supporting information S4.

To set the effects of our coupling into context, we compared both M-LPJGs and M-Ms simulated NPP for the four experiment locations. Since the NPP parameterised by the Miami Model forms the foundation of the M-M simulations, we wanted to test if the NPP simulated by LPJ-GUESS is more realistic. For the comparison we used NPP data derived from the MODIS 17ASHGFv061 dataset (Running and Zhao, 2021) as the average NPP of the area corresponding to the model domains. The MODIS data layers are derived from the RUE (radiation use efficiency) concept (Hatfield and Dold, 2019) and therefore are produced by a model themselves.

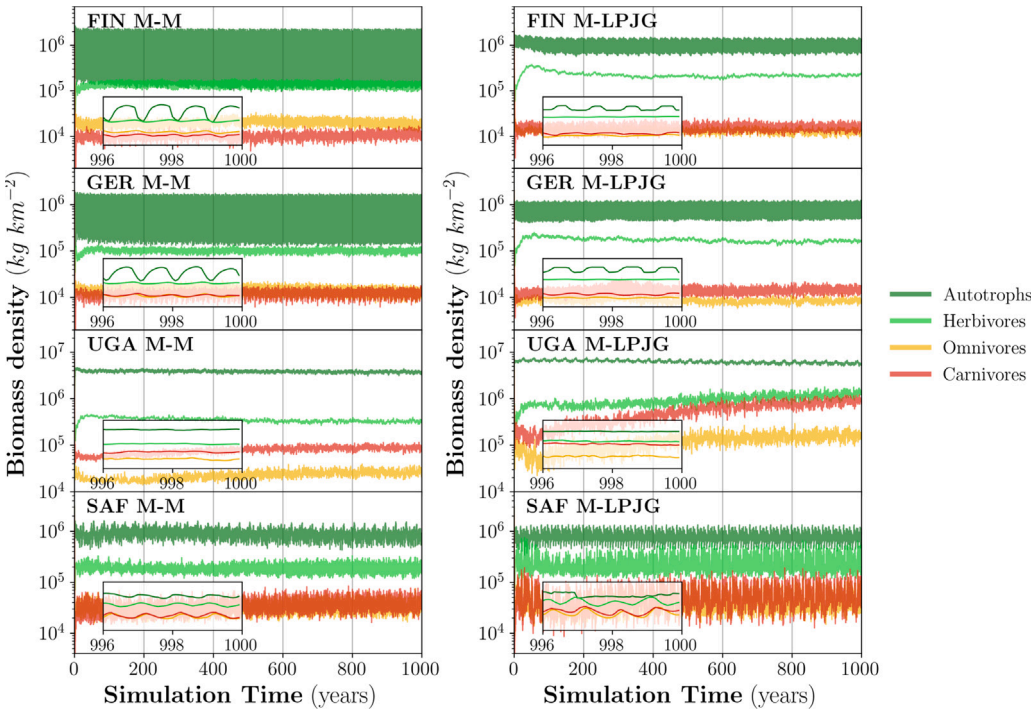

Fig. 2. Long-term analysis. Averages from 10 ensemble runs of wet biomass densities. The M-LPJG simulation on the right and the M-M simulations on the left. The zoomed insets are showing the last 4 years of the simulations to better visualise the annual fluctuations.

We also compared the results of our simulations with power-law relationships (Cebrian, 2004), derived from a huge body of literature on net primary production and herbivore biomass and consumption by primary consumers. Most authors estimate empirical data for herbivore biomass from a mean herbivore individual weight multiplied by the herbivore abundance, which is similar to the total herbivore body mass calculation in Madingley. Empirical data for consumption by primary consumers is commonly recreated based on animal evacuation, exclosures/enclosures, parameterisation of herbivore metabolism, reconstruction methods based on bite marks and leaf growth rates. Studies using these techniques derive their herbivory rate reconstruction by comparing ecosystem states with and without reduced herbivory stress. It is worth noting that Cebrian (2004) combined herbivore consumption and detritus consumption in one pool as primary consumption, while Madingley only includes herbivores. We derived power-laws for the same functional relationships from the last ten years of each simulation.

Since long-term measurement data is available for the GER and FIN sites, we included comparisons between Madingley and LPJ-GUESS model runs and data from Cebrian (2004), Rebmann et al. (2010) and Launiainen et al. (2022) in the supplementary information (S5).

3. Results

3.1. Experiment 1: Long-term analysis

The left side of Fig. 2 shows the simulated biomasses resulting from the M-M simulations, while the right side shows those from M-LPJG. In M-M, the simulations reach a state of dynamic equilibrium after about 100 years. The time needed for a simulation to reach equilibrium in M-LPJG ranges from about 100 years (locations FIN, GER, SAF) to about 500 years (UGA).

Simulated leaf biomass density in the two vegetation models differs markedly. In the M-LPJG simulations, the amount of evergreen leaf biomass barely changes over the course of a year, in contrast to the seasonal oscillation seen in deciduous leaf biomass. This is clearly visible, for example, in the boreal and temperate climate regions with a high seasonality – represented by FIN and GER M-LPJG. In the FIN, GER and SAF M-M setups – both evergreens and deciduous stocks fluctuate strongly over the course of a year, while also having a higher amplitude and lower winter minima when compared to M-LPJG simulations. In both, UGA M-M and UGA M-LPJG, the leaf biomass stocks fluctuate only little. Leaf biomass stocks in SAF M-LPJG are more variable than in SAF M-M.

In the FIN M-LPJG simulation, simulated carnivores and omnivores show similar biomass densities, while omnivore biomass density exceeds carnivore biomass density in FIN M-M. All other simulations show similar hierarchies in heterotroph biomass densities between the M-M and M-LPJG simulations. In all simulations, herbivores dominate heterotroph biomass densities.

3.2. Experiment 2: Canopy composition

As indicated already in Fig. 2, significant differences between LPJ-GUESS and the Miami Model emerge from the simulated vegetation composition. Fig. 2 shows simulated autotrophic biomass split into the evergreen and deciduous stocks for the M-LPJG and M-M setups. A more detailed pft composition for each location can be found in the supplementary information S2. In the FIN and GER location, the Miami Model simulates large seasonal fluctuations throughout a year for both evergreen and deciduous stocks. LPJ-GUESSs simulated vegetation stocks are much more stable throughout the year for evergreen leaf biomass and show the expected seasonal fluctuations in deciduous leaf biomass. Under sub-tropical and tropical climate conditions, M-LPJG simulates substantially less deciduous leaf biomass than M-M.

In SAF, variability in evergreen leaf biomass is higher in the M-LPJG simulations and less regular, likely due to fire impact in these fire-prone environments. While M-M is parameterised to burn a fixed percentage of leaf biomass annually depending on climatic conditions, M-LPJG uses the statistically-based fire model SIMFIRE-BLAZE, which simulates fire-frequencies, fire-intensities, fire-related fluxes and responses in vegetation (Launiainen et al., 2022; Rabin et al., 2017).

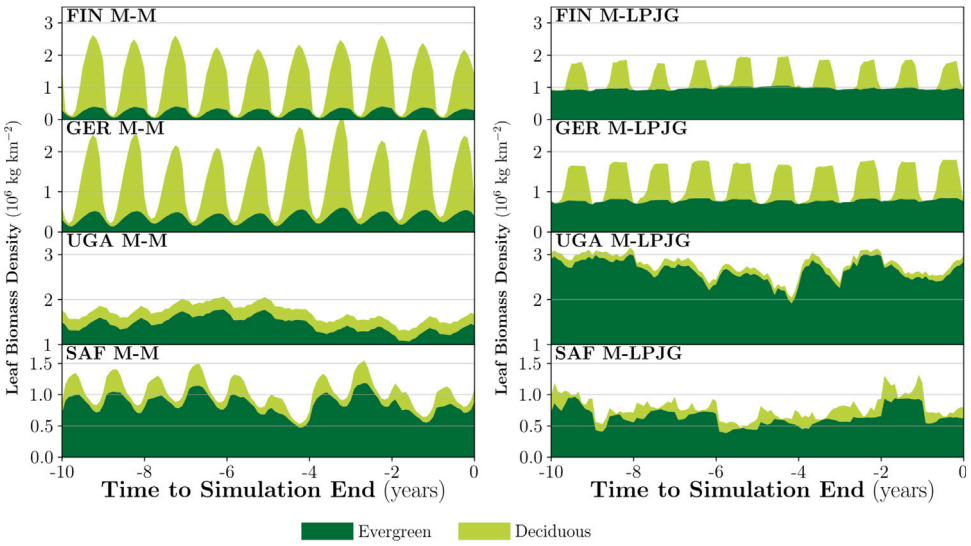

Fig. 3. Evergreen and deciduous composition. Stacked plots of the vegetations total leaf biomass during 10 years of a simulation — split into light green evergreen and dark green deciduous compartments.

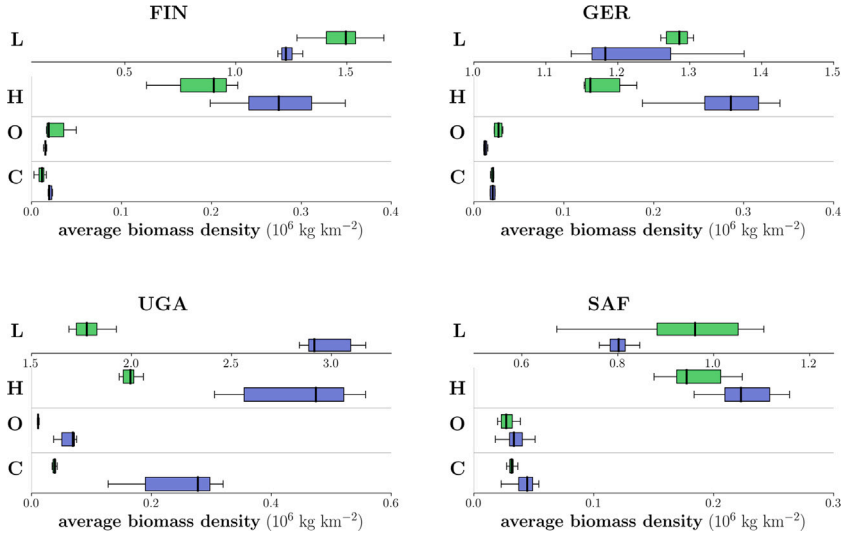

Fig. 4. Averaged biomass pools. Pools of leaf (L), herbivores (H), omnivore (O) and carnivore (C) biomass densities, averaged over the last ten years of the simulations. Medians and deviations from the medians are calculated from eight ensemble simulations. Due to the greater magnitude of the leaf biomass, it is shown on a separate scale (same unit as the other pools). Green boxes indicate the data from the M-M simulations, blue boxes indicate the data from the M-LPJG simulations. For comparison between sites, note the different axes scale.

3.3. Experiment 3: Community level analysis

All community level simulations show differences between the M-M and M-LPJG simulations (Figs. 4 and 5). The average leaf biomass is smaller in FIN M-LPJG (−16%), GER M-LPJG (−5%) and SAF M-LPJG (−15%) compared to the M-M results. In UGA, M-LPJG simulates 66% more average leaf biomass than M-M. The overall herbivore biomass of the M-LPJG simulations exceed those of the M-M simulations in every location (Fig. 3), most dominantly in UGA (+170%). Average carnivore biomass in the M-LPJG simulations is greater in FIN (+93%), SAF (+34%) and again most dominantly in UGA (+542%). Average omnivore biomass in the M-LPJG simulations is decreased in FIN (−39%) and GER (−51%), and is increased in UGA (+453%), compared to M-M.

In FIN and GER, all biomass fluxes besides L → H, H → C and C → O show similar medians in both M-M and M-LPJG simulations. In SAF all fluxes show a slight increase in M-LPJG up to +20%. In UGA, all fluxes show a significant increase in M-LPJG up to +500% (Fig. 5).

In FIN, GER and SAF with the M-LPJG coupling, the size distribution spectrum shows a tendency towards individuals with a higher abundance and lower biomasses (Fig. 6). In the M-LPJG runs at the UGA location, the high and low end of the body mass spectrum of endotherms shows higher individual numbers when compared to the M-M simulations. Especially ectotherms show larger individual numbers at the lower end of the body mass spectrum.

Under boreal and temperate climate conditions, the M-LPJG coupling showed the largest increases in the number of endotherm cohorts. In contrast, at the tropical and sub-tropical sites, ectotherm cohorts increase more in the runs using M-LPJG vegetation (Fig. 6). At all four sites, the M-LPJG coupling consistently results in larger cohort numbers of carnivore endotherms. In FIN M-M, the whole functional group of carnivore endotherms disappear in the first years of the simulation without any reestablishment afterwards. Herbivore endotherms are concentrated at the higher end of the body mass spectrum. In FIN M-LPJG, carnivore endotherms are present throughout the simulation and herbivore endotherms populate a wider range of the body mass spectrum.

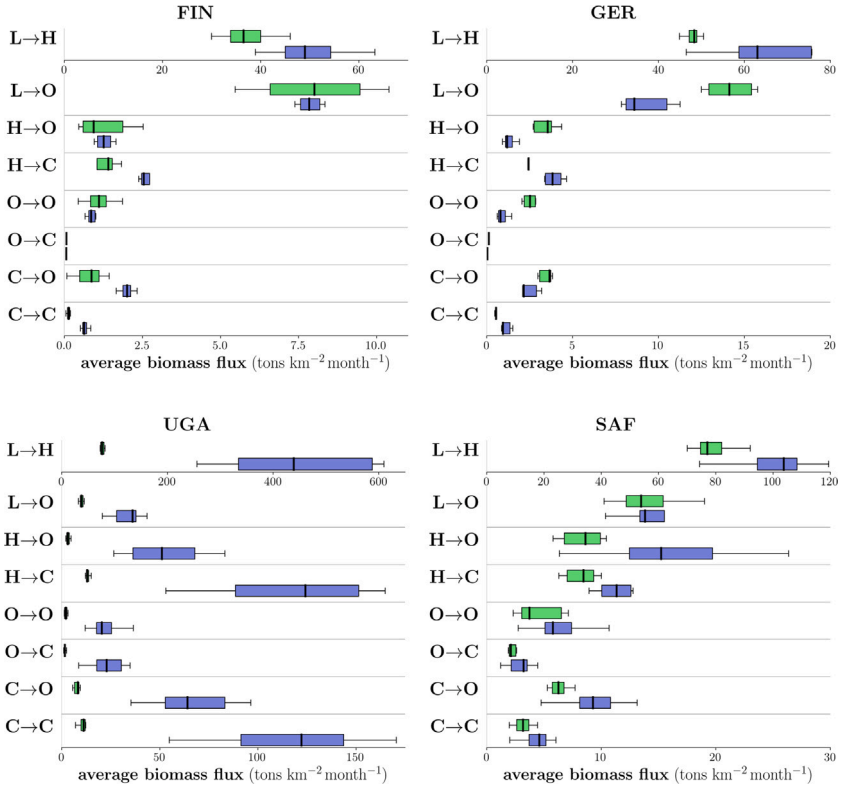

Fig. 5. Averaged biomass fluxes. Biomass fluxes between leaf (L), herbivores (H), omnivores (O) and carnivores (C) averaged over the last ten years. Medians and deviations from the median are derived from eight ensemble simulations. Due to the greater magnitude of L→H flux, it is shown on a separate scale (same unit as the other fluxes). Green boxes indicate the data from the M-M simulations, blue boxes indicate the data from the M-LPJG simulations.

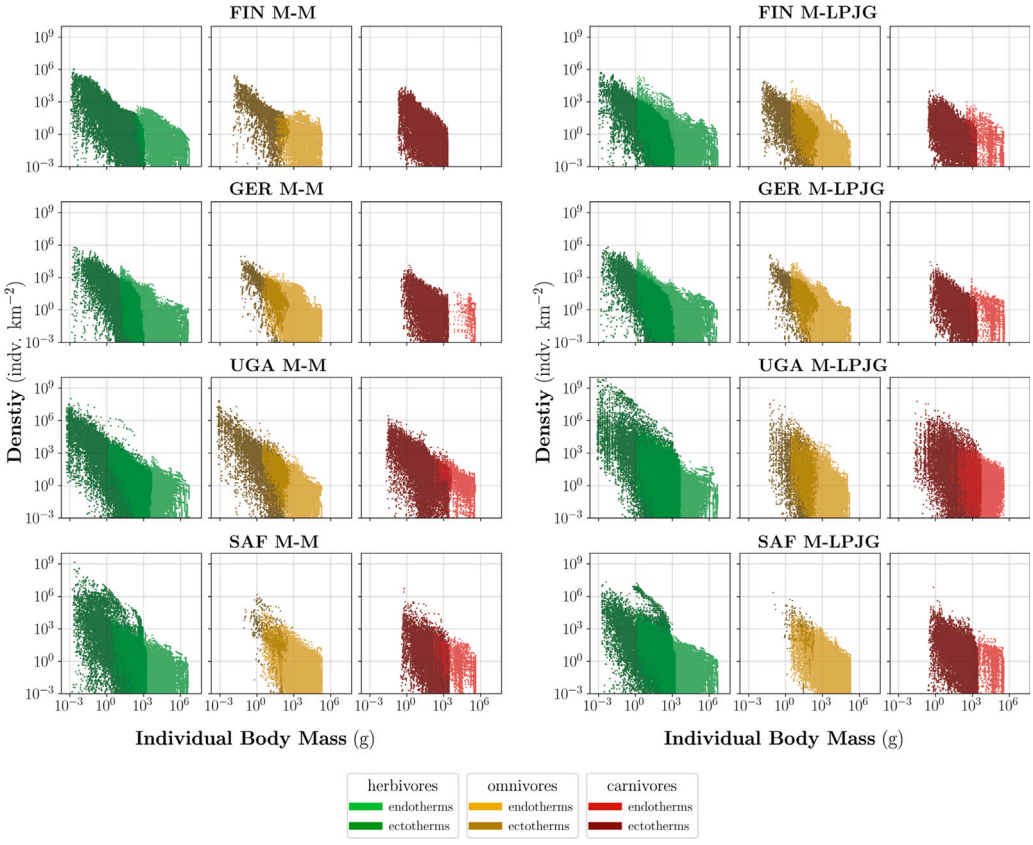

Fig. 6. Size distributions. The emergent size distributions, showing every cohort state during the last year of one simulation. Each marker represents one cohort state. The lighter colours represent endotherm cohorts.

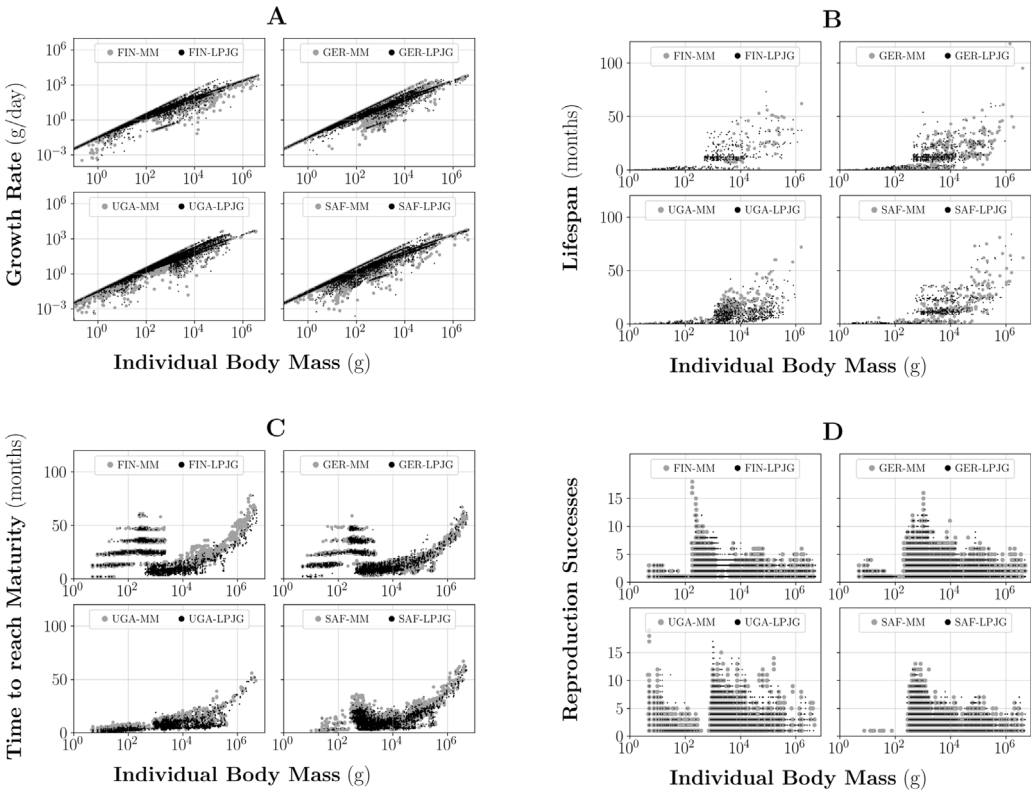

Fig. 7. Individual level characteristics. Every dot represents the state of a cohort during the last year of a simulation. Grey dots represent cohorts from M-M setups, while black dots represent cohorts from the M-LPJG setup. A shows the individuals growth rate. B shows the lifespan of the cohorts that have died (hence, the number of cohorts in B differs from the other graphs.) C shows the time cohorts need to reach their adult body mass. D shows the cohorts lifetime reproduction successes.

3.4. Experiment 4: Individual level analysis

The individual level analysis shows general similarities between the M-M and M-LPJG setups for each location (Fig. 7A). Growth rates are slightly larger in the M-LPJG runs. Most notable is an increased growth rate of the smallest individuals in SAF and UGA. The lifespan of bigger individuals (individuals that have body mass >100 g) decreases in the M-LPJG simulations for all locations (Fig. 7B). Consequently, the mortality rate for cohorts containing bigger individuals increases. This effect is most dominant in UGA. In FIN and SAF, the time endotherm cohorts need to reach maturity state decreases noticeably in M-LPJG (Fig. 7C). Besides an increased growth rate and a shorter time to reach maturity, the shorter lifespan seems to be the dominant effect, leading to the cohorts having a reduced lifetime reproduction success rate in all M-LPJG simulations (Fig. 7D).

3.5. Comparison to external sources

At all experiment locations, M-LPJG consistently predicts the NPP better than M-M when compared to the MODIS dataset (Fig. 8). The best LPJ-GUESS predictions were found in the FIN (−9%), GER (−5%) and SAF (−3%) setup, while the only larger difference was found in UGA (+17%). The M-M simulations show a larger gap between Miamis predicted NPP and the data derived from the MODIS dataset (FIN −21%, GER −20%, SAF +45% and UGA −25%).

Beyond comparing the vegetation model outputs to the MODIS V6.1 dataset, we also made an assessment of whether the realism of the entire model system output was increased. According to Cebrian (2004), terrestrial ecosystems NPP is related to herbivore biomass and herbivore consumption by the following logarithmic power laws:

$$\log(biomass) = -3.43 + 1.30 \cdot \log(NPP) \quad (2)$$

$$\log(primaryconsumption) = 0.24 + 0.82 \cdot \log(NPP) \quad (3)$$

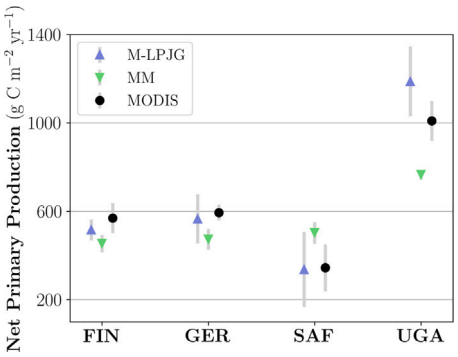

Fig. 8. Comparing simulated NPP to MODIS data. Blue triangles represent the domain average for M-LPJG simulation. Green triangles represent the domain average for M-M simulation. Grey bars mark the range of the standard deviation. Black dots mark the area average derived from the MODIS dataset.

We were able to determine similar shaped power-law relations from the M-LPJG simulations by applying a logarithmic fit for the last ten annual sums of herbivore biomass and consumption. We derived the following power-law relationships:

$$\log(biomass) = -1.75 + 1.03 \cdot \log(NPP) \quad (4)$$

$$\log(primaryconsumption) = -1.94 + 1.55 \cdot \log(NPP) \quad (5)$$

These power-law relationships are shown in Fig. 9. Notable is the high herbivore biomass and herbivory consumption in SAF M-LPJG, which is the ecosystem with the lowest simulated productivity.

Since the Miami model predicts a smaller range of NPP throughout diverse ecosystems when compared to M-LPJG, all data points for

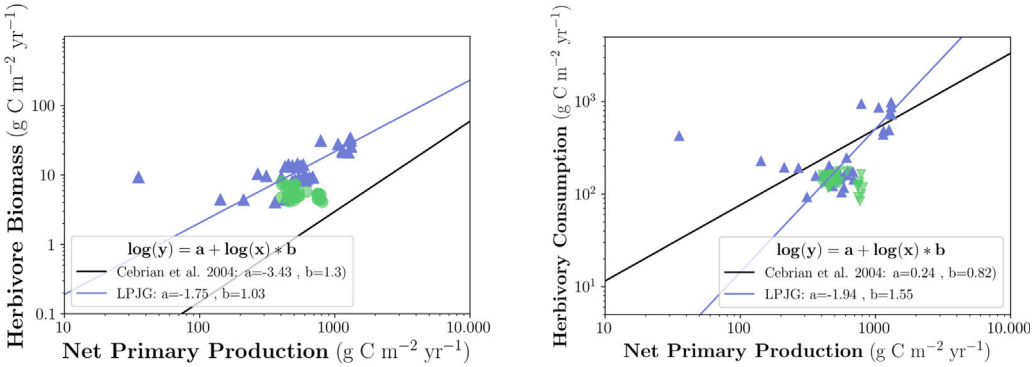

Fig. 9. Power-law relationships. Blue triangles represent an annual sum during a M-LPJG simulations. Green dots represent an annual sum during a M-M simulations. For the M-LPJG setups, herbivore biomass and herbivory consumption are related to NPP. There are no reasonable corresponding logarithmic fits for the M-M setups.

the M-M simulations are clustered in a narrow range. This renders a logarithmic fit for herbivore biomass and herbivory consumption unreasonable, so these are not provided here. However, it is worth noting, that in the M-M simulations both herbivore biomass and herbivory consumption consistently show lower values in ecosystems with slightly higher NPP, providing weak support for an inverse relationship in that model.

4. Discussion

The large differences between M-M and M-LPJG simulations show a complex interconnectivity of coupling-related effects throughout the experiments. To analyse their validity, we first want to explain the observed changes and the underlying processes. Secondly, we want to discuss the differences to the MODIS dataset and the power laws derived by Cebrian (2004).

4.1. Development of the animal population

The model reaches a dynamic steady state in all M-LPJG and M-M setups. The longer time needed for the UGA M-LPJG simulation is most likely caused by the much larger amount of edible leaf biomass simulated for this location in LPJ-GUESS, compared with Miami. Cohorts of heterotrophs were initialised in the same way for all four locations. Their subsequent growth is therefore not only limited by food availability, but also by climatic conditions and predation. UGAs warm climate lengthen the active time of ectotherms and thus increases their food uptake and metabolic cost. Therefore, UGA M-LPJGs larger vegetation biomass supply funnels through to the higher trophic levels which increases predation stress for the lower trophic levels. These interactions increase the growth limit of the cohorts, and thus result in a longer period necessary to reach the model systems dynamic steady state. This effect appears to be most visible in enhancing herbivore and carnivore biomasses. Omnivores also responded to the changes in vegetation stocks, but not as much as the other groups, possibly because while omnivores have the ability to feed both from plants and other cohorts, they do so with a less efficient assimilation strategy.

In contrast to UGA, leaf biomass was lower at the other three locations in the M-LPJG simulations compared to M-M. The larger total herbivore biomass in the M-LPJG runs was thus unexpected. Since the reported leaf biomass data represents the stock state after the cohorts feed from it, one might argue that the reduced leaf biomass stock simply reflects a larger degree of herbivory. However, this seemingly simple explanation does not capture the complexity of the underlying processes that affect the development of the emergent animal populations. In the following, we want to discuss the ecological responses to the coupling-related changes in total leaf biomass and varying climate conditions.

Total leaf biomass. is the chief alteration to the original Madingley model. All differences that can be observed between the M-M and M-LPJG setups originate from shifts in the simulated vegetation. In M-LPJG, more leaf biomass is available as a food source during the cold season compared to M-M. Thus, M-LPJG supports a larger biomass flux from autotrophs to herbivores over winter. The larger total cohort biomasses that correspond to the lower average leaf biomasses but higher minimum leaf biomasses (as computed in M-LPJG compared to M-M), indicates that total cohort biomasses are more sensitive to the minimum leaf biomass. This is plausible, since at least at locations with a temperate or boreal climate — the cohorts growth limitations are more likely to be reached during the cold season. In FIN M-LPJG, endotherms need significantly less time to reach maturity than in FIN M-M. This indicates that an increased minimum leaf biomass also increases the leaf biomass flux to herbivores on an individual level. Thus, the herbivores assimilate more biomass throughout the M-LPJG simulation and reach their adult body mass more quickly. A similar effect can be found in SAF M-LPJG, where a higher minimum in the leaf biomass pool results in a higher flux from autotrophic biomass to herbivores. This is quite remarkable since the average leaf biomass in SAF M-LPJG is lower than in SAF M-M and explains how despite the lower leaf biomass pool, the herbivore biomass pool can be higher in M-LPJG.

In three out of four locations, M-LPJG predicts a lower average annual leaf biomass when compared to M-M. This seems to shift the size distributions towards smaller individuals, most visible in the increased abundance of individuals lighter than 1 g (Fig. 6). This result is consistent with the increased number of cohorts going extinct in the M-LPJG simulations and their lower lifespans, which in turn reflects increased predation stress on the smaller individuals.

The larger total annual leaf biomass supports cohorts of heavier individual body mass in the M-M simulations. While this observation is consistent with the megafauna theory (Evans et al., 2012), the default Madingley version nonetheless overestimates the size of large herbivores by four to six times compared to field studies (Harfoot et al., 2014). It was also observed that the smaller the gap between the predicted M-M and the M-LPJG vegetation, the higher the herbivore biomass in the M-LPJG run (compare GER M-LPJG and SAF M-LPJG). This indicates that a uniform increase in vegetation biomass without changing its evergreen/deciduous composition still enhances herbivore biomass.

Climatic conditions. Under colder conditions, animals are less active and thus have less time to fulfil their metabolic cost (Harfoot et al., 2014). While ectotherms become inactive below a certain temperature threshold, endotherms constantly need to be active under tropical and boreal conditions alike. Climatic conditions thus contribute to the cohorts stress by enhancing the effect of calorific shortages.

Fig. 6 shows that the coupling leads to an increase in ectotherm herbivore abundance under warm climate (UGA and SAF). In these

locations, the smallest individuals, which are typically ectotherm herbivores, show overall higher growth rates in M-LPJG, compared to M-M. Fig. 7B shows this effect also on an individual level. In M-M, the smallest individuals, which are typically ectotherms, are showing a wide pattern of growth rates in similar weight classes. This is an indicator that most individuals are not reaching their maximum potential growth rate, therefore the amount of leaf-biomass seems to be the limiting factor. In contrast, in M-LPJG, the smallest individuals all have similar growth rates under similar climatic conditions. This again indicates that the higher leaf-biomass no longer limits the growth rate.

Under colder climate conditions (FIN and GER) the ectotherm herbivore abundance did not show significant changes due to the coupling. In these locations, the growth rates of similar individuals are not enhanced by LPJ-GUESS vegetation input significantly. We expect the climatic conditions to be the limiting factors in both M-M and M-LPJG simulations.

These two examples have shown that climatic conditions can weaken or enhance the effect of changes in leaf-biomass. As the most noticeable example, we want to highlight the extinction of carnivore endotherms in FIN M-M simulations. During the first few timesteps, the endotherm herbivore population grows faster in FIN M-LPJG as a result of a higher minimum in leaf biomass during the cold season than in FIN M-M. This keeps the total biomass of herbivores in FIN M-LPJG large enough to feed endotherm carnivores in contrast to the FIN M-M simulations. The reduced growth of endotherm herbivores in FIN M-M leads to the total herbivore biomass being too low to support a carnivore endotherm population. As a result, endothermic carnivores in FIN M-M go extinct during the first few timesteps. Since there are no mechanisms that would allow these extinct functional group to enter the simulation, besides the initialisation, they stay extinct for the rest of the simulation. After the first decades, the established herbivore population grows without the top-down control of predation and thus their body mass size distribution shows fewer, heavier individuals than in the FIN M-LPJG simulation. This effect of the absence of large carnivores in Madingley, leading to the non-regulated growth of the lower trophic levels, is consistent with observations (Elmhagen et al., 2010; Brose et al., 2019) and highlights the importance of representing all trophic levels in a simulation.

Overall, the individual level characteristics only show minor differences when comparing the M-LPJG simulations to the M-M simulations, but, at the same time, we observe huge variations in the traits on a community level. This leads us to the conclusion that relatively small changes in individual processes can lead to substantial changes in the dynamics of a whole animal community. Minor differences on the individual level also indicate that Madingley still successfully predicts ecological processes for individuals and thus still produces reasonable assumptions for animal communities.

4.2. Comparison to external sources

M-LPJG consistently predicts NPP that is closer to empirical observations than the NPP predicted by M-M. Madingleys chosen NPP parameterisation (Miami) does not seem to fit well for temperature or precipitation extremes (very hot, very arid or very wet). In arid ecosystems such as SAF, M-LPJG also includes wildfires in its simulations. While the Miami model predicts a lower NPP than LPJ-GUESS in FIN and GER, we see higher leaf biomass stocks in M-M rather than in M-LPJG. This is caused by Madingley assuming that 64% (FIN) and 68% (GER) of the monthly available NPP is allocated towards leaves (see also supplementary information S3). LPJ-GUESS is typically accounting about 30% of the allocation towards leaves (De Kauwe et al., 2014).

The simulation derived power-law for herbivore biomass to NPP is more consistent with empirical relationships in the M-LPJG setup. Still, while the power-laws slope is similar, the magnitude of the simulated herbivore biomass is higher than seen in the empirical data from Cebrian (2004). There is an ongoing discussion in the scientific community about whether a higher biomass density of herbivores increases the ecosystems productivity through accelerating nutrient cycles (Enquist et al., 2020), significantly reduces plant biomass through damaging individuals (Jia et al., 2018) or shifts ecosystems plant species distributions (Schmitz et al., 2014). The strength of these effects likely are highly site and ecosystem specific. We aim to include the effects described by the scientific community in our future model development, such as implementing C:N stoichiometry in Madingley, implementing a feedback loop from Madingley to LPJ-GUESS, affecting leaf area and photosynthesis, and installing a litter pool in Madingley to track animal faeces. Such additional model development will allow to explore further which process underpins the overestimation of herbivore biomass in Fig. 9. Still, the Madingley model can, for the first time, predict similar kinds of power-laws as observable in nature, which is a major improvement of the model and lays the foundation for future model developments.

In SAF M-LPJG, both herbivore biomass and herbivory consumption are overestimated when compared to the power-law relationships. We expect this to result from every cohort having access to 10% of the leaf biomass stock in Madingley. While this value may be accurate for large insect swarms, we find it unlikely for a herd of mammals to access 10% of the leaf biomass in an area of ~2.500 km^2 (one grid cell in SAF) over the course of one month. While the cohorts are limited by the accessible leaf biomass, they do not necessarily consume all of it, but only try to fulfil their metabolic cost. In SAF, herbivores consume a higher portion of the standing stock due to the ecosystems lower productivity.

Interpretation of previous Madingley publications. We have shown that Madingleys build in NPP parameterisation by the Miami is only predicting realistic NPP in one out of the four simulated locations. Even in European temperate forest, NPP is underestimated by 30%. In ecosystems with extremely low or high productivity, it is very likely that Miami has made a completely unrealistic NPP prediction. We have also shown that not only the average NPP, but also the Miamis high yearly fluctuations of both evergreen and deciduous stocks more specifically the vegetation stocks winter minima and the length of the growing season- are very likely to affect the development of animal populations. In conclusion, we expect that previous publications have underestimated the abundance and growth rates of ectothermic animals in high or low-productivity ecosystems, while also overestimating the cohorts lifespan and reproduction cycles in all terrestrial ecosystems.

4.3. Limitations and future priorities

While we explicitly chose the four experiment locations to represent ecosystems under different climatic conditions, it remains to be tested how M-LPJGs leaf biomass simulation compares globally to that of M-M and whether this will align herbivore biomass better with observations.

We assume that the improved modelling of the vegetation by LPJ-GUESS and thus shifts to more realistic canopy compositions enhance the realism of the ecological processes in Madingley. The next step will be the full coupling of both models and thus reduce the leaf mass from the individuals in LPJ-GUESS according to the herbivory activity in Madingley. During this process, we also want to make the leaf biomass accessible to the herbivores based on their traits, instead of giving every cohort access to 10% of the stocks. We expect this to also improve the representation of low-productivity ecosystems in out model system. In addition to the full coupling, we aim to implement a litter pool in Madingley and track animal faeces, which are currently escaping the model environment. There is an ongoing effort to include nitrogen in Madingley and to include this compartment of the code in the fully coupled version. This would enable further investigations if the model system can track an accelerated nutrient cycle and thus an enhanced ecosystem productivity.

Another plan we are pursuing is the implementation of different herbivory types, like grazing and browsing. A new version of Madingley is also being developed which would enable ground vs. canopy feeding.

4.4. Conclusion

The upcoming UN decade of restoration undoubtedly imposes huge challenges upon decision makers and emphasises the urgent need of understanding processes and interconnectivity in ecosystems. A large focus lies on nature-based solutions, and the increased interest in protecting animal population and biodiversity (European Commission, 2020). Modelling is a strong tool for making assessments on ecosystem functioning and interconnectivity of living organisms. With this study, we show that coupling the Madingley model with the process-based dynamic global vegetation model LPJ-GUESS is improving the realism of Madingleys modelled animal populations on multiple levels. Simulated animal cohorts were facing a wider range of net primary production and realistic fluctuations in seasonal vegetation biomass and composition. These changes lead to significant differences when compared to Madingleys default version, such as the persistence of whole ecological groups, which otherwise go extinct. We found general shifts in the animal populations towards smaller but more abundant individuals and demonstrated that our model system is consistently portraying and preserving all ecological groups, which is a major improvement. At the same time, the model still presents the underlying ecological processes, which is the foundation of the simulation of functional diversity. This ensures that that changes in the model output correspond to changes in the models boundary conditions and are in-fact not based on statistical disruptions in the food-chain or numeric instabilities.

Ultimately, we conclude that our implementations were in-fact improving the realism of the model systems prediction by comparing our results to empirical data. Madingley is a powerful tool in assessing an ecosystems functioning by modelling its whole trophic pyramid and we are keen to implement further processes and feedbacks in our model system in the future. With further development, out model system will help making informed decisions on ecosystem management in regards of animal biodiversity and overall ecosystem functioning.

4.5. Code availability

The LPJ-GUESS model code is managed and maintained by the Department of Physical Geography and Ecosystem Science at the Lund University, Sweden. The original Madingley model code is managed by the UN Environment Programme World Conservation Monitoring Centre (UNEP-WCMC) at the University of Cambridge, England. The intellectual property right for the translated version we used in this study is hold by the Radboud University in Nimwegen, Netherlands. Therefore, a DOI for both the LPJ-GUESS, as well as the Madingley model code cannot be provided. The source can be made available under a collaboration agreement under the acceptance of certain conditions.

CRediT authorship contribution statement

Jens Krause: Conceptualization, Methodology, Writing – original draft, Visualization. **Mike Harfoot:** Conceptualization, Methodology, Software, Writing – review & editing. **Selwyn Hoeks:** Software, Writing – review & editing. **Peter Anthoni:** Conceptualization, Software, Validation, Writing – review & editing. **Calum Brown:** Writing – review & editing. **Mark Rounsevell:** Writing – review & editing. **Almut Arneth:** Validation, Writing – review & editing, Supervision, Funding acquisition.

Declaration of competing interest

The authors declare that they have no known competing financial interests or personal relationships that could have appeared to influence the work reported in this paper.

Data availability

The authors do not have permission to share data.

Acknowledgements

Almut Arneth, Peter Anthoni and Jens Krause acknowledge funding via the Helmholz Foundation Impulse and Networking, Germany fund and the Helmholz ATMO programme, Germany. We also thank the reviewers for their constructive suggestion and the time they invested in supporting the review process of this study.

Appendix A. Supplementary data

Supplementary material related to this article can be found online at https://doi.org/10.1016/j.ecolmodel.2022.110061. The supplementary material shows climate input, model setup, further simulation results and validation comparisons.

References

Arneth, A., Shin, Y.-J., Leadley, P., Rondinini, C., Bukvareva, E., Kolb, M., Midgley, G.F., Oberdorff, T., Palomo, I., Saito, O., 2020. Post-2020 biodiversity targets need to embrace climate change. Proc. Natl. Acad. Sci. USA 117 (49), 30882–30891. http://dx.doi.org/10.1073/pnas.2009584117, URL http://www.pnas.org/lookup/doi/10.1073/pnas.2009584117.

Bar-On, Y.M., Phillips, R., Milo, R., 2018. The biomass distribution on earth. Proc. Natl. Acad. Sci. USA 115 (25), 6506. http://dx.doi.org/10.1073/pnas.1711842115, URL http://www.pnas.org/content/115/25/6506.abstract.

Berzaghi, F., Longo, M., Ciais, P., Blake, S., Bretagnolle, F., Vieira, S., Scaranello, M., Scarascia-Mugnozza, G., Doughty, C., 2019. Carbon stocks in central african forests enhanced by elephant disturbance. Nature Geosci. 12, http://dx.doi.org/10.1038/s41561-019-0395-6.

Brose, U., Archambault, P., Barnes, A.D., Bersier, L.-F., Boy, T., Canning-Clode, J., Conti, E., Dias, M., Digel, C., Dissanayake, A., Flores, A.A.V., Fussmann, K., Gauzens, B., Gray, C., Häussler, J., Hirt, M.R., Jacob, U., Jochum, M., Kéfi, S., McLaughlin, O., MacPherson, M.M., Latz, E., Layer-Dobra, K., Legagneux, P., Li, Y., Madeira, C., Martinez, N.D., Mendonça, V., Mulder, C., Navarrete, S.A., O'Gorman, E.J., Ott, D., Paula, J., Perkins, D., Piechnik, D., Pokrovsky, I., Raffaelli, D., Rall, B.C., Rosenbaum, B., Ryser, R., Silva, A., Sohlström, E.H., Sokolova, N., Thompson, M.S.A., Thompson, R.M., Vermandele, F., Vinagre, C., Wang, S., Wefer, J.M., Williams, R.J., Wieters, E., Woodward, G., Iles, A.C., 2019. Predator traits determine food-web architecture across ecosystems. Nature Ecol. Evol. 3 (6), 919–927. http://dx.doi.org/10.1038/s41559-019-0899-x.

Cardinale, B.J., Duffy, J.E., Gonzalez, A., Hooper, D.U., Perrings, C., Venail, P., Narwani, A., Mace, G.M., Tilman, D., Wardle, D.A., Kinzig, A.P., Daily, G.C., Loreau, M., Grace, J.B., Larigauderie, A., Srivastava, D.S., Naeem, S., 2012. Biodiversity loss and its impact on humanity. Nature 486 (7401), 59–67. http://dx.doi.org/10.1038/nature11148, Publisher: Nature Publishing Group. URL http://www.nature.com/articles/nature11148.

Cebrian, J., 2004. Role of first-order consumers in ecosystem carbon flow: Carbon flow through first-order consumers. Ecol. Lett. 7 (3), 232–240. http://dx.doi.org/10.1111/j.1461-0248.2004.00574.x, URL http://doi.wiley.com/10.1111/j.1461-0248.2004.00574.x.

Dangal, S.R.S., Tian, H., Lu, C., Ren, W., Pan, S., Yang, J., Di Cosmo, N., Hessl, A., 2017. Integrating herbivore population dynamics into a global land biosphere model: Plugging animals into the earth system: Plugging animals into the earth system. J. Adv. Model. Earth Syst. 9 (8), 2920–2945. http://dx.doi.org/10.1002/2016MS000904, URL http://doi.wiley.com/10.1002/2016MS000904.

De Kauwe, M., Medlyn, B., Zaehle, S., Walker, A., Dietze, M., Wang, Y., Luo, Y., Jain, A., El Masri, B., Hickler, T., Warlind, D., Weng, E., Parton, W., Thornton, P., Wang, S., Prentice, I., Asao, S., Smith, B., Mccarthy, H., Norby, R., 2014. Where does the carbon go? A model-data intercomparison of vegetation carbon allocation and turnover processes at two temperate forest free-air CO 2 enrichment sites. New Phytol. 203, http://dx.doi.org/10.1111/nph.12847.

Elmhagen, B., Ludwig, G., Rushton, S.P., Helle, P., Lindén, H., 2010. Top predators, mesopredators and their prey: interference ecosystems along bioclimatic productivity gradients. J. Anim. Ecol. 79 (4), 785–794. http://dx.doi.org/10.1111/j.1365-2656.2010.01678.x, Publisher: John Wiley & Sons, Ltd.

Enquist, B.J., Abraham, A.J., Harfoot, M.B.J., Malhi, Y., Doughty, C.E., 2020. The megabiota are disproportionately important for biosphere functioning. Nature Commun. 11 (1), 699. http://dx.doi.org/10.1038/s41467-020-14369-y.

European Commission and Directorate-General for Research and Innovation, 2020. Biodiversity and Nature-Based Solutions : Analysis of EU-Funded Projects. Publications Office, http://dx.doi.org/10.2777/183298.

Evans, A.R., Jones, D., Boyer, A.G., Brown, J.H., Costa, D.P., Ernest, S.K.M., Fitzgerald, E.M.G., Fortelius, M., Gittleman, J.L., Hamilton, M.J., Harding, L.E., Lintulaakso, K., Lyons, S.K., Okie, J.G., Saarinen, J.J., Sibly, R.M., Smith, F.A., Stephens, P.R., Theodor, J.M., Uhen, M.D., 2012. The maximum rate of mammal evolution. Proc. Natl. Acad. Sci. USA 109 (11), 4187–4190. http://dx.doi.org/10.1073/pnas.1120774109, arXiv:22308461, Edition: 2012/01/30 Publisher: National Academy of Sciences. URL https://pubmed.ncbi.nlm.nih.gov/22308461.

Harfoot, M., Newbold, T., Tittensor, D.P., Emmott, S., Hutton, J., Lyutsarev, V., Smith, M.J., Scharlemann, J.P., Purves, D.W., 2014. Emergent global patterns of ecosystem structure and function from a mechanistic general ecosystem model. PLoS Biol. 12 (4), e1001841. http://dx.doi.org/10.1371/journal.pbio.1001841, Publisher: Public Library of Science. URL http://dx.plos.org/10.1371/journal.pbio.1001841.

Harris, I.C., 2020. CRU JRA v2.1: a forcings dataset of gridded land surface blend of climatic research unit (CRU) and japanese reanalysis (JRA) data. Jan.1901 - Dec.2019. URL https://catalogue.ceda.ac.uk/uuid/10d2c73e5a7d46f4ada08b0a26302ef7.

Hatfield, J.L., Dold, C., 2019. Chapter 1 - photosynthesis in the solar corridor system. In: Deichman, C.L., Kremer, R.J. (Eds.), The Solar Corridor Crop System. Academic Press, pp. 1–33. http://dx.doi.org/10.1016/B978-0-12-814792-4.00001-2, URL https://www.sciencedirect.com/science/article/pii/B9780128147924000012.

Hickler, T., Prentice, I., Smith, B., Sykes, M., Zaehle, S., 2006. Implementing plant hydraulic architecture within the LPJ dynamic global vegetation model. Glob. Ecol. Biogeography 15, 567–577. http://dx.doi.org/10.1111/j.1466-8238.2006.00254.x.

Hoeks, S., Huijbregts, M.A.J., Busana, M., Harfoot, M.B.J., Svenning, J.-C., Santini, L., 2020. Mechanistic insights into the role of large carnivores for ecosystem structure and functioning. Ecography 43 (12), 1752–1763. http://dx.doi.org/10.1111/ecog.05191, URL https://onlinelibrary.wiley.com/doi/10.1111/ecog.05191.

Holdo, R.M., Sinclair, A.R.E., Dobson, A.P., Metzger, K.L., Bolker, B.M., Ritchie, M.E., Holt, R.D., 2009. A disease-mediated trophic cascade in the serengeti and its implications for ecosystem c. PLoS Biol. 7 (9), e1000210. http://dx.doi.org/10.1371/journal.pbio.1000210, Publisher: Public Library of Science. URL https://dx.plos.org/10.1371/journal.pbio.1000210.

Hooper, D.U., Adair, E.C., Cardinale, B.J., Byrnes, J.E.K., Hungate, B.A., Matulich, K.L., Gonzalez, A., Duffy, J.E., Gamfeldt, L., O'connor, M.I., 2012. A global synthesis reveals biodiversity loss as a major driver of ecosystem change. Nature 486, 105–109. http://dx.doi.org/10.1038/nature11118, URL https://www.nature.com/articles/nature11118.pdf.

Jia, S., Wang, X., Yuan, Z., Lin, F., Ye, J., Hao, Z., Luskin, M.S., 2018. Global signal of top-down control of terrestrial plant communities by herbivores. Proc. Natl. Acad. Sci. USA 115 (24), 6237. http://dx.doi.org/10.1073/pnas.1707984115, URL http://www.pnas.org/content/115/24/6237.abstract.

Kattge, J., Díaz, S., Lavorel, S., Prentice, I.C., Leadley, P., Bönisch, G., Garnier, E., Westoby, M., Reich, P.B., Wright, I.J., Cornelissen, J.H.C., Violle, C., Harrison, S.P., Van BODEGOM, P.M., Reichstein, M., Enquist, B.J., Soudzilovskaia, N.A., Ackerly, D.D., Anand, M., Atkin, O., Bahn, M., Baker, T.R., Baldocchi, D., Bekker, R., Blanco, C.C., Blonder, B., Bond, W.J., Bradstock, R., Bunker, D.E., Casanoves, F., Cavender-Bares, J., Chambers, J.Q., Chapin Iii, F.S., Chave, J., Coomes, D., Cornwell, W.K., Craine, J.M., Dobrin, B.H., Duarte, L., Durka, W., Elser, J., Esser, G., Estiarte, M., Fagan, W.F., Fang, J., Fernández-Méndez, F., Fidelis, A., Finegan, B., Flores, O., Ford, H., Frank, D., Freschet, G.T., Fyllas, N.M., Gallagher, R.V., Green, W.A., Gutierrez, A.G., Hickler, T., Higgins, S.I., Hodgson, J.G., Jalili, A., Jansen, S., Joly, C.A., Kerkhoff, A.J., Kirkup, D., Kitajima, K., Kleyer, M., Klotz, S., Knops, J.M.H., Kramer, K., Kühn, I., Kurokawa, H., Laughlin, D., Lee, T.D., Leishman, M., Lens, F., Lenz, T., Lewis, S.L., Lloyd, J., Llusià, J., Louault, F., Ma, S., Mahecha, M.D., Manning, P., Massad, T., Medlyn, B.E., Messier, J., Moles, A.T., Müller, S.C., Nadrowski, K., Naeem, S., Niinemets, U., Nöllert, S., Nüske, A., Ogaya, R., Oleksyn, J., Onipchenko, V.G., Onoda, Y., Ordoñez, J., Overbeck, G., Ozinga, W.A., Patiño, S., Paula, S., Pausas, J.G., Peñuelas, J., Phillips, O.L., Pillar, V., Poorter, H., Poorter, L., Poschlod, P., Prinzing, A., Proulx, R., Rammig, A., Reinsch, S., Reu, B., Sack, L., Salgado-Negret, B., Sardans, J., Shiodera, S., Shipley, B., Siefert, A., Sosinski, E., Soussana, J.-F., Swaine, E., Swenson, N., Thompson, K., Thornton, P., Waldram, M., Weiher, E., White, M., White, S., Wright, S.J., Yguel, B., Zaehle, S., Zanne, A.E., Wirth, C., 2011. TRY - a global database of plant traits: TRY - a global database of plant traits. Glob. Change Biol. 17 (9), 2905–2935. http://dx.doi.org/10.1111/j.1365-2486.2011.02451.x, URL http://doi.wiley.com/10.1111/j.1365-2486.2011.02451.x.

Launiainen, S., Katul, G.G., Leppä, K., Kolari, P., Aslan, T., Grönholm, T., Korhonen, L., Mammarella, I., Vesala, T., 2022. Does growing atmospheric CO2 explain increasing carbon sink in a boreal coniferous forest? Glob. Change Biol. n/a, http://dx.doi.org/10.1111/gcb.16117, Publisher: John Wiley & Sons, Ltd.

Lieth, H., 1975. Modeling the primary productivity of the world. In: Lieth, H., Whittaker, R.H. (Eds.), Primary Productivity of the Biosphere. Springer Berlin Heidelberg, pp. 237–263. http://dx.doi.org/10.1007/978-3-642-80913-2_12.

Lindeskog, M., Lagergren, F., Smith, B., Rammig, A., 2021. Accounting for forest management in the estimation of forest carbon balance using the dynamic vegetation model LPJ-GUESS (v4.0, r9333): Implementation and evaluation of simulations for Europe. Geosci. Model Dev. Discuss. 2021, 1–42. http://dx.doi.org/10.5194/gmd-2020-440, Publisher: Copernicus Publications. URL https://gmd.copernicus.org/preprints/gmd-2020-440/.

Newbold, T., Tittensor, D.P., Harfoot, M.B.J., Scharlemann, J.P.W., Purves, D.W., 2020. Non-linear changes in modelled terrestrial ecosystems subjected to perturbations. Sci. Rep. 10 (1), 14051. http://dx.doi.org/10.1038/s41598-020-70960-9.

Nichols, E., Peres, C.A., Hawes, J.E., Naeem, S., 2016. Multitrophic diversity effects of network degradation. Ecol. Evol. 6 (14), 4936–4946. http://dx.doi.org/10.1002/ece3.2253.

Pachzelt, A., Forrest, M., Rammig, A., Higgins, S., Hickler, T., 2015. Potential impact of large ungulate grazers on african vegetation, carbon storage and fire regimes: Grazer impacts on african savannas. Glob. Ecol. Biogeography 24, http://dx.doi.org/10.1111/geb.12313.

Pacifici, M., Foden, W.B., Visconti, P., Watson, J.E., Butchart, S.H., Kovacs, K.M., Scheffers, B.R., Hole, D.G., Martin, T.G., Akçakaya, H.R., Corlett, R.T., Huntley, B., Bickford, D., Carr, J.A., Hoffmann, A.A., Midgley, G.F., Pearce-Kelly, P., Pearson, R.G., Williams, S.E., Willis, S.G., Young, B., Rondinini, C., 2015. Assessing species vulnerability to climate change. Nature Clim. Change 5 (3), 215–225. http://dx.doi.org/10.1038/nclimate2448.

Rabin, S.S., Melton, J.R., Lasslop, G., Bachelet, D., Forrest, M., Hantson, S., Kaplan, J.O., Li, F., Mangeon, S., Ward, D.S., Yue, C., Arora, V.K., Hickler, T., Kloster, S., Knorr, W., Nieradzik, L., Spessa, A., Folberth, G.A., Sheehan, T., Voulgarakis, A., Kelley, D.I., Prentice, I.C., Sitch, S., Harrison, S., Arneth, A., 2017. The fire modeling intercomparison project (firemip), phase 1: experimental and analytical protocols with detailed model descriptions. Geosci. Model Dev. 10 (3), 1175–1197. http://dx.doi.org/10.5194/gmd-10-1175-2017, Publisher: Copernicus Publications. URL https://gmd.copernicus.org/articles/10/1175/2017/.

Rebmann, C., Zeri, M., Lasslop, G., Mund, M., Kolle, O., Schulze, E.-D., Feigenwinter, C., 2010. Treatment and assessment of the CO2-exchange at a complex forest site in Thuringia, Germany. Agric. Forest Meteorol. 150 (5), 684–691. http://dx.doi.org/10.1016/j.agrformet.2009.11.001, URL https://linkinghub.elsevier.com/retrieve/pii/S0168192309002500.

Running, S., Zhao, M., 2021. MODIS/Terra net primary production gap-filled yearly L4 global 500 m SIN grid V061. 2021. URL https://doi.org/10.5067/MODIS/MOD17A3HGF.061.

Schmitz, O.J., Raymond, P.A., Estes, J.A., Kurz, W.A., Holtgrieve, G.W., Ritchie, M.E., Schindler, D.E., Spivak, A.C., Wilson, R.W., Bradford, M.A., Christensen, V., Deegan, L., Smetacek, V., Vanni, M.J., Wilmers, C.C., 2014. Animating the carbon cycle. Ecosystems 17 (2), 344–359. http://dx.doi.org/10.1007/s10021-013-9715-7, Publisher: Springer US. URL http://link.springer.com/10.1007/s10021-013-9715-7.

Schmitz, O.J., Wilmers, C.C., Leroux, S.J., Doughty, C.E., Atwood, T.B., Galetti, M., Davies, A.B., Goetz, S.J., 2018. Animals and the zoogeochemistry of the carbon cycle. Science 362 (6419), eaar3213. http://dx.doi.org/10.1126/science.aar3213, URL http://www.sciencemag.org/lookup/doi/10.1126/science.aar3213.

Smith, M.J., Purves, D.W., Vanderwel, M.C., Lyutsarev, V., Emmott, S., 2013. The climate dependence of the terrestrial carbon cycle, including parameter and structural uncertainties. Biogeosciences 10 (1), 583–606. http://dx.doi.org/10.5194/bg-10-583-2013, Publisher: Copernicus Publications. URL https://bg.copernicus.org/articles/10/583/2013/.

Smith, B., Wärlind, D., Arneth, A., Hickler, T., Leadley, P., Siltberg, J., Zaehle, S., 2014. Implications of incorporating n cycling and n limitations on primary production in an individual-based dynamic vegetation model. Biogeosciences 11 (7), 2027–2054. http://dx.doi.org/10.5194/bg-11-2027-2014.

Sobral, M., Silvius, K.M., Overman, H., Oliveira, L.F.B., Raab, T.K., Fragoso, J.M.V., 2017. Mammal diversity influences the carbon cycle through trophic interactions in the amazon. Nature Ecol. Evol. 1 (11), 1670–1676. http://dx.doi.org/10.1038/s41559-017-0334-0.

Staver, A.C., Bond, W.J., 2014. Is there a 'browse trap'? Dynamics of herbivore impacts on trees and grasses in an African savanna. J. Ecol. 102, 595–602. http://dx.doi.org/10.1111/1365-2745.12230, URL https://besjournals.onlinelibrary.wiley.com/doi/pdf/10.1111/1365-2745.12230.

Wilmers, C.C., Schmitz, O.J., 2016. Effects of gray wolf-induced trophic cascades on ecosystem carbon cycling. Ecosphere 7 (10), e01501. http://dx.doi.org/10.1002/ecs2.1501, Publisher: Wiley-Blackwell.

Wramneby, A., Smith, B., Zaehle, S., Sykes, M., 2008. Parameter uncertainties in the modelling of vegetation dynamics—Effects on tree community structure and ecosystem functioning in European forest biomes. Ecol. Modell. 216, 277–290. http://dx.doi.org/10.1016/j.ecolmodel.2008.04.013.

Wårlind, D., Smith, B., Hickler, T., Arneth, A., 2014. Nitrogen feedbacks increase future terrestrial ecosystem carbon uptake in an individual-based dynamic vegetation model. Biogeosciences 11 (21), 6131–6146. http://dx.doi.org/10.5194/bg-11-6131-2014.

Ecological Modelling 492 (2024) 110706

Contents lists available at ScienceDirect

Ecological Modelling

journal homepage: www.elsevier.com/locate/ecolmodel

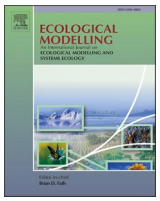

Corrigendum

Corrigendum to "How more sophisticated leaf biomass simulations can increase the realism of modelled animal populations" [Ecological Modelling 471 (2022) 110061]

Jens Krause [a,*], Mike Harfoot [b], Selwyn Hoeks [c], Peter Anthoni [a], Calum Brown [a], Mark Rounsevell [a], Almut Arneth [a]

[a] KIT-Campus Alpin, Institute of Meteorology and Climate Research (IMK-IFU), Garmisch-Partenkirchen, Germany
[b] UN Environment Programme World Conservation Monitoring Center, Cambridge, United Kingdom
[c] Department of Environmental Science, Radboud University Nijmegen, Netherlands

The authors regret that the data presented in Fig. 9 were incorrect. We created an algorithm to estimate each grid cell's area. This algorithm contained an error, which led to an overestimation of the calculated area and thus an underestimation of the herbivore biomass density and the herbivory consumption density. We corrected the algorithm and used the same model state and setup as in our original manuscript and repeated the simulations used to determine the power-law relationships. We expanded the analysis time-frame from 10 to 30 years to ensure that low-productivity ecosystems are represented well. The corrected power-law relationships are:

$$log(biomass) = 0.9 + 0.31 * log(NPP)$$

$$log(primary\ consumption) = 0.26 + 0.66 * log(NPP)$$

The corrected Fig. 9 is the following:

Our original claims still uphold with the corrected Fig. 9. Our model system shows a positive response of herbivore biomass density to the ecosystem's NPP, while the default Madingley model version is showing

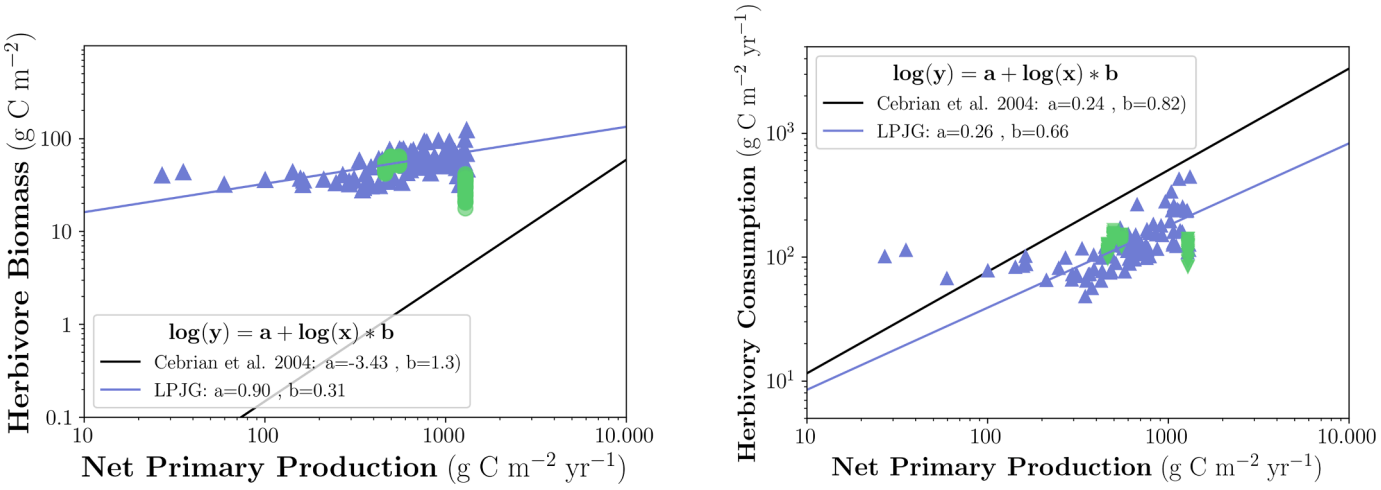

Fig. 1. Power-law relationships. Blue triangles represent an annual sum during a M-LPJG simulations. Green dots represent an annual sum during a M-M simulations. For the M-LPJG setups, herbivore biomass and herbivory consumption are related to NPP. There are no reasonable corresponding logarithmic fits for the M-M setups.

DOI of original article: https://doi.org/10.1016/j.ecolmodel.2022.110061.

* Corresponding author at: KIT-Campus Alpin, Institute of Meteorology and Climate Research (IMK-IFU), Garmisch-Partenkirchen, Germany
E-mail address: jens.krause@kit.edu (J. Krause).

https://doi.org/10.1016/j.ecolmodel.2024.110706

Available online 12 April 2024

a narrow range of NPP data points, and lacks a logarithmic relationship.

With the corrected grid cell area algorithm, the derived power-law relationship for herbivory consumption is showing a very close fit to (Cebrian, 2004).

The authors would like to apologise for any inconvenience caused.

Reference

Cebrian, J., 2004. Role of first-order consumers in ecosystem carbon flow: Carbon flow through first-order consumers. Ecology Letters 7, 232–240. https://doi.org/10.1111/j.1461-0248.2004.00574.x.